UNIVERSITÉ DU QUÉBEC À TROIS-RIVIÈRES

EN ASSOCIATION AVEC

UNIVERSITÉ DU QUÉBEC À MONTRÉAL

STRUCTURE ET FONCTION DES ÉCOSYSTÈMES PAR L'IMAGERIE : LA RELATION ENTRE HÉTÉROGÉNÉITÉ ET BIODIVERSITÉ

THÈSE PRÉSENTÉE
COMME EXIGENCE PARTIELLE
DU DOCTORAT EN SCIENCES DE L'ENVIRONNEMENT

PAR
IAN SEIFERLING

AVRIL 2017

UNIVERSITÉ DU QUÉBEC À TROIS-RIVIÈRES

DOCTORAT EN SC. DE L'ENVIRONNEMENT (Ph. D.)

Programme offert par l'Université du Québec à Montréal (UQAM)

en association avec

l'Université du Québec à Chicoutimi (UQAC)

l'Université du Québec à Rimouski (UQAR)

l'Université du Québec en Abitibi-Témiscamingue (UQAT)

et l'Université du Québec à Trois-Rivières (UQTR)

Cette thèse a été dirigée par :

Raphaël Proulx, Ph. D.	Université du Québec à Trois-Rivières
Directeur de recherche, grade	Rattachement institutionnel
Christian Wirth, Ph. D.	Leipzig University, Germany
Codirecteur de recherche, grade	Rattachement institutionnel

Jury d'évaluation de la thèse :

Raphaël Proulx, Ph. D.	Université du Québec à Trois-Rivières
Prénom et nom, grade	Rattachement institutionnel
Christian Wirth, Ph. D.	Leipzig University, Germany
Prénom et nom, grade	Rattachement institutionnel
Esther Lévesque, Ph. D.	Université du Québec à Trois-Rivières
Prénom et nom, grade	Rattachement institutionnel
Richard J. Ladle, Ph. D.	Federal University of Alagoas, Brazil
Prénom et nom, grade	Rattachement institutionnel
Christian Messier, Ph. D.	Université du Québec en Outaouais
Prénom et nom, grade	Rattachement institutionnel

Thèse soutenue le 17/11/2016

Surround yourself with people who make you happy. People who make you laugh, who help you when you're in need. People who genuinely care. They are the ones worth keeping in your life. Everyone else is just passing through — Karl Marx

I would like to acknowledge the many people to whom I learned from, helped achieve this work and most of all made it enjoyable. I thank my parents, Norm and Diane, for supporting my meanderings and helping me follow my interests unbounded. I thank my sister Dena - an artist with the curiosity of a scientist - for the distractions when distractions were needed. Satsuko for her unwavering support, motivation and for thinking all my ideas are great...even when they're not mine.

I give many thanks to Mario Liebergessell for the numerous occasions in which he gave his time to help my field work and project; I thank him more for his friendship, refreshing perspectives and our philosophical ramblings. Likewise, I thank Vera Holland for all her help and making long days in the field seem short. Thanks to Daniel Marra for all his help and inspiring talks while hiking Romanian hills (or drinking Romanian wine in the rain). I owe gratitude to Sophia Ratcliffe for her help in the field and data logistics, not least of all for securing us engine oil when lost in small German villages. Many thanks to Guillaume, Irene, Philippe and Charles in the lab for their help, perspectives and input on the research.

Thanks to Dr. Christian Wirth for his kind support, direction and inspiration. I consider myself lucky to not have just one great director, but two. I thank Dr. Michael Scherer-Lorenzen, the FunDivEurope site managers, support personnel and all my FunDivEurope colleagues; what an incredible experience, made so by the people involved.

I would also like to thank my many friends and colleagues at the Senseable City Lab who motivated and inspired me during my time there. Thank you to Dr. Carlo

Ratti for the opportunity and inspiration. Particular thanks to Erin Baumgartner, Moe Vazifeh, Anthony Vanky, Youjin Shin, Jonathon Sun, Newsha Ghaeli, Chaewon Ahn, Behrooz Hashemian and Iva Bojić for all the support while at SCL and making it such a fun and rewarding experience. Additional thanks to Behrooz and Moe who donated their own biological computing power (which is a lot in these two cases) to help work through computational problems.

Thank you to Dr. Oliver Sonnentag for his role on my proposal committee and his many valuable contributions and ideas to the research. Likewise, I thank Naik Nikhil who I was lucky enough to collaboration with. Big thanks to Daniel Sheehan at MIT Libraries for his GIS workshops and help to improve my GIS licks.

This research was supported by a Natural Sciences and Engineering Research Council of Canada (NSERC) research grant to R. Proulx, a Post-graduate NSERC scholarship to I. Seiferling, a Fonds de recherche du Québec - Nature et technologies (FRQNT) scholarship to I. Seiferling and a FRQNT internship grant and a NSERC scholarship to I. Seiferling. The invaluable experiences, learning and scientific achievements represented by this work would not have been possible without the support from NSERC and the FRQNT. Chapter 2 of the research presented here received funding from the European Union Seventh Framework Programme (FP7/2007-2013) under grant agreement no. 265171.

I owe my final gratitudes to Dr. Raphaël Proulx, who instead of offering me a short, relaxing summer internship in Germany as I requested, offered me a PhD. His level-headed guidance, humble friendship and creative ideas were a vital ingredient to all of the work we were able to achieve. I couldn't have asked for a better mentor and supervisor if I had programmed one myself. Average people talk about things, great people talk about ideas...Raphaël is one of the greats.

TABLE DES MATIÈRES

LISTE DES TABLEAUX

LISTE DES FIGURES

RÉSUMÉ

La biodiversité, l'hétérogénéité environnementale et le fonctionnement des écosystèmes sont devenus des concepts de base dans plusieurs domaines de la biologie. De nombreuses ressources et études scientifiques ont été consacrées à suivre la biodiversité, à quantifier les fonctions des écosystèmes, et les processus qui affectent ces trois concepts. Pour mesurer les impacts engendrés par les humains sur le monde naturel et pour définir des objectifs de conservation, ces trois concepts ont été utilisés comme des principes de référence pour définir les états d'un écosystème naturel et de la manière dont nous devrions procéder pour le préserver. En pratique, toutefois, un fort déclin d'espèces persiste ou augmente continuellement à travers la planète. Par ailleurs, des mesures disparates de biodiversité et d'hétérogénéité environnementale embrouillent notre compréhension de leur dynamique, leurs interrelations et l'établissement d'états de références. Afin de mieux comprendre les relations entre la biodiversité, l'hétérogénéité environnementale et le fonctionnement des écosystèmes, il est essentiel de définir et quantifier les tendances macro-écologiques avec des métriques non seulement calculables rapidement à de larges échelles, mais également comparables à travers les systèmes, tout en prenant compte de l'influence anthropogénique. Avec une amélioration de notre compréhension, nous pourrions développer des outils pour définir les caractéristiques et les représentations nécessaires au maintien ou même la restauration des fonctionnements écologiques et de l'intégrité des écosystèmes. L'objectif ultime serait l'intégration d'une telle perspective à l'échelle de tous les systèmes dans les politiques d'aménagement et de conservation. Pour y parvenir, les relations réciproques entre la diversité des espèces, l'hétérogénéité environnementale et les patrons saisonniers de croissance des plantes ont été examinés. L'emphase a été mis sur le développement et l'application de métriques qui décrivent les propriétés des écosystèmes en se basant sur des images digitales. Ces métriques génèrent une collection de données écologiques et atteignent de nouveaux niveaux de résolution spatiale et temporelle pour les mesures visuelles de patrons écosystémiques.

Premièrement, je présente un nouveau cadre conceptuel qui pourrait permettre de réconcilier les divergences observées jusqu'à présent dans les relations entre l'hétérogénéité environnementale (HE) et la biodiversité (BD). Les résultats révèlent que les écosystèmes fortement modifiés ou semi-naturels sont caractérisés par une dominance de relations HE-BD positives et négatives, respectivement, alors que les écosystèmes naturels montrent des réponses mixtes. Contrairement

à la vision traditionnelle stipulant que l'hétérogénéité environnementale entraîne nécessairement de la biodiversité, je montre que les écosystèmes naturels ne sont pas caractérisés par des niveaux maximum d'HE, mais bien par des niveaux intermédiaires. Ainsi, l'empreinte laissée par les humains sur les écosystèmes joue un rôle central dans la détermination de la nature des relations entre l'hétérogénéité spatiale et la biodiversité.

Ensuite, avec l'ancienne perspective révisée, j'examine la diversité en tant que vecteur de la dynamique écosystémique et pose la question : Est-ce que les variations de la diversité des espèces en forêt, définie ici par la composition des arbres, a un effet mesurable sur les patrons de croissance saisonniers ? En utilisant des photographies à intervalles et l'analyse d'images, les résultats mettent en évidence que la phénologie de la forêt n'est pas seulement une réponse de l'écosystème au climat, mais aussi un trait fonctionnel qui varie indépendamment du climat ; elle joue un rôle primaire dans la définition de la structure de la forêt et de l'allocation aux ressources. Par exemple, j'ai trouvé que la phénologie de la communauté du sous-bois est directement influencée par la diversité des arbres susjacents, le sous-bois a une croissance prolongée lorsqu'il est associé à une communauté riche en arbres aux étages supérieurs. Les résultats suggèrent que la diversité des arbres peut conduire à une efficacité accrue de la lumière qui se transfère des étages supérieurs vers le sous-bois.

Finalement, j'adapte des outils informatiques du domaine de la vision numérique pour quantifier les caractéristiques environnementales à partir de photographies digitales. J'utilise la vision numérique pour cartographier la distribution des arbres et d'autres types de végétation dans les paysages urbains. En utilisant des données d'images open-source de paysages de rue urbaines qui sont actuellement abondantes (images de Google Street View), je valide qu'un algorithme multi-étapes de la vision numérique segmente et quantifie avec précision le pourcentage de couverture d'arbres d'images de streetscape. La méthode constitue un avancement significatif par rapport aux efforts précédents pour quantifier le couvert d'arbres à l'aide de photographies, les anciens efforts utilisaient des métriques informatiques simples. En permettant l'utilisation de 'big data' et en réalisant des analyses rapides et automatiques avec des outils de la vision numérique, nous pouvons quantifier rapidement les caractéristiques des écosystèmes à échelles temporelles et spatiales rarement atteintes précédemment.

Durant cette recherche, j'ai découvert des patrons pouvant être généralisés qui mettent en lumière les interactions entre la diversité des espèces, l'hétérogénéité environnementale et le fonctionnement écosystémique des systèmes terrestres. Ce travail a également développé une nouvelle application d'analyse d'images et de photographies digitales pour quantifier, suivre et décrire rapidement les caracté-

ristiques d'un système. Il constitue une ligne prometteuse pour la recherche future dans l'évaluation rapide et la quantification de patrons environnementaux.

~

Biodiversity, environmental heterogeneity and ecosystem functioning have become core concepts in many fields of biology, with a great deal of scientific study and resources devoted to tracking biodiversity and quantifying the ecosystem functions and processes it effects. To measure the impacts humans are having on the natural world and define conservation goals, all three concepts have been used as benchmark features to define natural ecosystem states and how we should go about preserving them. In practice however, high rates of species loss persist or continue to increase around the globe. Moreover, disparate measures of biodiversity and environmental heterogeneity have complicated our understanding of their dynamics, interrelationships and the establishment of reference states.

Defining and quantifying macro-ecological patterns with metrics that are comparable across systems, account for anthropogenic influences and can be computed rapidly at large scales are essential to understanding the interrelationships between biodiversity, heterogeneity and ecosystem functioning. With an improved understanding, we may then develop tools to define the features and representations needed to maintain, or even restore, the ecological functioning and integrity of ecosystems. The ultimate goal being the integration of a systems-level perspective into land management and conservation policies. In an effort to contribute to this process, I examine the reciprocal relationships between species diversity, environmental heterogeneity and the seasonal patterns of plant growth. I focus on the development and application of digital image-based metrics of ecosystem properties. These metrics automate the collection of ecological data and achieve new levels of spatial and temporal resolution in the measurement of visual ecosystem patterns.

First, I present a new conceptual framework that could help reconcile the array of different environmental heterogeneity - biodiversity relationships that have been observed to date. The results reveal that highly-modified and semi-natural ecosystems are characterized by a dominance of positive and negative EH-BD relationships, respectively, whereas natural ecosystems show mixed responses. Against the traditional view that environmental heterogeneity necessarily supports biodiversity, I show that natural ecosystems are typified, not by maximum, but intermediate levels of EH. As such, an ecosystem's human footprint context plays a central role in defining the nature of the relationship between environmental heterogeneity and biodiversity.

Second, the former perspective is reversed and I examine diversity as the driver of ecosystem dynamics and ask the question of whether varying the species diversity of forests' defining component – trees – has measurable effects on their seasonal growth patterns. Using time-lapse photography and image analysis, the results evidenced that forest phenology is not only an ecosystem response to climate, but also a functional property that varies independent of climate; one that plays a primary role in defining forest structure and the allocation of resources. For example, I find that the understory community phenology is directly influenced by the overstory tree diversity, growing longer when associated with a species-rich overstory tree community. The results suggest that tree diversity may lead to increased light efficiencies that cascade from the overstory down to the understory.

Finally, I adapt computational tools from the computer vision field to quantify environmental properties from digital photographs. I use computer vision to map the distribution of trees and other vegetation in urban landscapes. By utilizing the open-source image data of city streetscapes that is now abundant (Google Street View images), I find that a multi-step computer vision algorithm accurately segments and quantifies the percent of tree cover in streetscape images. The method is a significant advancement from previous efforts to quantify tree cover in photographs which used computationally simpler, single-feature metrics. By making use of "big data" and achieving automated rapid analysis with computer vision tools, we can quickly quantify ecosystem properties at spatial and temporal scales rarely attainable before.

Through this research, I have uncovered generalizable patterns that shed new light on the interplay between species diversity, environmental heterogeneity and ecosystem functioning in terrestrial systems. This work has also demonstrated novel applications of digital photography and image analysis to rapidly quantify, track and describe ecosystem features; a promising line of future research towards the rapid assessment and quantification of environmental patterns.

INTRODUCTION

0.0.1 General overview

Central to ecology, and the understanding of how ecosystems operate and respond to perturbations, are the concepts of biodiversity [1], ecosystem functioning (EF) [2] and environmental heterogeneity (EH) [3]. At the core of this thesis, I will examine the interdependent relationships of species diversity and spatial heterogeneity, including an examination of forest phenology as a specific ecosystem function which relates to both. I will seek to identify a generalized relationship between EH and biodiversity at the landscape scale. I will also study how forest phenology at the community scale may represent a functional response to diversity. Within this research effort, and towards developing methodologies to explore those relationships, I focus on digital image-based metrics of ecosystem properties. These metrics automate the collection of ecological data and achieve new levels of spatial and temporal resolution in the measurement of visual patterns and features.

---

1. Depending on the specific discipline, the definition of biodiversity ranges from "the number of different species occurring in some location" to "all of the diversity and variability in nature". The 1992 United Nations Earth Summit defined biodiversity as "the heterogeneity among living organisms from all sources and the ecological complexes of which they are part."

2. Ecosystem functioning is the capacity of an ecosystem to provide services – directly and indirectly – underpinned by biophysical structures and processes (Scherer-Lorenzen, 2005).

3. Environmental heterogeneity is the spatial or temporal variation of a given resource, structure or biota in a given space.

0.0.2 Biodiversity, ecosystem functioning and the big biodiversity experiments

Biodiversity is a longstanding concept in many fields of biology, one that is increasingly used as a quality that is inherently optimized in natural ecosystems. As such, biodiversity is viewed as an intrinsic value that ought to be protected (Noss, 1990) and a benchmark to compare modified ecosystems to their natural analogues. Despite a global movement for biodiversity conservation and preservation, accelerating rates of species loss are evident across the globe (Ceballos *et al.*, 2015). With losses of global biodiversity, there has also been a rising concern that the functioning of ecosystems, and the services humans derive from them, may be compromised (Cardinale *et al.*, 2012) and inflict substantial costs on society (Naeem, 2002; Scherer-Lorenzen, 2013).

Consequently, researchers have sought to better understand the underlying and active role of ecosystem's biota and diversity in governing environmental conditions and processes, with cascading effects on the delivery of ecosystem services and human wellbeing (Cardinale *et al.*, 2012; Scherer-Lorenzen, 2013). Derived mainly from the establishment of several large-scale experimental grassland studies over the past 15 years (Tilman, 1999; Hector et Loreau, 2000; Roscher *et al.*, 2004), the current consensus is that biodiversity is an important determinant of ecosystem functioning and the services provided to mankind (Naeem, 2002; Scherer-Lorenzen, 2013). The main conclusions being that, increasing the species diversity of communities is associated with an increased mean (and a decreased variance) of several process rates (Hooper et al. 2005), namely primary productivity, increased temporal stability of system processes (Isbell *et al.*, 2009) and increased resilience to disturbances such as disease and drought (Thompson *et al.*, 2009; Keesing *et al.*, 2010; Grossiord *et al.*, 2014).

A complete understanding of the influence of biodiversity on ecosystem functio-

ning remains a challenge however, and most findings to date are based on research within grassland systems. Furthermore, a disproportionate number of studies focus solely on the diversity-productivity relationship. Identifying how functional traits may scale across ecosystem components, and thus identifying underlying mechanisms that link multiple processes to biodiversity, remain substantial challenges. Acknowledging these gaps, we must now investigate the relationship of diversity with understudied ecosystem functions such as phenology and also address those ecosystems that control a large portion of the carbon, nutrient and water balances of the earth – forests.

Forests constitute the world's largest terrestrial carbon sink and maintaining this ecosystem service is crucial for the Earth's greenhouse-gas balance. Within forest systems, trees are the key biological and structural feature, effecting biogeochemical cycles, water and energy exchange profoundly due to their large size and dominant role in creating system structure and complexity. As such tree diversity in forests likely effects system processes more profoundly than any other vegetation type. Unlike herbaceous plants for example, trees store large amounts of carbon and thus any change in growth and stand structure directly influences carbon sequestration. The work presented here will have a particular focus on forest ecosystems and their dominant feature, trees, but will also cover landscape scale analyses and patterns which can span ecosystem types and gradients between or within them.

0.0.3 From the top - down: Does environmental heterogeneity modulate biodiversity ?

In *Chapter 1* of this thesis, I will examine the biodiversity-EH-EF theme with a wide lens, not focussing on any specific taxonomic group, ecosystem type nor function, but asking whether spatial and temporal patterns across a landscape

can explain the levels and response of the biodiversity within them. That is, does environmental heterogeneity modulate species biodiversity across scales of space, ecosystem types and species taxonomies? This question does not seek to describe the complex array of mechanisms driving the dynamics between patterns of resources and the associated biodiversity. Rather, it will look to uncover generalizable patterns which may, in turn, explain variation in biodiversity across contemporary landscapes and the potential impacts of anthropogenic landscape modification on global biodiversity.

Environmental heterogeneity (EH) is the spatial or temporal variation of a given resource, structure or biota in a given space. Its relationship with biological diversity has been well studied, with numerous attempts by ecologists to quantify EH and explicate its role in begetting species richness, yet it remains a contentious subject. The "environmental heterogeneity hypothesis" (MacArthur et Wilson, 1967; Simpson, 1949), a cornerstone of ecology, asks whether EH orients the diversity of an ecosystem and implies that heterogenous conditions provide more niches and diverse ways of exploiting the resources, thus increasing species diversity (Tews *et al.*, 2004). Hence, the general expectation is that environmental heterogeneity–biodiversity (EH–BD) relationships should be positive. In fact, positive relationships supporting the EH hypothesis are well documented (Tews *et al.*, 2004; Palmer, 1994; Levin *et al.*, 2010; Kumar *et al.*, 2009), however non-significant and negative relationships are also prevalent in the literature (Tamme *et al.*, 2010; McKinney, 2008). I revisit this fundamental ecological relationship and aim to provide a novel and up to date framework that may account for both positive and negative relationship types through a statistically rigorous meta-analysis.

The EH-BD debate – proposed hypotheses

A number of recent studies have attempted to explain why we observe a mix of positive and negative EH-BD relationships when the longstanding niche-based EH hypothesis predicts only a positive relationship. Specifically, a few recent theoretical models explain the discrepancy through a predicted hump-shaped EH-BD relationship (Laanisto *et al.*, 2013; Smith et Lundholm, 2012; Bar-Massada et Wood, 2014; Bar-Massada, 2015; Allouche *et al.*, 2012). These recent works propose two different hypotheses to explain a unimodal hump-shaped EH-BD relationship and, thus, why the relationship may effectively switch from positive to negative: *i)* the microfragmentation (MF) hypothesis (Laanisto *et al.*, 2013) and; *ii)* the area-heterogeneity trade-off (AHTO) hypothesis (Allouche *et al.*, 2012; Bar-Massada et Wood, 2014). The MF hypothesis proposes that the "switch" from positive to negative is a factor of small-scale heterogeneity effects (*i.e.,* habitat loss and isolation occurring within a larger habitat patch or landscape) interacting with the taxa's foraging strategy (i.e., specialists *vs.* generalists). The AHTO hypothesis suggests that habitat patch area interacts with the taxa's population size and dispersal ability which can initiate local extinctions and, thus, cause the "switch" from positive to negative relationships to occur at some inflection point. Though the two hypotheses could be interpreted as conflicting, I believe that an inspection of the two indicate that they are in fact complimentary and relate to the same mechanisms, but operating at different scales. That is, both hypotheses suggest that positive EH-BD persist in natural habitats or landscapes and are driven by niche-partitioning processes (*i.e.,* the traditional EH hypothesis), but given a set of physical and biological interactions, neutral or negative relationships arise when some populations in an area experience local extinctions while others exhibit a neutral response. Those responses are the interaction between *i)* the physical features of habitat patch size, geometry and the resource constraints they impose

on biota ; *ii)* the biological features of niche breadth (dispersal ability and functional/foraging strategy); and *iii)* a temporal dimension which they interact and operate over (e.g., population size being a function of time).

Laanisto et al. (2013) define microfragmentation as the community level process of splitting habitat into a more heterogeneous environment that can have non-positive effects on the diversity through habitat loss and subsequent isolation. They provided support for the hypothesis through the results of a spatially explicit EH-BD simulation model in which they varied the ratio of generalist and specialist species across different configurations of spatial habitat heterogeneity (*i.e.*, structure in the form of patch size was varied while composition was constant). The model suggested that the relationship between heterogeneity and diversity is not always positive and that species' foraging strategy (a determinant of niche breadth) can determine how populations, and hence diversity, respond to these microfragmentation effects (Fig.1.1). The output showed that heterogeneity had differing effects on the diversity of specialist and generalist populations, wherein generalists remained largely unaffected by EH while the diversity of specialists responded non-linearly to increasing EH; increasing initially but responding negatively after an inflection point (Fig.1.1). The results are intuitive since generalists are defined as such by their adaptive abilities to utilize different resources in variable conditions and, as such, should be better adapted to heterogeneous habitats than specialists are (Tews *et al.*, 2004). On the other hand, generalists in the model were influenced by EH indirectly through the EH-BD dynamics of specialists and secondary interactions with them. When the model was devoid of specialists (Fig.1.1, panel B), the results showed a neutral-like community model wherein their *functional equivalence* (Hubbell, 2001) caused species diversity to be driven only by random processes. Laanisto et al.'s model not only gathered support for a hump-shaped EH-BD relationship, but it also evidenced that the "configurational

component" of environmental heterogeneity (Fahrig *et al.*, 2011) can, in of itself, have effects on species diversity. That is, simply increasing the diversity of habitat components, as previous models had focussed on, is an incomplete representation of the relationship. Increasing EH via configuration (i.e., fragmenting the system without adding new habitat types) appears to be a driving mechanism behind the presence of negative Eh-BD relationships. This finding suggests that the pattern and geometry of environmental features and structures is important to the EH-BD relationship and not just the compositional component of EH as emphasized in the bulk of the literature. In Chapter 1, I will support this concept that pattern is a critical feature of the EH-BD relationship, particularly so when landscape context and the effect of anthropogenic landscape modification (fragmentation) is taken into account. Drastically changing the configurational component of the landscape and habitat patches is, after all, precisely a result of fragmentation.

Thus, the Laanisto's et al. (2013) model and a few other previous works (Tews *et al.*, 2004; Smith et Lundholm, 2012; Kadmon et Allouche, 2007) indicate that environmental heterogeneity can affect community diversity in natural systems in much the same way we believe anthropogenic fragmentation does at the landscape level. This proposed mechanism is directly linked to the taxa's foraging or functional habits wherein local extinctions of specialist species can result from increasing EH in the form of small-scale patchiness. The model therefore addresses some, but not all parameters that define a species' niche breadth. For example, dispersal was highly constrained in the model by only allowing it to act on nearby habitats (nodes in the model's context) that were previously vacated by the loss of another species. In a series of studies formulating the AHTO, Allouche and Bar-Massada (Bar-Massada, 2015; Bar-Massada *et al.*, 2012; Bar-Massada et Wood, 2014; Allouche *et al.*, 2012) elaborate to explicitly model dispersal and thus add to the picture on how species' niche breadth and dispersal may interact with EH fea-

tures (habitat patch size and geometry, spatial scale and grain of EH) to produce a unimodal, hump-shaped EH-BD relationship.

The AHTO hypothesis describes a tradeoff between environmental heterogeneity and population sizes, which increases local species extinctions at high heterogeneity levels (Bar-Massada, 2015; Allouche *et al.*, 2012). The authors used both a spatially explicit meta-community model and empirical evidence from breeding bird datasets to quantify the roles of niche width and immigration rates on the type of the richness–heterogeneity relationship observed at the landscape scale. They found that patterns of species richness, species abundance, and extinction rates are consistent with the predictions of the area–heterogeneity tradeoff hypothesis and that empirical data better fit the unimodal pattern predicted by the AHTO than the linear and positive pattern predicted by classic niche theory. Like the Laanisto et al. model, these studies evidenced that both positive and negative EH-BD relationships can occur in communities but the AHTO extended the pattern to meta-communities (i.e., not only within habitat patches but across them). The results indicated that immigration rates between patches (i.e., meta-communities) and species' niche width interacted to determine the type of EH-BD relationship. Nonlinear relationships dominated in meta-communities comprised of species with wide niches but low inter-patch immigration rates, whereas positive EH-BD relationships dominated in communities comprised mainly of species with narrow niches and high immigration rates (Fig.1.2). These findings again are intuitive in that we would expect dispersal ability to be a primary determinant to how species respond to EH, specifically that species with high dispersal abilities are better adapted to cope with increasing EH and move across patchy landscapes to exploit resources. However, on the surface the results are somewhat contradictory to that of Laanisto et al. in the effect of niche breadth or foraging type (i.e., specialists with narrow niche breath *vs.* generalists with wide niche breadth). Here,

species with narrow niche breadth responded positively to metacommunity and landscape patchiness (i.e., EH), while species with wider breadths showed a more strongly unimodal-hump-shaped response (Fig.1.2). Regardless, all species types showed saturation and negative or neutral responses at high EH values (Fig.1.2. It was the inter-patch immigration, which was now allowed to act over long distances, that prevented local extinctions and drove the positive responses at low to intermediate EH levels.

What the Bar-Massada and Allouche studies concluded was that meta-communities comprised of generalist species are likely to exhibit unimodal richness-heterogeneity relationships as long as low immigration rates prevent rescue effects and the patches are small. The EH-BD relationship at the landscape scale is dictated by species' niche widths and inter-patch immigration rates; immigration rates, in turn, depend on the interaction between species dispersal capabilities and habitat connectivity. I argue the MF and AHTO hypotheses, both, highlight the roles of species traits and landscape structure in predicting the EH-BD relationship. Moreover, the two hypotheses are not at odds, they simply present a different lens by applying their models to slightly different scales and configurations but show that the same or similar EH-BD pattern (i.e., a generalized unimodal one) operates across these scales, albeit perhaps driven by slightly different mechanisms. At landscape and metacommunity scales, species generally appear to respond positively to increasing EH. Specifically, with adequate immigration levels over distances, species of both narrow and wide niche breaths avoid local extinctions; species with narrow breadths, however, do better as different species adapted to the new habitat patches can fill them and thus species richness increases. However, both species types saturate at some inflection point along the EH gradient and even respond negatively. What these two hypotheses and their studies show is that where this inflection point is depends on the spatial scale, dispersal abilities,

immigration rates and niche breadth. At small habitat scales, microfragmentation may operate and, while at the landscape scale specialists may have a strong positive response to EH, without far reaching dispersal abilities or adequate immigration rates the microfragmentation effects may quickly drive negative responses of diversity to EH. Generalists, or species with wide niche breadths, may respond less strongly to microfragmentation, but at large landscape levels they require high immigration rates to cope with increasing patchiness across the landscape. In all cases, I would argue that these studies support a generalized unimodal EH-BD relationship that may operate at multiple scales and wherein the inflection point on a hump-shaped EH-BD curve depends on the spatial scale and landscape context – that being the source of EH and its configuration or patterning (e.g., natural sources of EH like resource patchiness driven by underlying geological and biological factors *vs.* anthropogenic fragmentation).

These mathematical models hint at some potential mechanisms driving EH-BD relationships and, thereby, explain how neutral or negative relationships may arise. However, an empirically-based framework that is supported by the observational data across multiple spatial scales and ecosystems is still missing. Such a framework would be valuable in unifying these hypothesis and support a hump-shaped EH-BD relationship with observational evidence. The current state of knowledge does not adequately answer the questions of: how should EH be defined and measured, what accounts for negative EH-BD relationships and is there a generalized EH-BD relationship that applies to multiple ecosystems? In an effort to help answer these questions, *Chapter 1* presents a new perspective on the EH-BD relationship; one that could reconcile the array of relationships observed to date.

0.0.4 From the bottom - up: Does species biodiversity modulates the heterogeneity of seasonal growth patterns?

In *Chapter 2*, I narrow the lens on the biodiversity - EF and EH relationships, focussing on forest phenology – the seasonal growth patterns of forest ecosystems. I ask whether the species diversity of forest stands mediates stand-level phenology. Thus, wherein the previous chapter I examined whether increasing or decreasing EH has a predictable effect on the species diversity of the affected biological communities; in this chapter, I ask the reciprocal question of whether increasing or decreasing species diversity (trees in this case) has measurable effects on the forest community's (i.e., stand) seasonal growth and the system processes forest phenology drives.

Phenology is the study of the seasonality of plant growth. In forest ecosystems trees are ecosystem engineers, hence any change in their growth or structure profoundly impacts system processes (e.g., biogeochemical cycles, water and energy exchange), including the light environment in a top-down, vertically structured manner. Particularly in temperate forests which are defined by their strong seasonality, the spatial and temporal arrangement of tree leaves throughout the growing season is the cardinal strategy for light interception (Ishii et Asano, 2010) and the primary structure determining the light environment below.

Forest phenology has been extensively studied as a critical element of global change research, yet phenology does not only represent a response trait (i.e., an individual trait driven by abiotic factors such as climate), but also a functional trait (i.e., a trait that impacts fitness indirectly) (Jackson *et al.*, 2001). The seasonal timing of vegetation growth is not only sensitive to climate, but also has direct or indirect controls on light attenuation, productivity, fluxes of water, energy and carbon, and reproductive success (Kudo *et al.*, 2008; Ishii et Asano, 2010; Richardson *et al.*,

2013a). However, it remains unclear how species-specific phenologies (e.g., species identity) relate and generate the local community phenology via community composition and species diversity. If the timing of seasonal plant growth is not simply a response to exogenous environmental cues, but also depends on community composition, an unexplored yet important question is then raised: what is the role of species diversity in determining the seasonal growth patterns of plant communities ?

Measuring forest phenology

Leaf development will be the key variable of interest and how I quantify and track forest phenology. I measure the leaf development of forest stands using *in-situ* time-lapse digital imagery which provides fine-scale spatial and temporal estimates of leaf development not achieved by the more traditional methods of remote sensing. Phenological research requires long-term (years to decades) observations of the vegetation, at varying scales of space, time and species assemblages. To date, there's been a heavy reliance on obtaining such data from remote-sensing instruments mounted on spacecraft or manned aircraft. However, the spatial and temporal resolutions of satellite and even aerial imaging are often relatively coarse and not suited to local-scale investigations. Other methodologies, and particularly those used in grassland or forest understory communities, have traditionally included visual assessment, point sampling, or *in-situ* transects. The high labour inputs and logistical issues of extensive field sampling are self apparent, but they also carry limitations related to observation errors (consistency, continuity and objectivity). The coincidental development of fast, efficient, objective and informative image processing and automated metrics with the availability of low-cost conventional digital image sensors offer some tools to address these gaps and sampling challenges.

Close-range image applications in ecology

Close-range (*syn.* ground-based or near-surface) digital cameras and image sensors can achieve fine-scale (e.g., "plot-level") representations of vegetation and its structure, while their low costs allow us to deploy them at fairly wide extents. The challenge of, likewise, achieving high temporal resolutions can then be addressed by the automation of image capturing at high frequencies (repeat or time-lapse digital imaging) with the addition of intervalometers or packaged time-lapse digital cameras. Indeed, conventional digital cameras taking repeated images of the landscape at high frequencies (several images per day) over several months or even years is increasingly garnering attention for phenological research (Abdulkadir *et al.*, 2012; Abrams, 1995; Balvanera et Aguirre, 2006; Bakker *et al.*, 2000; Graham *et al.*, 2010). Typically, such applications of digital cameras are characterized by a small network of cameras mounted on instrumentation towers or look out points, thus capturing horizontal or oblique views of vegetation canopies (Bennett *et al.*, 2000; Sonnentag *et al.*, 2012; Richardson *et al.*, 2010). Images obtained from such installations are generally standard digital photographs of the visible part of the electromagnetic spectrum (combined brightness levels of the Red-Blue-Green color channels). Sensors or modified digital cameras capable of capturing multispectral data, such as the near-infrared (NIR) channels, are very useful for studying vegetation but remain rare in most applications of conventional digital cameras or ground-based imaging. Having said that, the cost and size of such sensors continues to decline and they are more and more being deployed to survey vegetation and measure their dynamics at close ranges. In the study presented in Chapter 2, I will deploy low-cost time-lapse digital cameras in a network of forest plots in order to capture daily photographs of stand structure and development.

Once acquired, a key feature of digital images is that they can be mathematically

manipulated in numerous ways to detect and enhance patterns, classify elements and thereby estimate ecological features or "indicators" (Proulx et Parrott, 2009). Often measuring and recording analogous features in the field manually takes significant labour, time or even expensive specialized equipment (e.g., hemispherical light meters). Comprised of three bands (red, green, and blue – RGB), RGB imagery has been shown to be an inexpensive and effective way to estimate plant cover and biomass (Luscier *et al.*, 2006; Lukina *et al.*, 1999), record the timing of phenological events such as the green-up (Liang *et al.*, 2012; Morisette *et al.*, 2009) and plant senescence (Adamsen *et al.*, 1999), and to estimate leaf area (Przeszlowska *et al.*, 2006). We can consider that forest light regimes, vegetation structure (e.g., leaf morphology, leaf angle, leaf surface) and space-filling (i.e., the spatial distribution of biomass) in forest overstorey and understorey layers are all important determinants of ecological processes at various scales (Trichon *et al.*, 1998; Endler, 1993; Valladares *et al.*, 2002). Thus, feature extraction from digital images has a high potential for estimating and quantifying a large number of ecosystem processes, structures and dynamics since it is a representation of light, scene structure and geometry. For instance, Proulx and Parrott (2009) demonstrated that heterogeneity in forest light, derived from close-range digital images and measured using an information theoretic metric (mean information gain), can serve as an indicator of the structural complexity of the vegetation.

I will focus here on the application of vegetation indices derived from time series of ground-level digital cameras and the application of those indices to track the leaf development of forest plant communities. The use of vegetation indices in remote and near-surface sensing of both natural vegetation stands and crops is not new, as cited above, but the field is young and still developing. In particular there is an open challenge to derive estimates of foliage presence and condition from simple RGB information that are comparable to those achieved by multispectral or even

chemical measurements. For example, studies for crop and weed detection have been performed using different spectral bands and combinations for vegetative indices (Homer *et al.*, 2015; Xian *et al.*, 2011; Yang *et al.*, 2003; Wenhua Mao *et al.*, 2003; Wang *et al.*, 2001; El-Faki *et al.*, 2000; Woebbecke *et al.*, 1995). Some such metrics use only the red, green and blue spectral bands. Several forest ecosystem studies have now followed suit and used a "greenness" index computed on daily time series to track relative changes in vegetation cover (Ahmad *et al.*, 2007; Crimmins et Crimmins, 2008; Sonnentag *et al.*, 2012; Richardson *et al.*, 2009a)

A limitation with using RGB brightness levels (i.e., digital photographs) is that they are highly influenced by the scene illumination. However, with the current technology, scene illumination can be fairly well standardized by a combination of the camera's light sensor and autoexposure to standardize illumination at capture time and histogram equalization or other post-processing methods to standardize the image brightness across images post-capture. Moreover, variation in the RGB brightness levels can be suppressed by a nonlinear transform of RGB digital numbers to rgb chromatic coordinates (Gillespie *et al.*, 1987; Woebbecke *et al.*, 1995), defined as:

$$r_{cc} = \frac{R}{(R+G+B)} \qquad g_{cc} = \frac{G}{(R+G+B)} \qquad b_{cc} = \frac{B}{(R+G+B)}$$

This transformation of the color brightness channels to chromatic coordinates is the basis for a number of color-based vegetation indices that have been developed. The objective function of these indices has mainly been to distinguish the green plants from other scene elements (soil/residue, background and other non-foliage features) in images and, subsequently, to improve on that distinction. Perhaps the most widely applied indices to describe canopy greenness are the green chromatic

coordinate (g_{cc}) as seen above or the excess green (ExG) defined as:

$$ExG = 2G - (R + G + B)$$

The output of vegetation indices such as the excess green and normalized difference indices are typically further transformed using an Otsu threshold value (Otsu, 1975) in order to convert the near-binary index to a fully binary index. As such the result is a binary "green mask" which simply differentiates green pixels (take on a value of 1) from non-green pixels (take on a value of 0) in the image.

The excess green index, in particular, has been shown to be somewhat advantageous over the other color indices because it enhances the signal of green material over that of all else, thereby more accurately distinguishing green plants from the background. Moreover, and similar to the rgb chromatic coordinates, excess green can minimize the effects of variation in scene illumination between images. In forest ecosystems which display a strong seasonal signal in leaf development, increasing and decreasing canopy greenness might be indicative of the increasing and decreasing amount of photosynthetically active green leaves and their condition during spring and autumn. Thus, and in addition to simply creating a "binary green mask", daily values of canopy greenness as described by a color index such as excess green have been linked to seasonal changes in net ecosystem carbon dioxide exchange, canopy photosynthesis, and other important biophysical measures (Ahrends *et al.*, 2008; Richardson *et al.*, 2013a, 2009a).

I will use a relatively novel vegetation index developed by Meyer et Neto (2008) which has rarely been applied in the study of natural vegetation phenology; the

excess green - excess red (ExG - ExR):

$$ExG = 2G - (R + G + B) \qquad ExR = 2R - (R + G + B) \tag{1}$$

$$ExG - ExR \tag{2}$$

This index was initially developed within the field of crop science in order to improve on indices distinguishing between weeds and the soil background in images. It was shown to be a substantial improvement over the commonly used excess green and the normalized difference indices (Meyer et Neto, 2008). In some scene contexts (e.g., distinguishing green plant parts from wheat straw backgrounds), the ExG - ExR index was up to 55% more accurate than the excess green and normalized difference indices with the Otsu transformation. The ExG - ExR index has the additional slight advantage in that it has a fixed, built-in zero threshold, and therefore does not need an Otsu or any user selected threshold value in order to produce the binary green mask result.

Thus, this fixed zero threshold, unsupervised vegetation index of ExG - ExR, represents a promising new method for the automated measurement and tracking of plant phenology using commercial color digital cameras. Its improved ability to separate plants and backgrounds for image sets should apply particularily well to the complex structure of forest stand scenes – green leaves amongst the complex and cluttered arrangement of brown tree trunks and sky, along with green understory vegetation distributed amongst brown litter and organic material, deadwood and other non-green substrates.

Limitations of single feature, unsupervised vegetation indices from ground-based digital images

Despite these promising applications of vegetation indices computed on time-series of ground-based or close-range color images, several important limitations or

challenges should be noted. While camera autoexposure and the ExG - ExR index is able to minimize the effects of changes in scene illumination, it can not eliminate, or standardize them between image time series, completely. Weather and sky conditions (e.g., clear full sun sky vs. full cloud cover) will still cause noticeable variations between image brightness and color channel values; particularly in very low cost cameras that struggle to produce properly exposed images under low-light conditions. These factors will undoubtedly produce some noise in the time series data of index values. However, since my objective is to track the seasonal leaf development of forest stands, the absolute value of the greenness time series' is not critical. It is the relative values and trend in the greenness signal that is of primary importance here and as such, any illumination-caused noise between sequential values can be controlled for in large part by fitting a smoothing function to the time series data as will be detailed in Chapter 2.

Perhaps an often overlooked technical aspect of these methodologies is the digital camera choice. If we consider the large variety of cameras, sensors and image file formats, understanding the role of these hardware-based parameters fundamental for interpreting the resulting signal in a phenological framework (Sonnentag *et al.*, 2012). The questions of whether differences in imaging sensor technologies are relevant for phenological research and what the optimal data format is for the application should be considered in this emerging field of study just as sensor type, quality, wavelength sensitivity properties and resolution are of key importance to studies deriving geo- or bio-physical information from satellite imagery. While they are continuing to be benchmarked and qualified, in a comparison of different digital cameras, Sonnentag *et al.* (2012) has noted that camera and image file format choice might be of secondary importance for phenological research. They found that autumn patterns of changes in *gcc* and *ExG* from images in common JPEG image file format were in good agreement. Moreover, as will be detailed further in

Chapter 2, my study employs only one type of digital camera across all field sites and plots, thus variations between sensor detection parameters should be minimized. Nevertheless, it has been noted that there remains a general lack of reporting of vegetation index accuracy in the studies employing these methodologies (Meyer et Neto, 2008). A future challenge for the inter-comparison and longterm reliability of digital camera-derived phenological data will be to quantify these differences between the camera and file format types, generate transformation functions and further validation of their biological and ecological interpretation.

0.0.5 Applications of computer to measure complex ecological properties and patterns – moving beyond single-feature metrics.

In *Chapter 3*, I investigate and develop new automated tools for rapidly quantifying ecosystem features and visual patterns. The data derived from such metrics, or in some cases we may term them "ecological indicators", may enable us to further study and understand biodiversity–EF relationships and, in turn, improve the methods we use to manage and conserve ecosystem services. The methods offer finer-scale spatial and temporal resolutions over current datasets, while achieving high rates of throughput, cost and time efficiently.

This research objective is initiated in *Chapter 2* in which I apply time-lapse digital photography and derive unsupervised, single-feature metrics from them (e.g., greenness indices) to quantify the seasonal growth patterns of forest stands. In *Chapter 3* I move beyond these single-feature-based image metrics and look to the rapidly advancing field of computer vision to apply more complex, supervised learning models. These methods use multiple image features, either computed as bags-of-features or generated by artificial neural networks, to first segment environmental real-world features represented in an image (e.g., trees) and, second, derive and quantify useful measures of those features (e.g., percent tree cover).

As the accessibility and capabilities of digital imaging continue to rapidly grow, researchers have begun to explore the merits of digital photography in various ecological applications (Graham *et al.*, 2010; Granados *et al.*, 2013; Mellin *et al.*, 2012; Proulx *et al.*, 2014; Crimmins et Crimmins, 2008; Olea et Mateo-Tomas, 2013; Rousselet *et al.*, 2013). A key feature of digital photographs is that they can be mathematically manipulated in numerous ways to detect and enhance patterns and classify objects. What's more, analytical and mathematical advances have been complimented with advances in computing power and data storage. Thus, if images and image-based metrics can be shown to represent ecosystem properties that have traditionally been measured and collected with difficulty (i.e., involving large amounts of resources, man power and time), their value becomes obvious. What's more, mathematical derivations of environmental properties, represented in images, may also be able to capture higher-level ecosystem features that are otherwise very difficult to quantify and describe (e.g., heterogeneity of light, structural diversity or heterogeneity, leaf angle). Computational power and data technologies also enables researchers to collect, aggregate and analyze high volumes of image data captured at very high levels of temporal and spatial resolution; i.e., high-throughput at fine-grain resolutions with the potential to be applied at large extents.

Beyond single-feature image metrics, computer vision scientists are teaching computers to see and under stand the world at astounding rates of success. However few disciplines outside of the strict artificial intelligence fields (e.g., robotics, medical devices, driverless cars, web analytics) have utilized these advancements. Yet, if computer vision algorithms can learn to detect features of an environmental scene, it stands that those algorithms can be used to objectively quantify real-world features and their spatial distribution within a landscape for a multitude of applications. Higher-level ecosystem properties (e.g., forest stand complexity) have

traditionally been quantified through many manual measurements and labour intensive multi-step analyses. A powerful advantage of machine learning methods to quantify environmental patterns is the ability to identify complex and non-linear patterns that may not be observable otherwise or only intuitively so.

The specific objective of the third research chapter will be to apply computer vision tools to begin to develop automated assessment tools to measure, map and track environmental features of ecological importance. Specifically, I will apply computer vision algorithms that have become well-accepted within their own field (Hoiem *et al.*, 2005; Naik *et al.*, 2014a) to map and measure trees. To do so in an urban landscape context, I will also utilize the open-source image data of city streetscapes that is now abundant – Google StreetView Images (Google Inc., 2014)

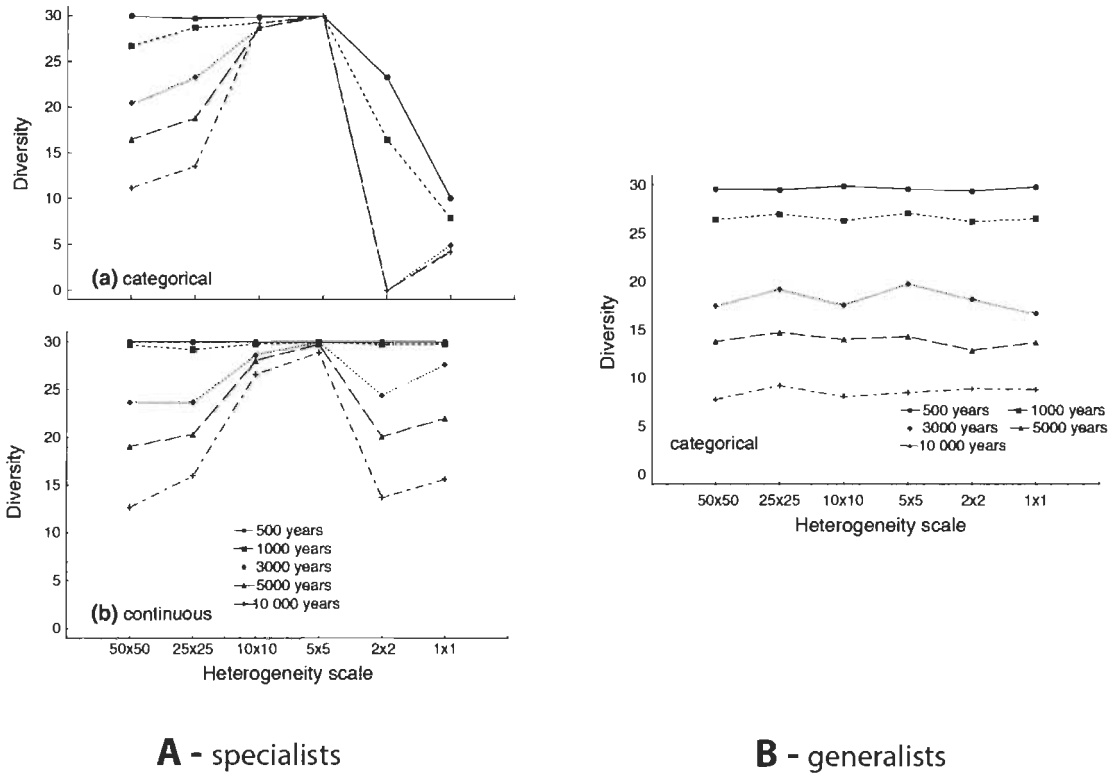

Figure 0.1: Figures 2 & 3 taken from Laanisto et al. (2013) – *Microfragmentation concept explains non-positive environmental heterogeneity-diversity relationships.* The heterogeneity scale corresponds to patch sizes in model landscapes (low heterogeneity at left and high heterogeneity at right); diversity is measured as Simpson's Reciprocal index. Panel A shows the results of a simulation model wherein habitat patch size was varied, but only specialist species populations were included. Results of a categorical and b continuous framework are also shown in Panel A but only a categorized framework is shown in Panel B. Lines show results for varying time frames.

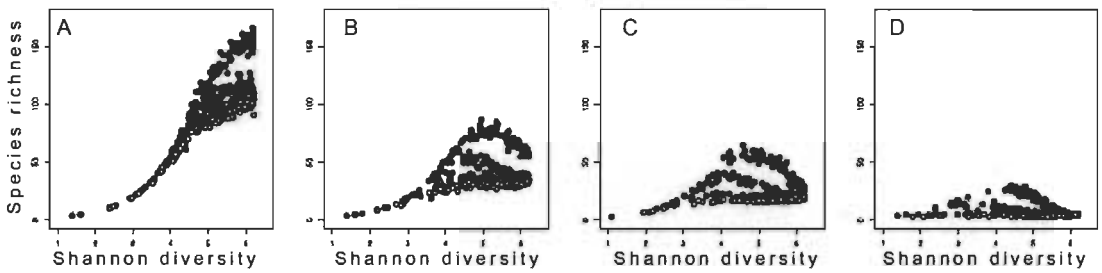

Figure 0.2: Figure 2 taken from Bar-Massada (2015) - *Immigration rates and species niche characteristics affect the relationship between species richness and habitat heterogeneity in modelled meta-communities.* (A–D) correspond with different species niche widths (A–very narrow, B–narrow, C–intermediate, and D–wide). Curves denote inter-patch immigration rates, with circle colors depicting the value of the z parameter (0.2–black, 0.1–blue, 0.05–green, and 0.025–white), reflecting increasing levels of inter-patch immigration rates.

CHAPITRE I

DISENTANGLING THE ENVIRONMENTAL HETEROGENEITY - SPECIES DIVERSITY RELATIONSHIP ALONG A GRADIENT OF HUMAN FOOTPRINT

1.1 Abstract

Des décennies de recherche ont tenté de définir une relation générale entre l'hétérogénéité environnementale et la biodiversité en conservant comme référence l'hypothèse traditionnelle MacArthurian basé sur les niches. Selon cette hypothèse, une hétérogénéité croissante favoriserait la biodiversité en diversifiant les ressources. Les études ont toutefois fréquemment rapporté des relations négatives ou non significatives. Pour la plupart d'entre elles, l'hétérogénéité environnementale a été définie le long d'un gradient de stochasticité croissante, vers un désordre total. L'élaboration d'un nouveau cadre conceptuel permettrait de concilier ces observations divergentes. Suite à une revue approfondie de la littérature, nous testons le concept selon lequel, la relations entre l'hétérogénéité environnementale et la biodiversité dépend de l'empreinte humaine auquel l'écosystème est soumis (l'anthorpocline). Les résultats révèlent que les écosystèmes fortement modifiés sont caractérisés par une dominance de relations positives entre l'hétérogénéité environnementale et la biodiversité, les écosystèmes semi-naturels par une dominance de relations négatives, alors que les écosystèmes naturels montrent des réponses mixtes. Ce cadre conceptuel apporte une perspective nouvelle sur les écosystèmes naturels. Ils ne sont ni caractérisés par des niveaux maximaux, ni pas des niveaux minimaux d'hétérogénéité, mais par des niveaux intermédiaires.

~

Decades of study have attempted to define a generalized environmental heterogeneity - biodiversity relationship, with the traditional MacArthurian niche-based hypothesis remaining as the dominant reference point ; i.e., increasing heterogeneity promotes biodiversity by increasing resource opportunities. However, studies have frequently reported negative or non-significant relationships. In a vast

majority of them, environmental heterogeneity was defined along a gradient of increasing randomness, towards complete disorder. A new conceptual framework could help to reconcile the array of observed relationships. Using an extensive literature review, we test a conceptual framework proposing that the direction of environmental heterogeneity - biodiversity relationships is contingent on the level of human footprint to which an ecosystem is subjected (the anthropocline). The results reveal that highly-modified and semi-natural ecosystems are characterized by a dominance of positive and negative environmental heterogeneity - biodiversity relationships, respectively, whereas natural ecosystems show mixed responses. Out of this novel framework arises the revised perspective that natural ecosystems are characterized, not by maximal or minimal, but by intermediate levels of environmental heterogeneity.

keywords: environmental heterogeneity, biodiversity, complexity, habitat heterogeneity hypothesis, habitat heterogeneity, niche theory, human footprint, fragmentation, conservation management.

abbreviations: EH, environmental heterogeneity ; EH-BD, environmental heterogeneity - biodiversity ; RD, relationship direction.

1.2 Introduction

Environmental heterogeneity (EH) is the spatial or temporal variation of a given resource, structure or biota in a given area. Its relationship with biological diversity has been well studied, with numerous attempts by ecologists to quantify EH and explicate its role in begetting species richness, yet it remains a contentious subject. The "environmental] heterogeneity hypothesis" (MacArthur et Wilson, 1967; Simpson, 1949), a cornerstone of ecology, generally implies that heterogeneous environmental conditions provide more niches and diverse ways of exploiting the resources, thus increasing species diversity (Tews *et al.*, 2004). Accordingly, the general expectation is that environmental heterogeneity–biodiversity (EH–BD) relationships should be linear and positive. Though positive relationships supporting the EH-hypothesis are well documented (Kumar *et al.*, 2009; Palmer, 1994; Levin *et al.*, 2010), non-significant and negative relationships are also prevalent in the literature.

If more EH should beget more species through mechanisms such as niche differentiation, two questions become evident:

1. what accounts for negative or non-significant EH-BD relationships and ;
2. does increasing the spatial variation of ecosystem components (in particular via human modifications) always represent a set of suitable conditions for biodiversity to be maintained or at some point along the EH gradient is biodiversity lost rather than gained ?

Answers to these conundrums have been sparse in the literature. Recently, two meta-analyses suggested that EH-BD relationships are predominantly negative when studied at smaller spatial scales (Tamme *et al.*, 2010), or when considering animal taxa within landscapes of low- to mid-urbanization level (McKinney, 2008). Moreover, Allouche *et al.* performed an analysis of breeding bird data corrected

for sampling area to support their prediction that relationships are negative for species with narrow niches, but that EH has a general unimodal effect on species richness.

1.2.1 Revisiting environmental heterogeneity

Perhaps the first pressing problem when it comes to understanding EH-BD relationships is how to define and measure heterogeneity. Traditionally, EH has been measured on an unbounded gradient ranging from low to high spatial or temporal variation, with the observed values ranging somewhere in between these extremes (Fig.1.1). For instance, most measures of environmental variation for a given area (e.g., coefficients of variation, standard deviation, landscape texture, edginess, interspersion metrics) adhere to this definition. However, a limitation arises in that the results of any such attempt to quantify the EH-BD relationship lack a reference point on the heterogeneity gradient, thus preventing cross-study comparisons.

Since the EH gradient not only exists within ecosystems, but spans across all ecosystems and levels of the human footprint, the second pressing problem is how to organize the EH gradient between ecosystems. Proulx and Parrott (Proulx et Parrott, 2009; Parrott, 2010) proposed that natural ecosystems (i.e., ecosystems subject to no, or little, human modification) should be considered neither uniformly organized nor completely disordered, but rather as "complex" systems. Accordingly, natural ecosystems should fit between the two heterogeneity extremes, at some intermediate level of EH (Fig.1.1). Indeed, environmental conditions within natural ecosystems typically reveal some intermediate level of spatial or temporal patterning (i.e., are neither uniform or disordered) at one or several scales of observation (Legendre et Legendre, 1998). For example, in a recent study Seiferling et al. (Seiferling *et al.*, 2012) quantified the spatio-temporal landscape heteroge-

neity of vegetation cover both inside and outside 114 large protected areas around the world. While the pattern of vegetation cover was consistently more heterogeneous outside protected areas, the results revealed that the heterogeneity inside their borders averaged around c.a. 0.5 on a scale bounded between 0 (complete uniformity) and 1 (complete disorder). In other words, the patterns of natural vegetation cover within protected natural areas presented a great deal of EH, well above uniformity, yet well below complete disorder.

1.2.2 A new conceptual framework for the EH-BD relationship

In acknowledging that natural ecosystems retain some intermediate levels of EH, we may consider what happens to such an ecosystem if the amount of human modification is increased. Initially, novel environmental conditions are created at the expense of pre-existing natural ones (i.e., a human expansion phase ; Fig.1.1). The conversion of natural lands to small farms, low levels of urbanization, road development, or the dissemination of diffuse acoustic and chemical stressors, along with the alteration of food-web dynamics through resource harvesting would all constitute examples of this modification. The net result of this human expansion will, generally, be an increase of EH. During this phase, species diversity in several taxonomic groups may decline because species with larger home ranges or specialized resource requirements may be extirpated and, therefore, negative EH-BD relationships dominate. Even in situations where multi-species coexistence in patchy habitats appears to persist, species may exhibit extinction debts wherein local extinction is just a matter of time (Tilman et May, 1994; Vellend *et al.*, 2006).

As the human footprint further increases from early phases of semi-natural states, natural habitats dwindle in size and frequency, pushing the ecosystem into a phase of human intensification (i.e., human modification of ecosystems from semi-

natural to highly-modified states; Fig.1.1). Farms become farmlands and towns are replaced by high levels of urbanization, leaving behind only remnants of the original ecosystems. During this phase, biodiversity may further decline because only a few species are adapted to live in such homogenized habitats or are able to sustain the environmental stressors for long periods. Additionally, coexistence among competitor species may no longer be possible given the lack of EH, driving further losses of biodiversity through competitive exclusion (Amarasekare, 2003).

Natural ecosystems can also be converted directly to intensively modified states by processes like clear-cutting forest for agriculture or urban development (i.e., rapid homogenization; Fig.1.1). State shift theory, for example, would categorize such rapid homogenization as a "sledgehammer" effect (Barnosky *et al.*, 2012). Nonetheless, as the pattern of resources, biota and structures in ecosystems becomes more uniform, eventually biodiversity collapses. Examples of such highly-modified ecosystems include intensive agricultural lands, or very densely populated areas with extensive paved and building cover. The EH-BD relationships in such homogenized ecosystems are now positive since an addition of EH increases habitat or resource opportunities, which should promote niche partitioning and species coexistence (Fig.1.1).

This succession of ecosystem modifications by human activities describes a gradient of resulting EH that we may term the "anthropocline". The framework presented here begins with the anthropocline forming the x-axis of a generalized EH-BD relationship (Fig.1.1), wherein the three ecosystem categories described before are positioned along a gradient of increasing EH: highly-modified/uniform ecosystems, strictly-natural/intermediate ecosystems, and semi-natural/disordered ecosystems (Table 1.1). Highly-Modified ecosystems are characterized by environmental conditions that have been intensively modified or regulated by human activity (e.g., agriculture-dominated ecosystems), and characterized by few, if any,

small remnant patches of natural habitat. Strictly-Natural ecosystems are characterized by environmental conditions considered to exist in a most highly natural state, as found in areas where human activity is limited in intensity and extent. Semi-Natural ecosystems are characterized by environmental conditions that are, on average, subjected to relatively low to moderate levels of human management and resource extraction. Semi-natural systems may also be defined as containing patches of both highly-modified and strictly-natural ecosystems.

In addition to the anthropocline, spatial scale can influence how the EH is measured by researchers or perceived by taxa (Levin, 1992; Palmer et White, 1994; Stohlgren *et al.*, 1997; Tews *et al.*, 2004). Within its defined ecosystem context, each study represents a local gradient of EH that is nested within a broader gradient forming the anthropocline (Fig.1.1). Hence, if we assume EH is measured at scales that the taxa experience and that the observational grain and extent of each study are nested within the anthropocline gradient, then there should be no interaction between spatial scale and ecosystem category. In other words, over a certain range of scales positive or negative EH-BD relationships should not be more or less common within a given ecosystem category. Certainly, exceptions will exist to the predictions made by the anthropocline framework and many other factors may be involved (e.g., the specific taxonomic groups, the kind of EH variable measured). Although this study will investigate the larger role of human footprint context on EH-BD relationships, we are not implying it as the only factor influencing these associations.

The objective of this paper is (1) to present a conceptual framework of the EH-BD relationship that is contingent on the anthropocline and (2) to assess our conceptual framework with data extracted from the literature. In our data synthesis, EH represents any measure of "variation" in the vertical, horizontal, or temporal distribution of environmental conditions (i.e., abiotic or biotic variables) in

terrestrial or wetland ecosystems. The term BD refers to any measures of species relative abundance or richness, and does not explicitly include functional or genetic diversity per se. Specifically, we suggest that every study examining an EH-BD relationship can be accurately characterized by one of three ecosystem categories and, thus, also be positioned on the anthropocline (Fig.1.1). We expect to find that highly-modified ecosystems are typified by positive EH-BD relationships and semi-natural ecosystems are characterized by negative relationships, whereas natural ecosystems show mixed EH-BD responses including negative and positive correlations. That is to say, we will infer a generalized EH-BD relationship between ecosystems from the joint responses of individual studies (Fig.1.1).

1.3 Materials and Methods

1.3.1 Literature review

We performed a literature review of all peer-reviewed scientific papers to date, which empirically tested for BD-EH relationships (Appendix B). In our literature review we screened the ISI Web of Science, Scopus and Google Scholar for publications that correlated some measure of EH, or synonyms, with some measure of species diversity (animal or plant) or synonyms (see Appendix A, Table A1). Multivariate models that involved at least one input variable related to EH were included. We consider our literature search to be exhaustive at the date it was performed because we began the search using focused keyword terms (e.g., "spatial heterogeneity AND biodiversity relationship") and, subsequently, expanded it to very broad, encompassing terms (e.g., "heterogeneity OR variability AND diversity OR richness") until we were confident that no new studies were identified. To our knowledge, this is the first systematic literature survey on the EH-BD relationship that includes results across, both, taxonomic level and spatial scale. This literature search yielded 433 peer-reviewed scientific articles.

A data synthesis was then performed on the 433 studies, wherein a record was created for each EH-BD relationship. Thus, one study could yield more than one record if it reported more than one unique measure of EH. Any article that did not report a statistically tested relationship result between EH and diversity (i.e., like an R-value, r^2-value, partial r^2-value, F-statistic, t-statistic or Z-score) was eliminated from the database. Likewise, if the EH metric used was not a true measure of spatial or temporal heterogeneity, the study was eliminated. For an EH metric to be considered, each data point must describe the spatial or temporal variation of some environmental variables within a broader, and defined, sample area. We identified numerous studies that used the term heterogeneity in their title, or to describe an explanatory variable, and yet did not measure any true pattern of EH. Often such studies measured an environmental variable (e.g., primary productivity, elevation, sea depth, soil nutrients) across space, whereas each data point contained no information of spatial or temporal variation.

For each BD-EH relationship reported in a study, we then identified a set of explanatory variables hypothesized to have an effect on the direction of EH-BD relationships. If these variables could not be identified in a study, the study was eliminated from the dataset. 830 unique records (i.e., lines containing BD-EH relationships) from 114 studies formed the final dataset (see Appendix A, Table A1).

Variable selection and categorical grouping The relationship direction (RD) for a record denotes the overall correlational direction (positive, negative or non-significant) of the relationship between EH and BD ; that is, it answers the question of how did diversity respond to increasing EH in that particular ecosystem ? If a study reported no significant association between an EH variable and diversity, the RD was always categorized as non-significant. To each study, we assigned an ecosystem category (highly-modified, strictly-natural, semi-natural) according

to the description of the study's spatial extent by their author(s) and its strict correspondence with one of the ecosystem categories defined in Table 1.1. To attest the robustness of our approach, we asked six academic fellows to assign an ecosystem category to ten studies chosen randomly from our meta-analysis on the basis of the definitions in Table 1.1. Overall, 98% of the respondent's classifications matched ours. In the only mismatched case, the respondent matched one ecosystem to two of the categories.

We acknowledge that several factors other than the human footprint on ecosystems may influence the direction of EH-BD relationships. Accordingly, we identified and extracted four other explanatory variables from each study. Firstly, the spatial scale of a sampling design can influence how the environmental conditions, and thus EH, are measured by researchers or, alternatively, perceived by taxa (Tews *et al.*, 2004; Stohlgren *et al.*, 1997; Palmer, 1994). Complicating the topic of spatial scale however, is the differing uses and definitions of the term scale among authors. Our interpretation is that spatial scale can be decomposed into three components: spatial extent (i.e. the whole area under study), spatial grain (i.e., the dimension of the sampling units) and sample size (i.e., the number of sampling units or sampling intensity). We extracted the spatial extent, spatial grain and sample size from each study. Due to reporting inconsistencies across studies on the observational extent and grain values, it was not possible to express spatial scale in quantitative terms for all records. For these three continuous variables, the statistical analysis was conducted on a subset of the database that contained only records complete with quantitative spatial extent, grain and sample size values. All records in the database contained sample size values, but 115 out of 870 records did not explicitly contain spatial grain values and 29 records did not contain spatial extent values.

Secondly, EH-BD relationships may differ across taxonomic groups as organisms exploiting different resources may respond differently to EH (Palmer, 1994; McKin-

ney, 2008). Accordingly, for each study, we recorded whether the reported measure of species diversity (i.e., the study's response variable) pertained to plant or animal taxonomic groups. Lastly, the type of statistical analysis used could potentially bias this dataset if one of the model types consistently identifies significant EH-BD relationships more than others. We therefore identified whether the statistical model type included one (univariate) or several EH variables (multivariate) as the third control variable in our analysis. It must be noted that comparatively few studies have measured temporal variation of an environmental variable and related it to species diversity. In our resulting database, only 9 out of the 114 studies included a temporal component in EH. As such, the analysis and discussion are primarily in the context of spatial EH.

1.3.2 Statistical analyses

To test for an effect of spatial scale on the EH-BD relationships we entered the three components of scale (i.e., extent, grain and sample size) as continuous predictor variables in a recursive-partitioning model for classifying the direction of EH-BD relationships. We did not include studies for which we were not able to clearly identify both the spatial grain and extent and, as such, 140 of 870 records were removed for this part of the analysis. We built the recursive partitioning model with the "rpart" R package (R Core Team, 2013).

To test our conceptual anthropocline framework we performed a two-step procedure. The first step involved a graphical output and interpretation and the second involved a Chi-square correspondence analysis with constrained permutations to rigorously test the statistical significance of the graphical interpretation, while accounting for a study effect. In step one, the relative frequency of each EH-BD relationship direction (i.e., positive, negative or non-significant) across each level of the explanatory variable (i.e., human footprint categories and for all other

explanatory variables) was tabulated and subsequently plotted. In step two, a Chi-square test with constrained random permutations was performed to identify if any of the perceived excesses or rarities in the frequencies were statistically significant (pp. 230-233 in (Legendre et Legendre, 1998)). Constrained permutation tests for nested designs (e.g., studies within ecosystem categories) are rooted on the concept of exchangeable units, which are groups of observations that are equally likely to have occurred in any order when the effect being tested does not exist (Manly, 2007). The null hypothesis for an exact test of the fixed effect can be phrased as: groups of observations within each study (the random effect) can be permuted across levels of the fixed effect (Anderson et Braak, 2003). In the context of our study, steps of the constrained permutation test were as follows: 1) calculate the pivotal statistic χ^2_{obs} for the chi-square correspondence analysis between the predictor variable and EH-BD relationship directions ; 2) randomly permute among groups of EH-BD relationship directions nested within each study ; 3) calculate χ^2_{null} for the correspondence analysis between the predictor variable and the permuted groups of relationship directions ; 4) repeat the above two steps 9999 times and ; 5) the probability p of accepting the null hypothesis is the number of times χ^2_{null} falls above χ^2_{obs}, divided by 10 000. The hypothesis was that, for a given explanatory variable (e.g., ecosystem categories along the anthropocline) and within each of its levels, the relative frequencies of observed positive, negative or non-significant EH-BD relationships are larger (an excess) or smaller (a rarity) than those obtained under the null model. Rejection of the null model at an alpha rate of 0.05 indicated in what circumstances there was either an excess or a rarity in the direction type of EH-BD relationships.

The non-significant relationship direction type was included in the graphical output as we deemed it important to make these data visible for the reader. However, since non-significant results are often underreported in ecology (Jennions et Mol-

ler, 2002), we ultimately chose to remove these relationships from the recursive-partitioning and correspondence analyses due to the impossibility of controlling for such issues.

1.4 Results

The majority of the EH-BD relationships evaluated from the reviewed literature suggested positive associations (547), however non-significant (190) and negative (93) RDs were also numerous.

None of the three components of spatial scale entered the recursive-partitioning model, suggesting that spatial extent, spatial grain and sample size did not have a direct effect on the direction of EH-BD relationships. Furthermore, we found no interaction between the spatial scale components and the ecosystem categories defining the anthropocline (Fig.1.2). Although studies in the highly impacted ecosystem category were conducted at a higher spatial extent or grain than studies in the semi-natural category, there was no interaction with the anthropocline gradient (Fig.1.2, plates A & B). In other words, studies categorized as either "highly impacted" or "semi-natural" were not more likely to report a positive or negative EH-BD relationship.

The chi-square permutation tests on the relative frequencies of RD types across explanatory variable levels revealed significant differences among the ecosystem categories (Table 1.2). No other significant differences from randomized tests of frequency values were identified in the other explanatory variables. Regarding ecosystem categories, the analysis revealed a significant excess of positive EH-BD relationships and a significant rarity of negative relationships in highly-modified ecosystems (Table 1.2 & Fig.1.3). Results reversed in semi-natural ecosystems, showing a significant excess of negative RDs, while at the same time, a significant rarity of positive directions (Table 1.2). In strictly-natural ecosystems there was

no difference between the relative frequencies of positive and negative EH-BD relationship directions (Fig.1.3).

Considering the remaining two explanatory variables (i.e., taxonomic group and statistical model type), the correspondence analysis identified no significant excesses or rarities amongst any of the relative frequencies of RDs across ecosystem categories (Table 1.2; for graphical representations see Appendix A, Fig.A1). Finally, we note that cases of non-linear modeling and EH-BD relationships were present in the literature, however the number of such records (n=26) was too small to affect our final results or warrant a RD level of its own (see Appendix A, section III).

1.5 Discussion

1.5.1 Position on the anthropocline predicts the type of EH-BD relationship

This synthesis tested for the potential effects of ecologically relevant explanatory variables on the direction of EH-BD relationships. The results indicated that the anthropocline axis, as defined by three ecosystem categories denoting the level of human footprint, has a predictable effect on the nature of EH-BD relationships. In particular, there was no dominance of positive or negative EH-BD relationships in strictly-natural ecosystems, suggesting that biodiversity responds unimodally to increasing EH when the full human footprint gradient among ecosystems is considered. On the other hand, if the position on the anthropocline is shifted to highly-modified or semi-natural ecosystems, the respective frequency of positive or negative EH-BD relationships is reversed.

1.5.2 Other explanatory variables: the effect of spatial scale

The analysis suggested that studies classified in the highly-modified ecosystem category were conducted more commonly at a higher spatial extent or grain than

studies in the semi-natural category, but that these components of scale did not interact with the anthropocline gradient in explaining the direction of EH-BD relationships. The influence of spatial scale is a contentious issue and has been the focus of several theories aimed at explaining why EH-BD relationships are not consistently positive (Borcard et al. 2004 ; Tews et al. 2004 ; Allouche et al. 2012). As observers we ask ourselves at what scale do the taxa operate and respond to variability, at what scale do the habitat structures exist, and over what spatial area may the two interact ? In practice, it can be reasonably assumed that researchers have adequate a priori knowledge of these parameters to design their studies' grain and extent accordingly. Simply put, it must be assumed that researchers measure EH at observational scales that the taxa experience. Alternatively, if a study's scale is too coarse or small to capture EH-BD interactions one should expect only a weakening of the relationship, but not a reversal of direction. In support, studies in which EH-BD relationships were tested at multiple spatial scales, while position on the anthropocline does not change, show that the direction of the relationship was generally consistent even when spatial extent and grain decreased (Dufour *et al.*, 2006; Kumar *et al.*, 2009; Bar-Massada *et al.*, 2012). In those cases, only the magnitude of the relationship was affected by the changes in spatial scale and our results appear to be in line with those evidence.

Our results indicated no obvious effect of taxonomic grouping or statistical model type on the direction of the EH-BD relationships. Thus, our findings support the expectation that the nature of EH-BD relationships is dependent on the position along the anthropocline and that this effect is generally consistent across spatial scales, taxonomic groups and statistical model types.

1.5.3 Reconciling the anthropocline EH-BD framework with other theories

For decades ecologists have worked under the paradigm that EH promotes species diversity by increasing opportunities for niche-partitioning (the EH-hypothesis). Not only do our results show that the position along an anthropocline alters this relationship, but the prevalence of negative EH-BD associations in strictly-natural and semi-natural ecosystems provides further evidence to the viewpoint that the EH paradigm is incomplete. The anthropocline framework suggests that natural ecosystems are characterized by intermediate levels of EH and that the operative effects of niche-partitioning on species diversity may be restricted to highly-modified settings. Consequently, when patterns of EH are too high on the anthropocline, niche-partitioning no longer operates because viable habitats are lost rather than created. The outcome of this dynamic, and in agreement with another recent meta-analysis (Allouche *et al.*, 2012), would be a unimodal EH-BD relationship.

Previous studies have identified several factors that could explain a departure from positive EH-BD relationships, among those include: spatial scale (Lundholm, 2009; Rocchini *et al.*, 2010), species identity (e.g., specialists vs. generalists, rare vs. common species) (Tews *et al.*, 2004), area-heterogeneity tradeoffs (Allouche *et al.*, 2012), or the superseding effect of other biophysical influences on diversity patterns such as primary productivity (Kerr, 2001). All of these factors are supported by evidence and may indeed play a role in driving EH-BD relationships, particularly in natural ecosystems. However, the previous theories describing EH-BD relationships may also lack some generality. For example, measuring only topographic heterogeneity has limitations as it ignores the many other measures of EH that exist (over 430 records in our synthesis measured biotic features of EH for example) and, in some cases, is a weak predictor of species richness

when compared to other variables like productivity, energy or alternative indirect measures of EH (Kerr et Packer, 1997; Johnson *et al.*, 2003). The novelty of the anthropocline framework is that it presents a generalized EH-BD relationship without excluding the influence of other factors such as those evidenced by previous studies.

1.5.4 Is the picture complete ?

Though the literature synthesis supports the anthropocline framework, further questions can be raised. Firstly, why do we see so many positive and negative EH-BD relationships in strictly-natural ecosystems and a general lack of unimodal ones ? The simple answer is that linear modeling has been by far the most common analytical tool of past studies, while non-linear analyses are still rarely in use. It may also be that a majority of studies have not captured the full gradient of EH. If we conceptualize each study falling on the anthropocline, each one may only represent a short section, either in the positive or negative direction, of the uni-modal EH-BD curve, as was depicted by the blue lines in Fig.1.1.

Secondly, does the human expansion phase from strictly-natural to semi-natural ecosystems exacerbate species loss, or may ecosystem modifications increase species richness if the rate of species introductions outpaces native species extinctions (Sax et al. 2005) ? For sessile organisms like plants, the high EH characterizing semi-natural ecosystems can, in fact, translate into greater spatial turnover in community composition (Niemelä, 1999) and increased species richness (Wania *et al.*, 2006). Conversely, non-sessile animals, and particularly those with large ranges, are expected to respond negatively to increasing EH. This dichotomy between plant and animal responses to increasing EH during landscape diversification is well supported in the literature. For example, in cases where formerly natural landscapes have undergone low to intermediate levels of urbanization, animal taxa

experienced a net species loss, whereas plant species richness typically increased (McKinney, 2008). On the other hand, if one is concerned only with native plant species, the response to increasing EH beyond natural and semi-natural states may be similar to that of animals. The process of urbanization, for example, generally results in an expansion of alien plant species, but the decline of native species (Kühn et Klotz, 2006). Regardless of taxonomic group, since extinctions often occur generations after ecosystem modification, it may be the case that any initial gains in species diversity due to introductions is, on the long term, negated by a future ecological cost of human activities ; i.e., an extinction debt. Metapopulation models have shown that even moderate ecosystem modification by humans is predicted to cause time-delayed but deterministic extinctions (Tilman et May, 1994). Empirical studies have also shown that extinction debts are a common outcome in many cases of ecosystem modification, particularly for species with low turnover rates (Kuussaari *et al.*, 2009; Vellend *et al.*, 2006).

1.5.5 The environmental complexity-heterogeneity relationship

Natural ecosystems have long been thought of as complex systems, wherein the conditions for sustaining biodiversity are optimized (Nicolis et Prigogine, 1977; Fath *et al.*, 2004), but attempts to quantify complexity or define what and how ecosystem features contribute to complexity has lagged behind. It has, however, become clear that complex structures and dynamics are distinct attributes of natural ecosystems, which can be empirically tested and measured (Parrott, 2010). Complexity has been defined as a balance between the two extremes of order and disorder (Parrott, 2010; Langton, 1992; Levin, 1992). If natural patterns represent environmental optimums in terms of supporting biodiversity, then it may be useful to describe and quantify those patterns directly in terms of complexity rather than heterogeneity. Heterogeneity increases linearly with pattern disorder ; consequently EH-BD relationships have generally been measured and interpreted

on an unbounded, unreferenced axis of heterogeneity. Complexity metrics, on the other hand, are often a convex function of heterogeneity, attributing their highest values to systems of intermediate heterogeneity. Bearing the aforementioned in mind, we may reformulate the conceptual EH-BD relationship into a complexity-biodiversity relationship (Fig.1.4).

The concept of environmental complexity is not without its own shortcomings however. Confusion in the terms used to define habitat complexity and the measures used to quantify it has limited our understanding of its role in influencing species distributions and trophic interactions (Kovalenko *et al.*, 2012). Adding to this uncertainty is the fact that, while there is evidence for the role of environmental complexity in begetting species diversity, many of the mechanisms behind this effect remain ambiguous. Being underexplored highlights the importance of assessing complexity in a consistent manner; namely, viewing complexity as an ecosystem attribute and using metrics that are defined by a known baseline between complete uniformity and complete disorder (i.e., bounded and referenced).

1.6 Conclusion

Increasing environmental heterogeneity is not always good. Deciphering the underlying mechanisms of EH-BD relationships and identifying what is the right amount of environmental heterogeneity needed to enhance or maintain biodiversity is a difficult task. This task has been complicated by the use of multiple heterogeneity measures, as well as the difficulties to establish reference states (i.e., positioning EH on the anthropocline axis). Yet, recognizing macro-ecological patterns, and in particular those that quantify the modification of ecosystems, is essential to forecasting of ecosystem state shifts.

Contemporary studies often suggest that EH should be incorporated into ecosystem management for such purposes as protected area selection and assessment

(Miller *et al.*, 2011). Yet very few management plans use quantitative measures of EH to define their goals. If the response of biodiversity across the EH gradient is being misinterpreted, undesired conservation and management effects would seem a foregone result. Thus, for EH to be used as a benchmark of an ecosystem's state, EH-BD relationships should be understood in a context relative to its position on the anthropocline axis. A unified use of bounded EH metrics would allow future studies to "normalize" their position on the anthropocline by referencing with the extremes found in other ecosystems. Ideal measures of EH may be those that distinguish complex patterns against uniform or disordered patterns.

1.7 Supplementary Materials – Appendix 0.1

Appendix 0.1.1 - 0.1.3: Expanded details on the literature review, additional explanatory variables tested and how meta-data with polynomial model results were treated.

Appendix 0.1.4: Literature reference list of all studies used in the meta-analysis.

CONCEPT			DEFINITION	EXAMPLES
[HTML]E1EEFF	Environmental Heterogeneity (EH) [HTML]E1EEFF(spatial and temporal patterns of ecosystem features increasing from uniform to disorder)	Any measure of variation in the vertical, horizontal, or temporal distribution of environmental conditions within ecosystems; i.e., each extracted record from a reviewed study has a measure of EH	Standard deviation of time-series values, landscape fragmentation metrics, diversity of physical structures or resources	
[HTML]FBE5E5	Anthropocline [HTML]FBE5E5(spatial and temporal patterns of different human footprint levels)		A gradient of increasing EH according to the level of human footprint between ecosystems; i.e., each reviewed study has a human footprint category	Highly-modified, strictly-natural and semi-natural ecosystems
[HTML]E6FBE6		Highly-modified Ecosystems	Areas intensively modified or regulated by human activity, typically dominated by agricultural and urban centers (low EH)	Cropland, cultivated land, plantations, seeded pasture, any intensive agricultural landuse
[HTML]E6FBE6		Strictly-natural Ecosystems	Protected or remote areas with low human density and restricted resource extraction(intermediate EH)	Protected areas, remote areas and landscapes with low human density and restricted resources extraction
[HTML]E6FBE6		Semi-natural Ecosystems	Areas which are neither strictly-natural, nor highly-modified, but retain components of both (high EH)	Managed forests, uncultivated grazing land, broad spatial extents (e.g., regional to continental in extent) that encompass both natural and modified ecosystems

Tableau 1.1: Summary table of the main concepts defining the anthropocline framework. The first column lists the concepts. The second column lists the definitions of environmental heterogeneity, followed by the anthropocline and the three ecosystem categories that form its axis (positioned along a gradient of increasing environmental heterogeneity). The third column lists examples for each concept.

Explanatory Variable	Explanatory Category levels	EH-BD Relationship Direction	Chi-square Statistic	p-value
Ecosystem type	Highly-modified	negative	-2.354	**0.027**
	Highly-modified	positive	0.903	**0.038**
	Strictly-natural	negative	-0.231	0.408
	Strictly-natural	positive	0.131	0.465
	Semi-natural	negative	2.918	**0.011**
	Semi-natural	positive	-1.397	**0.007**
Taxonomic Group	Plant	negative	-0.575	0.261
	Plant	positive	0.261	0.301
	Animal	negative	0.683	0.301
	Animal	positive	-0.259	0.261
Model Type	Uni-variate	negative	-0.099	0.362
	Uni-variate	positive	0.065	0.425
	Multi-variate	negative	0.294	0.425
	Multi-variate	positive	-0.078	0.362

Tableau 1.2: Table of explanatory categorical variables, their levels and the chi-square probabilities for each EH-BD relationship direction type (positive or negative). Probability values below 0.05, as shown in bold, were considered significant. A negative chi-square probability values indicates that the relative frequencies of observed EH-BD relationships are smaller (a rarity) than those obtained under the null model. Positive chi-square probability values indicate that the relative frequencies of observed EH-BD relationships are larger (an excess) than those obtained under the null.

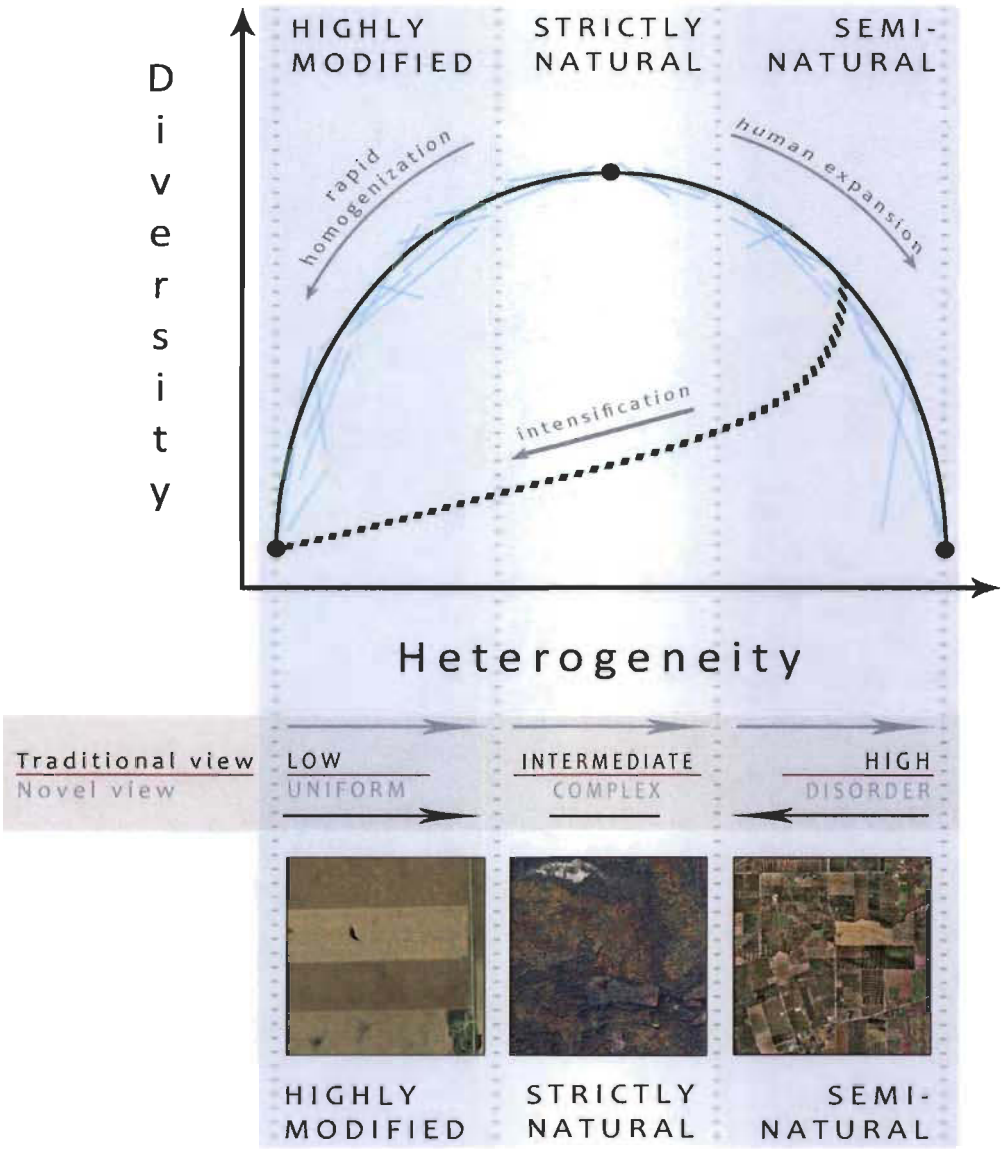
HIGHLY MODIFIED
STRICTLY NATURAL
SEMI-NATURAL
Diversity
rapid homogenization
human expansion
intensification
Heterogeneity
Traditional view
Novel view
LOW
UNIFORM
INTERMEDIATE
COMPLEX
HIGH
DISORDER
HIGHLY MODIFIED
STRICTLY NATURAL
SEMI-NATURAL

Figure 1.1: The anthropocline heterogeneity-biodiversity framework. The green curve represents the response of biodiversity (y-axis) across a gradient of increasing heterogeneity in the environmental conditions (x-axis). The environmental heterogeneity axis is partitioned into three ecosystem categories defining the anthropocline: *i)* Highly-modified ecosystems; *ii)* Strictly-Natural ecosystems and; *iii)* Semi-Natural ecosystems. The blue response lines along the green curve represent EH-BD relationships contributed by individual studies and regrouped on the basis of their ecosystem category. In this way, our hypothesis infers a generalized EH-BD relationship from the joint responses of all studies. Human activities can push natural ecosystems in either direction along the anthropocline; towards a semi-natural state via the progressive modification of environmental conditions (human expansion), or towards a highly-modified state via the abrupt homogenization of environmental conditions (rapid homogenization). Further intensification of human activities in semi-natural ecosystems can lead to a highly-impacted state (dotted line).The lower panel of image boxes illustrates a landscape-scale scene (U.S. Geological Survey (USGS), 2009) for each ecosystem category on the anthropocline axis.

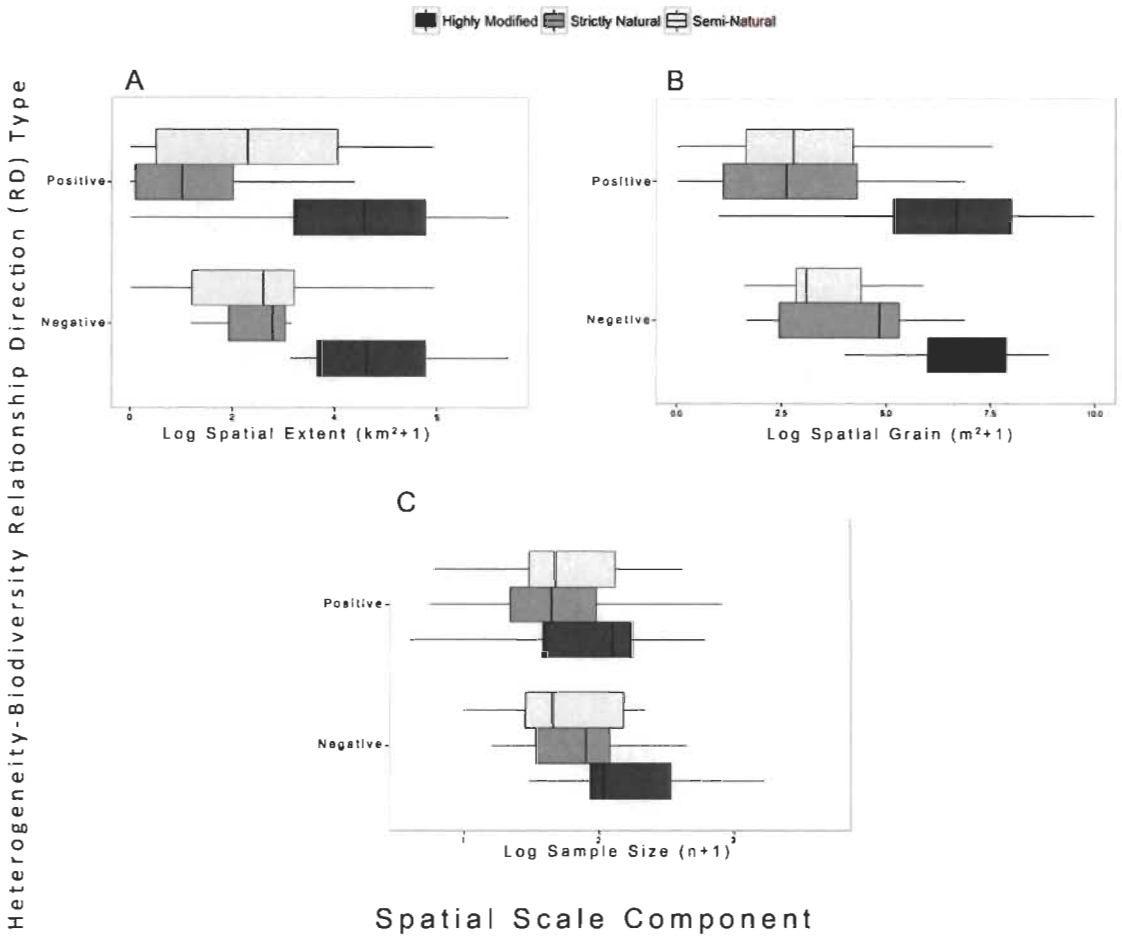

Figure 1.2: Box-plot distributions of each component of spatial scale (x-axes) for different combinations of ecosystem category (legend) and EH-BD relationship direction (y-axes). The three scale components are the spatial extent (panel A), the spatial grain (panel B) and the sample size (panel C). The spatial extent, grain and sample size distributions were log transformed and were computed on per study averages because some studies reported more EH-BD relationships (i.e. contributed more values) than others.

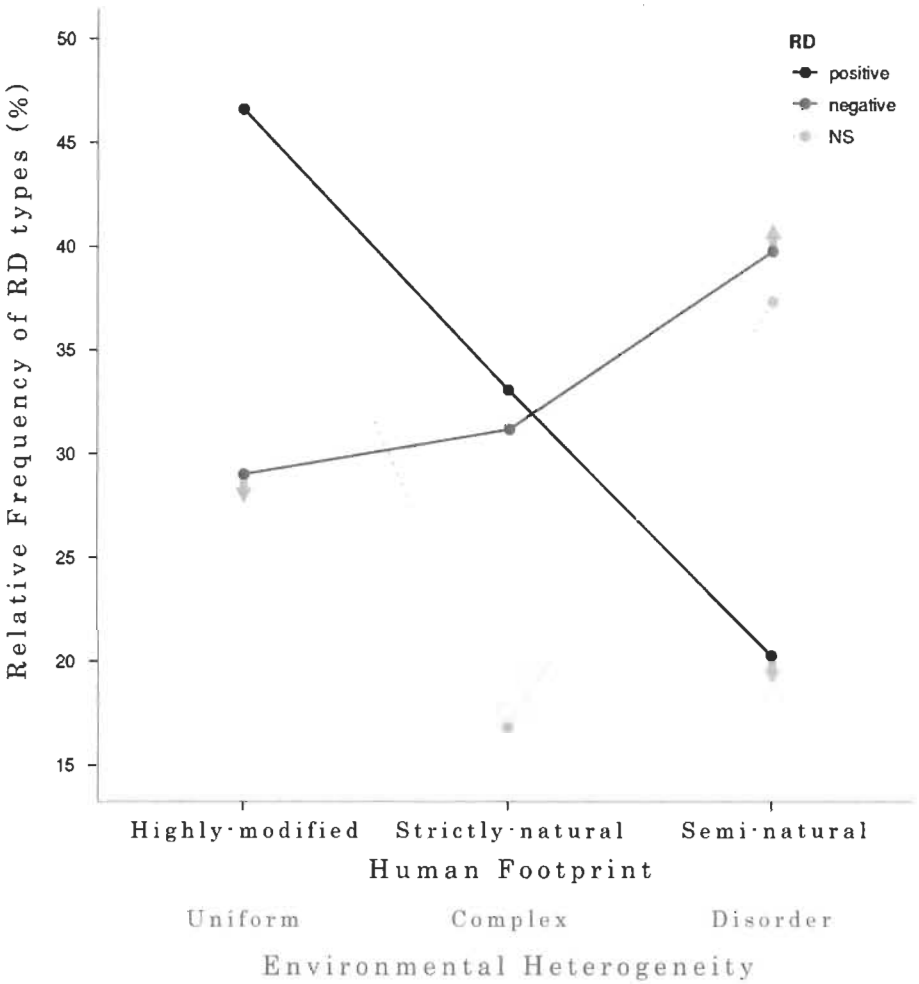

Figure 1.3: Relative frequency of environmental heterogeneity-biodiversity relationship direction (RD) types across ecosystem categories and their associated heterogeneity patterns (i.e., the anthropocline axis). Points with grey arrows directed up denote a significant excess of the RD frequencies within the level, while points with grey arrows directed down denote a significant rarity of the RD frequencies as determined by a correspondence analysis with constrained permutations. Points with no arrows showed no significant difference at an alpha rejection rate of 0.05.

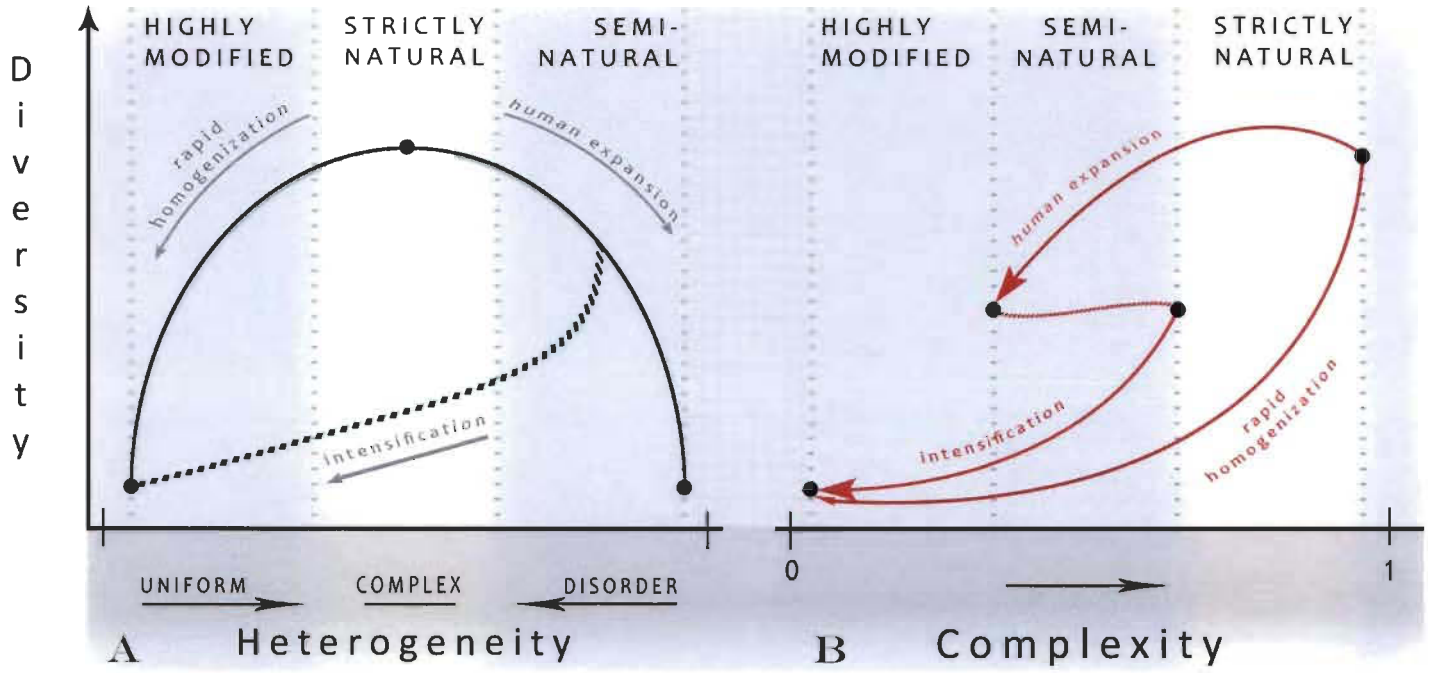
Diversity
HIGHLY MODIFIED
STRICTLY NATURAL
SEMI-NATURAL
rapid homogenization
human expansion
intensification
UNIFORM
COMPLEX
DISORDER
A Heterogeneity
HIGHLY MODIFIED
SEMI-NATURAL
STRICTLY NATURAL
human expansion
intensification
rapid homogenization
0
1
B Complexity

Figure 1.4: The anthropocline complexity-biodiversity framework: A) The generalized environmental heterogeneity-biodiversity relationship presented in the introduction. B) The adapted environmental complexity-biodiversity relationship in which heterogeneity is replaced by complexity on the anthropocline axis. Complexity increases along the x-axis and is bounded between 0 (low complexity) and 1 (high complexity). The solid curves indicate the expected response of species diversity as an ecosystem is modified by human activities from its initial natural state. Human expansion leads to a semi-natural ecosystem typified by disordered environmental patterns (decreasing complexity); human intensification further progresses the ecosystem to a highly-modified state (further decreasing complexity). Rapid homogenization of strictly-natural ecosystems leads directly to a highly-modified state.

CHAPITRE II

SIGNIFICANCE OF TREE DIVERSITY FOR THE COMMUNITY PHENOLOGY OF EUROPEAN FORESTS

2.1 Abstract

La phénologie a joué un rôle primordial dans les recherches sur les changements globaux, et ce, en tant que réponse climatique de l'écosystème. Toutefois, elle n'est que rarement quantifiée comme un trait fonctionnel ayant la capacité d'aussi varier indépendamment du climat. Plus spécifiquement dans les écosystèmes forestiers, les variations phénologiques de la végétation affecteraient profondément les processus du système puisque les patrons de croissance saisonniers des arbres définissent l'architecture de la canopée, autant en espace qu'en temps. Ceci soulève la question suivante, toujours si peu explorée malgré son importance indéniable : Quel rôle joue la diversité des espèces dans les patrons de croissance saisonniers des forêts ? Pour étudier cette question, nous avons utilisé des estimés hauterésolution de la synchronisation de la croissance des plantes d'un réseau de parcelles de forêts paneuropéennes distribuées le long d'un gradient de diversité en arbres. Une fois les conditions climatiques et édaphiques considérées, la phénologie des forêts tempérées est principalement un produit de la composition en espèces via la contribution relatives des phénologies spécifiques à chaque espèce. De plus, nous suggérons que ces variations phénologiques à l'échelle de la communauté forestière mènent à un compromis entre l'interception de la lumière de la canopée et la lumière disponible pour la communauté du sous-bois. En effet, nous avons observé que la diversité d'espèces d'arbres a un effet relativement très positif sur les communautés du sous-bois. Ces communautés du sous-bois situées sous une canopée diversifiée en arbres croissent significativement plus longtemps que celles observées sous une canopée moins diverse. Alors que les activités humaines et les changements climatiques continuent d'altérer la composition des écosystèmes forestiers tempérés, ces découvertes révèlent la nécessité de quantifier la phénologie spécifique à l'espèce et de l'incorporer à des modèles de biosphère. Les variations de patrons de croissance saisonniers des communautés associées à différents niveaux

de diversité de peuplements, pourraient avoir de grandes implications sur les fonctions et services clés écosystémiques comme, par exemple, pour la séquestration du carbone.

~

Phenology has played a principle role in global change research as an ecosystem response to climate, however it is rarely quantified as a functional property that may also vary independently of climate. Variation in the phenology of plant species and communities likely affects forest ecosystem processes since the seasonal growth patterns of trees will influence the canopy architecture in both space and time. The unexplored question of what role does species diversity play in determining the seasonal growth patterns of forests is raised. We use stand-level estimates of the timing of leaf development and duration from a pan-European network of forest plots distributed across a tree diversity gradient to investigate this question. Upon accounting for regional climatic and edaphic conditions, the leaf phenology of temperate forests is primarily a product of species composition via the relative contributions of species-specific phenologies. A community phenology emerges from mixing tree species at the stand-level and, as such, generates variation in leaf development and duration both within and between regions. Moreover, we suggest that tree diversity leads to increased light opportunities for plants forming the understory. In turn, we find that tree species diversity has a relatively strong positive effect on the understory communities, wherein those growing under diverse tree canopies maintain green foliage for longer periods than those growing under less-diverse canopies. As human activities and climate change continue to alter the composition of forest ecosystems, these findings reveal the necessity to quantify species-specific phenologies and incorporate them into biosphere models. Our findings suggest that community variation in growing season patterns has strong implications on key ecosystem

functions and services such as carbon sequestration.

keywords: phenology, forests, species diversity, functional diversity.

abbreviations: GSL, growing season length ; SOS, start of the growing season ; EOS, end of the growing season ; DOY, day of year ; RGB, Red-green-blue ; ROI, region of interest ; RF, random forests [of regression trees].

2.2 Introduction

The study of the seasonality plant development – *phenology*[1]– has gained a prominent role in ecology as a critical element of global change research and ecosystem responses to climate change Walther *et al.* (2002); Morisette *et al.* (2009). Recent work is indicating that water and energy fluxes, surface heat budgets and net carbon uptake in forest ecosystems are intimately tied to seasonality, climate and the response of the vegetation to both (Richardson *et al.*, 2013a; Dragoni *et al.*, 2011). For example, recent observations of extended growing seasons reported gains of 5.6 - 5.8 $g\,C/m^2$ for each additional growing day in deciduous broadleaf forests (Richardson *et al.*, 2013a). These observations not only illustrate to what degree ecosystems are responding to climate change, but they also underscore the sensitivity of ecosystem processes to changes in phenology.

While tree phenology responds to exogenous environmental cues (e.g., climate, precipitation and soil), it is also determined by species-specific and endogenous factors (Augspurger et Bartlett, 2003; Jackson *et al.*, 2001). Some species leaf and flower at the same time, others separate the timing of these events such that different resource acquisition or allocation strategies lead to different phenological traits. For example, shade-tolerant species can utilize reserves or adjust morphological and physiological traits to benefit from sun flecks or canopy gaps (Augspurger, 2013; Augspurger et Bartlett, 2003) ; while shade-intolerant species can optimize carbon gains by exploiting light windows in the early and late season (Ishii et Asano, 2010).

Yet study of forest phenology has typically focused on either local variation between species (Augspurger, 2008) or species-indiscriminate regional variation (i.e.,

1. Phenology is the study of the seasonal timing of biological events such as the timing of bud burst in spring, the ripening of fruit, or the coloring of leaves in fall. Our use of the term *phenology* will refer to the specific case of the seasonal timing of plant leaf development and duration.

long-range measures like satellite imagery that aggregate many individuals into one value – a pixel). Global vegetation models frequently use only one plant functional type to represent temperate broadleaf deciduous tree phenologies (Jeong et Medvigy, 2014) and few studies to date have investigated the influence of tree species diversity on community phenology.

The phenology of trees partly defines the forest canopy structure and, in turn, its control on light attenuation, productivity, fluxes of water, carbon uptake and sequestration and reproductive success (Richardson *et al.*, 2013a; Ishii et Asano, 2010; Kudo *et al.*, 2008). Recent theoretical models have suggested that, with increasing tropical tree diversity, temporal niche differences (i.e., phenological complementarity through phenotypic plasticity) may enhance light capture and, thus, is a driver of the productivity – diversity relationship (Sapijanskas *et al.*, 2014). However, such models may be "jumping the gun", so to speak, as measures of species-specific phenologies have not been able to achieve together the temporal and spatial resolutions required to investigate these dynamics in forests.

The spatial and temporal development of tree leaves throughout the season is the cardinal strategy for light interception in temperate forests (Ishii et Asano, 2010). As such, the enhancing and stabilizing effects of tree diversity on productivity and carbon storage may be mediated by phenology, particularly by the seasonal duration of leaves; what we define here as the growing season length (GSL). Understory species, including herbs, small shrubs and tree saplings, are known to adjust their phenology in response to the seasonality of the light environment; specifically by utilizing the open canopy periods either before canopy leafing in spring or after senescence in autumn (Ishii et Asano, 2010; Augspurger, 2008). At the stand-level, mixing tree species with complementary crown architectures and phenological traits may result in spatially and temporally structured canopies that intercept a greater portion of incoming solar radiation (e.g., Jucker *et al.*, 2014). At the regional or landscape levels, whether or not a "portfolio" of communities

translates into significant spatial variation in the GSL of forest stands and, in turn, to what degree understory phenology, fitness and responses to light availability may be influenced are unknown.

The objective of this study is to address *the role of tree species diversity in determining the leaf emergence and duration of plant communities in a range of forest ecosystems*. To do so, we use species data and image-derived estimates of the timing of leaf emergence, senescence and duration from a network of permanent forest plots distributed across Europe. First, we examine whether a relationship exists between tree community GSL and tree species diversity. We hypothesize that, as tree diversity increases, stands with short GSLs will become rare. Due to the control that the canopy structure imposes on the below-canopy environment, we also expect that tree species composition and diversity will have top-down effects on the understory phenology.

2.3 Methods

2.3.1 Study design and gradient of tree species diversity

This study was conducted across a network of permanent forest plots, spanning the primary bioclimatic gradient of the European continent and representing the major European forest types: boreal forests in Finland, hemi-boreal forests in Poland, beech forests in Germany, mountainous beech forests in Romania, thermophilous deciduous forests in Italy and Mediterranean mixed forests in Spain (`http://www.fundiveurope.eu`). All plots were established in mature forest stands that differed primarily by tree species richness (stochastic or management driven) while variation in other environmental factors and management history was minimized as much as possible (*SI Appendix 2–A* Table S1). As such, while regions differed strongly from one another in terms of climate, the 30 X 30 m plots within each region shared similar elevation, topography and soil quality. In total, the network comprises 209 plots and 16 target species (*SI Appendix 2–A* Table S2), several of which were present at more than one region. A full study

design and plot selection description can be found in (Baeten *et al.*, 2013) and in the supplementary information *SI Appendix 2–A*. Due to the theft of the cameras in the majority of plots in Romania, we have removed this region from the present study. The dataset analyzed and presented here comprises 181 plots between five regions.

2.3.2 Community phenology and growing season estimation

Recent developments in image analysis techniques have illustrated that time-lapse photographic datasets can yield highly accurate estimates of the timing of key phenological events (*e.g.,* leaf flushing, start of growing season and end of season senescence), across a variety of ecosystem types and at spatio-temporal resolutions rarely achieved by satellite image datasets (Sonnentag *et al.*, 2012; Richardson *et al.*, 2009b; Meyer et Neto, 2008; Bater *et al.*, 2011). Images from commercial-grade digital cameras represent combined brightness levels of the red-green-blue (RGB) color channel information and can be separately extracted and summarized through color indices such as excess green (Sonnentag *et al.*, 2012). Calculated across image scenes captured at recurring time intervals (*e.g.,* hourly, daily, weekly), a time-series of a greenness index may be employed as a proxy of plant biomass development and seasonal growth.

We installed RGB cameras with intervalometers in each permanent forest plot according to a standardized setup (see *SI Appendix*) and acquired images three times daily for the length of a growing season. In the German region, images were acquired for two consecutive growing seasons so as to compare potential inter-annual variation in the methodology. The side-view image scenes captured the general vertical profile and extent of the plot and during image post-processing, three regions of interest (ROI) were manually delineated: plot understory, mid-story and overstory or canopy. The ROIs were delineated manually for each plot time-series. The understory ROI was selected to maximize the area in the image

covering forest floor and the herbaceous, saplings and small shrub components (i.e., $<$ 1.3m as estimated by a trained botanist) ; the image area covered by live tree trunks was minimized. The overstory ROI was selected to maximize the image area covered by adult and canopy trees and leaves ; this usually included the upper image edge, down to the area where no branches or leaves were associated with trees ($>$ 7.5 cm dbh). The midstory ROI was selected to maximize the image area covered by young trees ($<$ 7.5 cm dbh) and tall shrubs ($>$ 1.3 m), but to also minimize the image area potentially covered by distant canopy tree foliage. A binary excess green index (Meyer et Neto, 2008) calculated the proportion of green pixels within each ROI for each image in a time-series. Each ROI defines a stratum in the forest stand, inclusive of all plant biomass visible from the camera's viewpoint. To identify the seasonal trends in growth, we applied a smoothing spline function to each time-series and, subsequently, the start of season (SOS) and end of season (EOS) dates were extracted from the first derivative of the function (White *et al.*, 1997). Finally, we defined the resulting GSL of the plot ROI or strata as the number of days between the SOS and EOS. For further detail on the camera equipment, installation procedure, ROI, example images and phenological image analysis see *see SI Appendix 2–A*.

2.3.3 Statistical Analysis

Our statistical analysis employed a random forest (RF) of regression trees (Breiman, 2001; Siroky, 2009; Liaw et Wiener, 2002) (*SI Appendix 2–A* provides expanded details). The RF algorithm is an ensemble-based approach in which multiple decision trees are built on a subset of data (out of bag or bootstrapped sample) and predictor variables. The final model decision is based on a voting system of all the potential random variable trees that have been created. Essentially, random forest regresses the predictor variables as many times as the user requires, introducing an element of randomness each time, and voting for the most popular model.

Rather than traditional indirect variable subset selection methods (e.g., statistical significance and Akaike's Information Criterion), the random forest algorithm provides a novel method of determining variable importance. It operates without excluding variables that may be ecologically important, but correlated with other predictor variables. As such, a RF model is particularly well suited for assessing the relative importance of predictor variables to the response when, for example, climate is likely a determinant. RF models are also better suited at finding limiting gradients, as would be expected if species rich forest stands become more rare as growing season length increases, rather than correlating gradients. The variable importance scores in RF may be used to identify ecologically important variables for further examination and interpretation. The randomForest package in R (Liaw et Wiener, 2002) was used to construct RF models for each of the three stand strata (i.e., ROIs): overstory, midstory and understory. For regression trees, the random forests provides two measures of predictor variable importance:

1. the mean decrease in the accuracy of predictions in the out of bag samples when a given variable is excluded from the model (%IncMSE), hereafter termed variable MSE-importance.
2. a measure of the total decrease in node impurity that results from splits over that variable and averaged over all trees (IncNodePurity), hereafter termed variable node purity.

What is labelled cross-validated r-square for each RF model represents the explained variance as measured by how well the out-of-bag, cross validation, predictions explain the target variance of the training set. We elaborate on these points and the application of the RF algorithm in the *SI Appendix 2–A* but it should be noted that negative cross-validated r-square values are possible if the out-of-bag variance is much greater than the original variation in the data.

As the primary objective of this study was to explore the potential role of tree

species diversity in determining stand-level phenology, our analysis took plot EOS and GSL dates as the response variables of interest and tree species richness as the principle predictor variable of interest. Tree species diversity was calculated as e^H, where H is the Shannon diversity of tree species. Although the experimental design only took into account the target tree species while not counting other tree species that may have been present with less than 10% abundance, our measure of tree diversity included all species present in the plots even if under the 10% cutoff (see *SI Appendix 2–A* for further description of the experimental design). It is clear that environmental conditions and stand structure affect the phenology of individual trees and, thus, phenology. Upon examination of a preliminary correlation analysis between a suite of climatic, structural and environmental variables and the response phenological variables, we also selected and included: annual mean temperature, annual mean precipitation, mean diurnal temperature range, latitude, exposition, mean age of canopy trees, year of image sampling and a proxy measure of seasonal mean below-canopy illumination as predictor variables in the final models (*SI Appendix 2–A*).

Image-derived greenness values as a proxy for phenology is clearly influenced by leaf habit. Though evergreen species typically do display a discernible growth pattern using this methodology (*e.g.*, greenness values increase when new needles flush in spring), the fact that their foliage remains green year-round mutes the growth signal and puts into question the accuracy of the derived phenophases, particularly if compared to those of deciduous trees or communities. Acknowledging this methodological limitation, we performed all statistical models using the full dataset, as well as three successive subsets in which an evergreen filter removed plots dependent on their relative abundance of evergreen tree species. The evergreen filter sizes were:

i) no plots removed (*i.e.*, full dataset).

ii) removal of plots with 66% or more evergreen trees.

iii) removal of plots with 33% or more evergreen trees

iv) removal of plots in which 5% or more of the trees are evergreen species.

We discuss the limitations and evergreen bias of image-derived phenologies further in *SI Appendix 2–A*.

2.4 Results

2.4.1 Community-level phenologies of mixed forests across Europe

Across study regions, the range and means of plot-level growing season length (GSL ; defined here as the seasonal leaf duration) were within those observed by independent datasets (Richardson *et al.*, 2010; Churkina *et al.*, 2005; Wang *et al.*, 2005 ; see also Table S3 in the SI Appendix for summary statistics of the plot phenologies). We found a strong linear correlation between the GSL and the end of the growing season (EOS) among all forest stands (Pearson's r-square = 0.90). The spring start of the growing season (SOS) displayed very little variation between stands and occurred on or soon after camera installation (Table S3, SI Appendix), suggesting the "true" SOS may not have been captured. For these reasons, we hereafter used the EOS date as our key phenological variable of interest and in remainder of the analysis. Considering intra-regional differences in stand phenology, we found that the within-region variation in stand overstory EOS overlapped among all regions with the exception of Finland (Fig. 2.1). In particular, plots of the Spanish and Italian regions displayed a wide range of EOS values.

2.4.2 Canopy tree phenology and tree species diversity

In all regions, low tree diversity plots accounted for the earliest EOS dates, while EOS variation in high-diversity plots was both reduced and shifted towards high EOS dates (i.e., later EOS and long seasonal leaf duration) (Fig. 2.1). However, random forest (RF) models indicated no significant relationship between stand-level tree diversity and EOS date for the overstory layer (Fig. 2.2 and, specifically,

the means of plot EOS were not significantly different considering low vs. high tree diversity. We note that a trend was consistent particularly amongst the German, Finland and Poland regions, wherein later EOS dates (i.e., longer growing seasons lengths) were more common with increasing plot tree diversity and early EOS dates (i.e., short growing season lengths) were increasingly rare with increasing plot tree diversity.

2.4.3 Top-down control of tree species diversity on community phenology

Tree species diversity was one of the key determinants of understory EOS among all potential environmental predictors, according to the RF models (Fig. 2.2). The MSE-variable importance score of tree species diversity to EOS date was highest for the understory stratum and was the highest ranked predictor variable when considering plots dominated by deciduous species (i.e., with sequential filtering of stands out of plots containing evergreen species). With a progression down the forest strata, tree diversity becomes an important predictor of the EOS date relative to all other predictor variables tested (Fig. 2.2).This effect of increasing importance of species diversity with successive filtering of conifer presence held true for all three forest strata, but not for the other predictor variables. The importance of climatic and edaphic drivers to EOS varied as latitude, annual mean temperature and precipitation were also consistently ranked high, while exposition and mean diurnal temperature range were ranked with low importance (Fig. 2.2). Stand age structure appeared to have little influence as a predictor variable while, on the other hand, below-canopy light availability was a relatively strong predictor of EOS in the models. Cross-validated r-square values indicated that the models had very low predictive power for the overstory and midstory layers. However, the understory layer showed robust patterns across regions in terms of the variable importance scores and model fit parameters. Node purity, the other variable importance score used in RF models, showed similar patterns

to that of the MSE scores (*SI Appendix 2–A* Table S4 & Fig. S1).

Understory EOS appeared strongly associated with tree species diversity, regardless of bioclimatic region (Fig. 2.3). Specifically, plots with low tree species diversity (i.e., less than 3 species) tended to have early EOS dates, while plots with high tree species diversity (i.e., above 2 species) tended to have late EOS dates. This relationship was even more pronounced when considering deciduous trees only (Fig. 2.3). Understory plant communities associated with species rich stands were active (i.e., stayed green) 29 days longer than those associated with species poor stands and up to 61 days longer in one region – Italy. The result was consistent across regions with the exception of Finland wherein the pattern appeared weak or dissimilar. Since the Finnish region was characterized by only three target tree species, two of which are conifers, the filtering of plots with evergreen species served only to leave plots dominated by one species.

2.5 Discussion

Our results highlight four parallel insights. First, *in-situ* digital photography and simple image color metrics can address a significant resolution-gap in phenological research, namely that of community phenologies, both within and across ecosystems. To date, this study is the first to deploy these novel techniques across such an extensive range of bioclimatic conditions, multiple forest types and a gradient of tree species richness. Second, the EOS, and hence also GSL, values we obtained from this approach agree with the range of values observed in previous studies with overlapping geographic areas and employing either long term observational data (Chmielewski et Rotzer, 2001) or remotely-sensed estimates (Wang *et al.*, 2005). The stand-level EOS values compare particularly well to the carbon uptake period (Churkina *et al.*, 2005) in terms of the observed range of values (days) between the SOS and EOS. Third, intra-annual variation between community phenologies is not explained by regional environmental conditions such as annual temperature,

precipitation or soil differences. Fourth, the species structure and composition of the community appears to be an important driver of the understory community phenology.

2.5.1 Community-level phenologies of mixed forests across Europe

Temperature and precipitation have been considered the primary drivers of GSL in studies to date and the key predictive parameter in phenological models (Diez *et al.*, 2012). Thus, that the GSL of some forest stands may be comparable from boreal to Mediterranean-mixed forests and yet also displayed a large amount of intra-regional variation is an unexpected result. We cannot rule out the possibility that some of this variation is due to the method used to quantify plant phenology. A limitation of our photographic *in-situ* estimation of phenology is that the determination of the key phenology events (e.g., EOS) is sensitive to the shape of the image-derived greenness curve and aberrations in it (i.e., anomalous peaks or sharp decreases). For example, the leaf duration and GS metrics we derive can by influenced by visual differences in tree species leaves that are not directly related to phenology *per se* such as deciduous leaves, which display clear leaf-out, green-up and senescence phases, *vs.* evergreen leaves which display only subtle seasonal changes in the greenness of their leaves. Apart from these considerations, our expert-based evaluation of all phenology trends did not justify the use of further selection/exclusion criteria, which illustrates the robustness of the approach.

Considering all forest stands, we observed a relatively broad range of EOS values and, hence, duration of stand-level GSL. To our knowledge, such range of spatial variation within regions has not been documented or explicitly noted to date. In the case of tree phenologies estimated from remote sensing, regional variation may simply get lost at coarse temporal or spatial extents. The relative large amounts of stand-level phenological variation displayed within the Italian and Spanish sites could be due to the moderate seasonality of Mediterranean climates and the in-

fluence of seasonal precipitation (i.e., an annual dry and wet season). For example, some plots containing winter-growing tree species may senesce early in the summer, while others remain active with green leaves throughout the summer. These species phenological traits could explain the high variation and strongly differentiated early-growing vs. late-growing EOS patterns observed in the two regions.

2.5.2 Canopy tree phenology and tree species diversity

Upon accounting for regional climatic and edaphic conditions, we suggest that the phenology of temperate forest overstory communities is primarily a product of the relative contributions of species-specific phenologies. Stands with diverse overstory communities tended to have a higher frequency of late EOS dates (longer growing season) and fewer early EOS observations than did those with a less diverse overstory communities (Fig. 1.1 & *SI Appendix* Fig. S1), but a clear diversity effect on EOS was not detected. Therefore, at the stand-level, tree diversity does not necessarily lead to longer growing seasons, but a full gradient of tree diversity does lead to a large portfolio of phenological responses within a region. Sapijanskas *et al.* (2014) used a mechanistic model to show that species-specific phenologies were the strongest driver of enhanced light capture but, on its own, phenological complementarity of mixtures did not outperform their best species. This finding is supported by our results since, on average, diversified tree canopies had a higher frequency of longer GSLs at the community level, yet several stands of low tree diversity achieved equally long growing seasons.

Previous studies indicated that recent increases in forest productivity can be explained by longer vegetative seasons (e.g., Dragoni *et al.*, 2011). Though we did not find a positive effect of tree diversity on overstory EOS or GSL, we note that stand composition and influence does influence the stand-level phenology. Variation in the GSL of stands generally decreased with increasing stand-level tree diversity due to fewer of them displaying a short growing season, while still displaying an

EOS as late as the latest-growing monospecific stands – evidence of an averaging effect of mixing species' phenological traits at the community level with a bias towards longer GSLs. That these results were evident at a local scale of 900 m^2 plots, totalling 16.3 ha in area (all plots and regions combined), highlights the functional significance of tree diversity - phenology relationships when scaled to the ecosystem or landscape levels. For example, the community phenology that emerges from stand composition and diversity will have implications on seasonal carbon uptake and other key ecosystem fluxes of temperate mixed forests.

2.5.3 Top-down control of tree species diversity on community phenology

Understory communities that grew under diverse tree mixtures maintained, on average, longer GSL than did communities growing under less diverse stands. A previous study of the FunDivEUROPE plot network has inferred that mixed tree communities with complementary crown architectures optimize the canopy space and in turn light interception, thus enhancing productivity (Jucker *et al.*, 2015). We should expect that community tree diversity is a strong determinant of the understory light availability in both space and time and so too the phenology of understory plants. For example, overstory complementarity associated with high tree species diversity may act to reduce understory light availability and, as a result, the understory growing season may shorten. Alternatively, the understory GSL may be extended by a diverse overstory via species turnover over time or by displaying phenological plasticity to compensate for periods of low-light conditions. The later response has been previously observed in temperate forest understory communities (Augspurger et Bartlett, 2003). Other studies have evidenced that understory plant species may exploit frequent light gaps produced by a species-diverse overstory (e.g., Franklin et Van Pelt, 2004). In agreement, our proxy measure of below-canopy light availability showed strong evidence that it is an additional important predictor of understory EOS (see *SI Appendix* for details

on how below-canopy light availability was estimated).

Paradoxically, our results suggest that diverse overstory communities, with higher packing densities (e.g., Jucker *et al.*, 2015), may also allow more light to reach the understory during canopy development than less diverse communities do. While previous studies showed that increasing tree diversity leads to crown expansion of individuals and increased canopy packing density (Pretzsch, 2014; Jucker *et al.*, 2015), ground coverage by tree crowns has not been shown to increase with mixing (Pretzsch, 2014). Structural features of forest canopies are typically based on snapshot measurements and, thus, their temporal dynamics may be overlooked in this context. Accounting for the temporal variation in canopy development that is associated with increasing tree diversity may then resolve the packing density – light availability paradox. In particular, temporal heterogeneity in understory light availability, wherein diverse overstory communities develop their foliage at differing times or rates, could increase understory light availability during canopy development relative to species poor communities which develop at the same time.

2.6 Conclusion

Recent studies suggest that increasing tree diversity may act to optimize canopy packing, thus driving positive diversity-productivity relationships (Jucker *et al.*, 2015). We suggest that high tree diversity also allows sufficient light to penetrate to the understory and enables longer-growing understory communities. As determined by tree diversity and composition, the spatial and temporal structure of the canopy strongly influences the understory phenology across European forests. Understory communities growing under diverse overstories grew, on average, up to 22% longer than those growing under pure or less-diverse overstories. While the understory contribution to forest standing biomass is relatively small, understory species can have disproportionate impacts on energy flow and nutrient dynamics (Fridley, 2012; Muller et Bormann, 1976).

Forest phenology has traditionally been quantified and modelled inter-annually, at the landscape level and as a function of latitude and temperature. However, we argue that substantial variation in forest phenology exists between communities and is independent of environmental forcing to a large extent (i.e., latitude and local to regional climate).

Previous studies and current biosphere models are contradictory regarding the drivers of autumn phenology, including dependence on photoperiod, temperature or both and leading to large differences in predicted terrestrial energy, water and carbon cycles (Jeong et Medvigy, 2014). As human activities and climate change continue to alter the compositional make up of temperate forest systems, these findings reveal the necessity to quantify or estimate species-specific phenologies, particularly their autumn leaf senescence, and incorporate them into phenological and terrestrial biosphere models.

2.7 Supplementary Materials – Appendix 0.2

In Appendix 0.2 we describe in more detail the study methodology, including a full and detailed description of the study plot network (FunDivEurope) and summary statistics for the plot descriptors (Table S1), a full list of target tree species in each study region (Table S2), camera hardware and sampling regime, image-based estimation of community phenology, predictor variables of interest used in the primary statistical analysis (random forests models), reasoning for and application of random forests models, the evergreen bias limitation of the methodology and the removal of plots in the Finland region. Furthermore, we make available all summary statistics for the plot phenologies of each study region and provide additional supplementary results figures (Table S3). We also make available additional statistical results (Table S4 & Figs. S1 – S2).

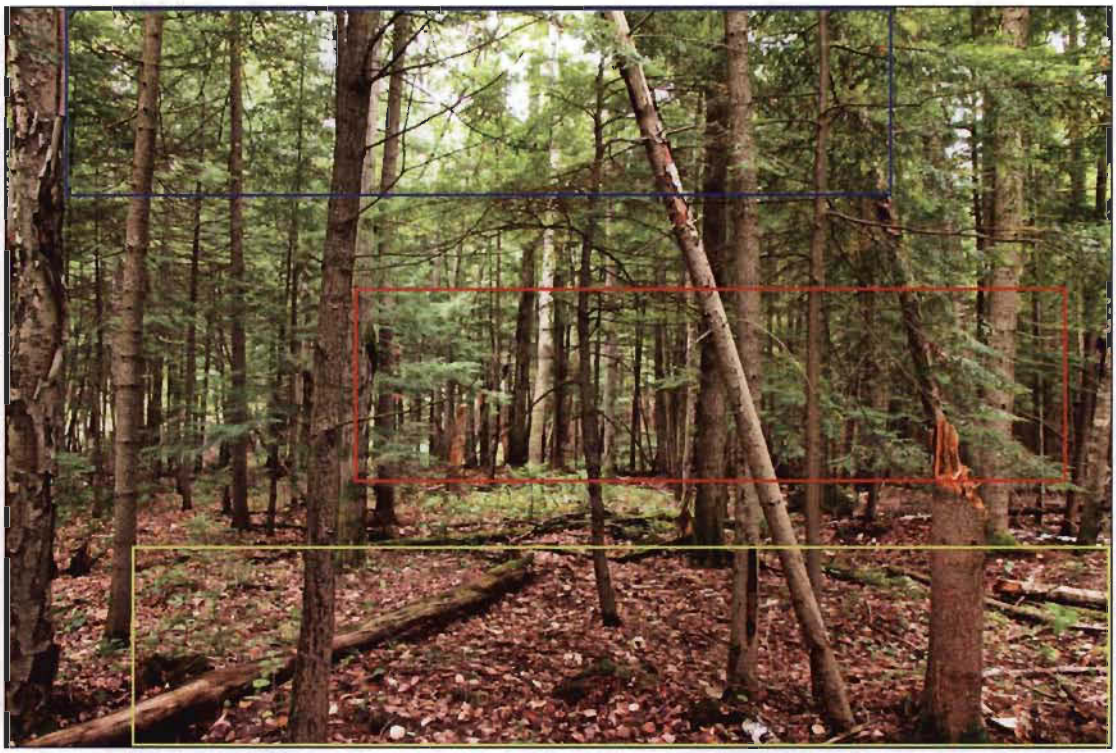

Figure 2.1: Single image taken from the time-series of side-view photographs for one of the study plots (German region). The colored boxes delineate the manually selected regions of interest (ROI) for the plot time-series images: overstory (blue), midstory (red) and understory (yellow).

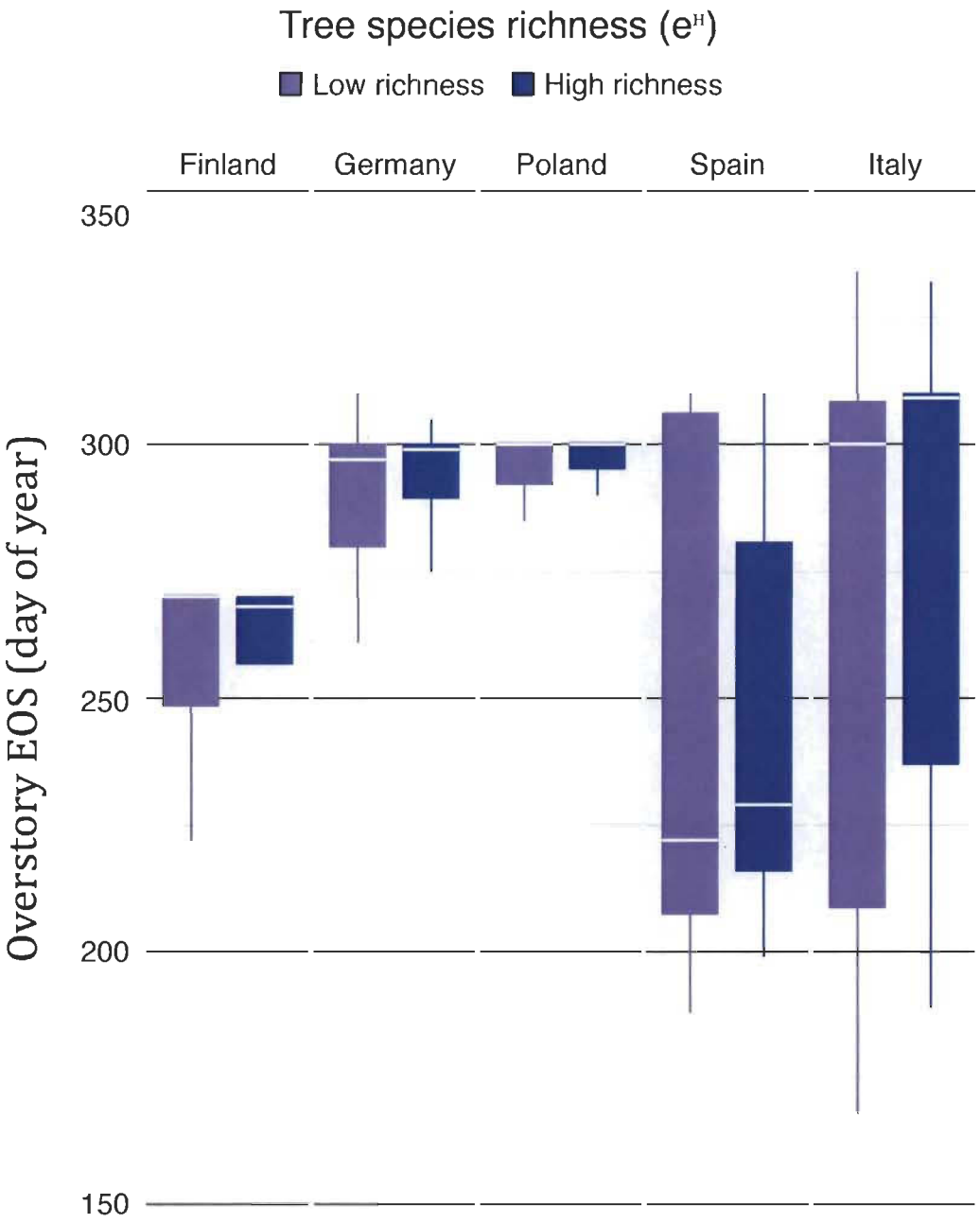
Tree species richness (e^H)
Low richness
High richness
Finland
Germany
Poland
Spain
Italy
Overstory EOS (day of year)
350
300
250
200
150

Figure 2.2: Variable mean squared error (MSE) importance scores for each predictor of the growing season length of each forest strata. For each panel, the x-axis indicates the evergreen filter level wherein the RF models were run at each level. The evergreen filter size is displayed as the inverse of values, such that with increasing values, the tolerance for evergreen presence decreases and, thus, more plots are removed. At 0 no plots are removed and at 100 plots containing any amount of evergreen trees are removed. The results of a random forests model show that the importance of tree species diversity ($\mathbf{e}^{\mathrm{H}}$) in predicting growing season length increases from the overstory layer down to the understory layer. The equivalent figure showing the predictor variable node purity scores is available in the appendix (SI Appendix 2–A)

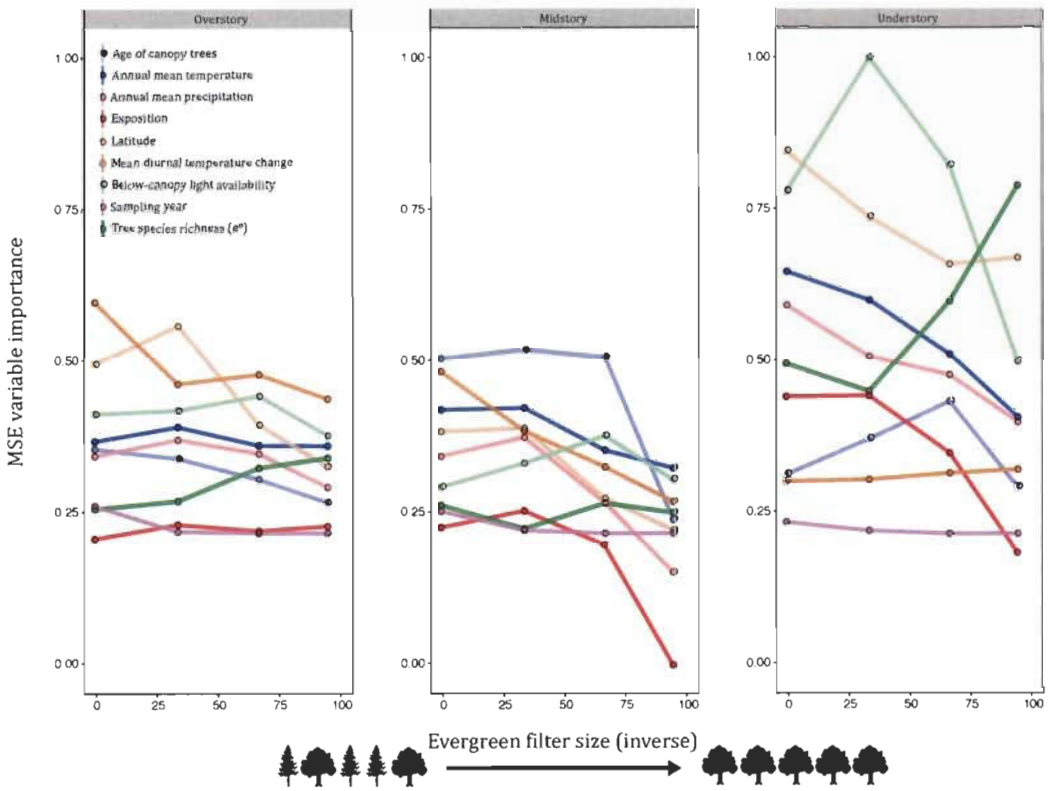
Overstory
Midstory
Understory
Age of canopy trees
Annual mean temperature
Annual mean precipitation
Exposition
Latitude
Mean diurnal temperature change
Below-canopy light availability
Sampling year
Tree species richness (α)
MSE variable importance
1.00
0.75
0.50
0.25
0.00
0
25
50
75
100
Evergreen filter size (inverse)

Figure 2.3: For each region, boxplots of stand understory growing season length grouped as short *vs* long growing seasons and compared across the gradient of tree species diversity (x-axis). The growing season length of the understory strata significantly increases with the tree species diversity ($\mathbf{e}^{\mathrm{H}}$) of its associated overstory community. This pattern holds true across all study regions and increases in strength with successive removal of plots containing evergreen species (reading the figure panels from top to bottom and then left to right); the pattern is highlighted by the slope of the blue line in each panel which represents a linear regression model fit to all plots in the study.

CHAPITRE III

GREEN STREETS — QUANTIFYING AND MAPPING URBAN TREES WITH STREET-LEVEL IMAGERY AND COMPUTER VISION

3.1 Abstract

Les outils traditionnels pour cartographier la répartition des espaces verts urbains sont restreints, soit à cause de leur coûts ou besoins en main d'œuvre élevés, soit par leur faible résolution spatiale dû à la structure spatiale complexe des paysages urbains. De plus, ces outils n'observent pas le paysage urbain comme notre perspective le ferait, or ils ne peuvent connaître de quelle manière un citoyen expérimente sa ville. Nous testons une application novatrice de vision numérique pour quantifier la couverture d'arbres urbains à l'échelle d'une rue. Pour cela, nous utilisons des données open source d'images très abondantes aujourd'hui ; de streetscape en ville (Google Street View). Nous démontrons qu'un algorithme à plusieurs étapes de vision numérique segmente et quantifie avec précision le pourcentage de couverture d'arbres dans les images de streetscape. En modélisant par la suite les relations entre les images le long des segments de rues de ville, nous sommes capables de prolonger ces représentations d'image et d'estimer la quantité de la couverture d'arbres dans les paysages de rue d'une ville entière avec un haut-niveau de précision. Bien que la méthode ne constitue pas un remplacement des méthodes de télédétection de haute-résolution (e.g., LiDAR aérien) ou des campagnes de terrain intensives, elle fournit une nouvelle métrique multi-fonction de la couverture forestière urbaine permettant de quantifier la présence et la répartition des arbres selon le même point de vue que nous, en tant que citoyens, expérimentons le paysage urbain.

~

Traditional tools to map the distribution of urban green space have been hindered by either high cost and labor inputs or poor spatial resolution given the complex spatial structure of urban landscapes. What's more, those tools do not observe the urban landscape from a perspective shared by our own and hence, how citizens experience a city. We test a novel application of computer

vision to quantify urban tree cover at the street-level. We do so by utilizing the open-source image data of city streetscapes that is now abundant (Google Street View). We show that a multi-step computer vision algorithm segments and quantifies the percent of tree cover in streetscape images to a high degree of precision. By then modelling the relationship between neighbouring images along city street segments we are able to extend this image representation and estimate the amount of perceived tree cover in city streetscapes to a relatively high level of accuracy for an entire city. Though not a replacement for high resolution remote sensing (e.g., aerial LiDAR) or intensive field surveys, the method provides a new multi-feature metric of urban tree cover, one that quantifies tree presence and distribution from the same viewpoint in which we, as citizens, experience and see the urban landscape.

keywords: urban trees, computer vision, streetscapes, tree cover, greenspace.

abbreviations: FOV, field of view ; GSV, Google Street View.

3.2 Introduction

With the growing consensus that nature and multi-functional ecosystems are intrinsic to sustainable cities, decision makers, designers and the broader public alike are looking to trees as urban keystone flora that provide natural infrastructure and services – to reduce air pollution, support biodiversity, mitigate heat island effects, increase land value, improve aesthetics and even improve human health (Kardan *et al.*, 2015; Lothian, 1999; Lovasi *et al.*, 2008; McPherson *et al.*, 1997; Nowak *et al.*, 2014; Thayer et Atwood, 1978). Urban tree effects may even extend to cultural and psychological behaviours with, for example, a high abundance of street trees being linked to urban scenes that were perceived to be safe (Naik *et al.*, 2014b). The fact remains however that urban trees come with costs and are currently threatened by climate change, pests and diseases. Conflicting land uses and cost-benefit tradeoffs cause contention at many levels of society. Such contentions can be alleviated through a better understanding of the role of trees in the complex and cluttered landscapes that are cities. To this end, tools to quantify and monitor presence, abundance and health of urban trees are needed. Governments, particularly cash-strapped ones, are evermore looking for low-cost ways to establish baseline data, manage and engage the public on urban trees.

Traditionally, urban tree cover has been quantified using coarse-scale methods developed for naturally forested landscapes and exposure to "nature" as an urban quality indicator has been quantified by measuring the total land area covered by greenspace (i.e., city park area) in cities (Richardson *et al.*, 2013b; Schroeder, 1986; Fuller et Gaston, 2009). In either case, these methods primarily rely on long-range remotely-sensed image processing to classify landcover (i.e., satellite imagery such as LANDSAT, ortho-aerial photographs or, more recently, LiDAR) (Homer *et al.*, 2007) or data derived from field surveys (Kardan *et al.*, 2015). Substantial drawbacks exist within each case, many of which present particular

challenges in an urban context. For example, traditional remote-sensing techniques for vegetation cover have, most often, been based on moderate-resolution imagery (e.g., 30 m in the case of openly available data) which has limited utility at the scale of cities. Recent efforts exploiting high resolution active sensing like LiDAR are proving well-suited for urbanscapes (MacFaden *et al.*, 2012), however they can be hindered by specialized proprietary software, high data-acquisition costs and significant labour inputs. On the other hand, field-based surveys lack the automation and the scale of big data sets (i.e., low-throughput), are prone to sampling errors (Dickinson *et al.*, 2010) and require enormous organizational efforts. These methodological impediments also make it difficult to achieve periodic resampling to asses changes in tree cover and health over time.

Chiefly through machine learning models, computer vision scientists are teaching computers to see the world at astounding rates of success. However, few disciplines outside of the strict artificial intelligence fields (e.g., robotics, driverless cars, software) have utilized these advancements. One of the few examples bridging ecology and computer vision technologies is the mobile app, Leafsnap, which identifies plant species using automatic visual recognition (Kumar et al. 2012). If a computer can learn to detect and quantify features of an environmental scene from digital photographs (i.e., scene understanding), it stands that those algorithms can be used to objectively quantify real-world features and their spatial distribution within a landscape for a multitude of applications. For instance, Naik et al. have developed computer vision algorithms that process street-level imagery to quantify urban appearance (Naik *et al.*, 2014b)), urban change (Naik *et al.*, 2015), or even socio-economic indicators (Glaeser *et al.*, 2015). Opportunely, we now also have access to entire cities in the form of geo-tagged, street-level images.

Using Google Street View images that represent a ground-based perspective of city streets – *streetscapes* – and which cover a city-wide extent, we develop and test a new method of rapid quantification and mapping of urban vegetation, specifically

trees. The method applies a trained predictor to segment the amount of tree cover in a given image of a city streetscape using multiple image features. We aim to demonstrate that we can quantify the presence and perceived cover of street-side trees with high spatial resolution at the city-scale by: *i)* sampling a series of sequential neighbouring image scenes of the streetscape ; *ii)* predicting the amount of tree cover present in them and ; *iii)* modelling the relationship between the tree cover of these neighbouring view-points. To estimate the accuracy and utility of this approach we compare our method to contemporary remote-sensing techniques used to estimate urban tree canopy cover (i.e., object-based image analysis (OBIA) of high-resolution LIDAR data and multispectral imagery).

The goal of this study is to present a novel method of measuring trees in a city at extremely high-throughput ; one that may not replace existing techniques, but offers clear benefits such as being relevant to the human perspective (*the perceived tree cover*), cheap, independent of proprietary software and easily scaleable across cities.

3.3 Methods

3.3.1 Study areas and image datasets

We collected data on urban tree cover by using 456,175 geo-tagged images from the two cities of New York (336,998 images) and Boston (119,177 images) in the United States. However, for the vast majority of the results presented, we focus on New York because the best-suited tree canopy cover maps and street tree survey data we could acquire were of New York. Images were sourced from the Google Street View (GSV) application program interface (API) (Google Inc., 2014), were acquired in 2014 and represent a ground-level, side-view perspective of the city streetscape (Fig. 3.1 C). All image collection points along city roads were downloaded for a target city and this resulted in a GSV image roughly every 15 meters along a given roadway ; these image samples are hereafter referred to as *GSV sampling points*. However, due to the protocol of the GSV system the

15 m interval could deviate by approximately +/- 5 m. Given this, we define a neighbour sample points as two GSV sampling points on the same road segment and a minimum of 10 m and maximum of 20 m apart. Some GSV sampling points, road segments or areas of the city did not have data for various reasons (e.g., corrupt or missing data, no-coverage area). Notwithstanding those instances, the sampling regime covered the full extent of the cities' official boundaries, though for the case of New York it did not cover Staten Island (Fig. 3.1 A & B).

Each digital photograph (Red-Green-Blue color channel jpeg image) was acquired from the GSV API at a resolution of 400 by 300 pixels, at a 90° horizontal field of view, 90 heading (east) and a 10° pitch. The level of pitch was chosen in order to optimize the capture of the streetscape (i.e., decrease the amount of foreground composed only of roadway). Fixing the image heading to 90 east for every sampling point allowed us to compare how the road-to-image orientation would affect the metrics and, ultimately, the ability to estimate tree cover. As such, all sampling points were grouped into one of four categories based on their road orientation, given 22.5° intervals around 360°: 1) N-S: GSV sampling points lying on roads that are oriented in a north-south direction (+/- 22.5° from 0° or 180°); 2) E-W: GSV sampling points lying on roads oriented in an east-west direction (+/- 22.5° from 90° or 270°); 3) NW-SE: GSV sampling points lying on roads oriented in a diagonal northwest- southeast direction (+/- 22.5° from 135° or 315°); 4) NE-SW: GSV sampling points lying on roads oriented in a diagonal northeast-southwest direction (+/- 22.5° from 45° or 225°).

In order to estimate the real-world surface area covered by each GSV image, we modelled the 2-dimensional (horizontal and vertical) surficial field of view (FOV) represented in an image at each sampling point; i.e., the camera's horizontal field of view (90°) and depth of field projected onto the earth's surface. We computed this FOV polygon for each GSV sampling point which was then projected on the horizontal surface plane to associate a surface area with the sampling point (Fig.

3.1). The length of the polygon (i.e., length of the right-angle bisector) represents the approximate image depth of field. However, in reality the depth of field varies with the presence, size and proximity of objects occluding the horizon. We assume that a given length should, on average, be representative of an urban streetscape. Therefore, we varied this depth of field parameter and created four levels: 15 m, 25 m, 35 m and 45 m from the GSV sampling point. In addition to the road-to-camera orientation groups, we run our analysis at each of these depth of field levels in order to determine which provides the best spatial context for predicting real-world tree cover.

3.3.2 Tree detection using Computer Vision

We estimated the total area covered by trees in each image by applying a multi-step image segmentation method developed by Hoiem *et al.* (2005). On a per-image basis, the objective of the method is to model geometric classes that depend on the orientation of a physical object with relation to the scene and with respect to the camera. Specifically, each image pixel is classified into one of a few geometric classes: *i)* the ground plane; *ii)* surfaces that stick up from the ground (vertical surfaces); *iii)* part of the sky plane. Further, vertical surfaces are subdivided into planar surfaces facing left, right or towards the camera and either porous (e.g. trees and their leafy vegetation) or solid (e.g. a person or lamp post) non-planar surfaces. Although this recognition approach differs from those that instead model semantic classes (e.g., car, house, person, vegetation), it has proven exceptionally powerful and efficient in cluttered outdoor scenes like urban streetscapes and, most relevant to our application here, in distinguishing human built structures from natural ones like trees.

The algorithm operates by first grouping image pixels into *super-pixels*, which are groups of pixels assumed to share a single label (e.g., ground or sky) and respect coarse-level segment boundaries (e.g., edges) (Felzenszwalb et Huttenlocher,

2004). The algorithm then groups regions of the image into homogenous segments using a standard segmentation algorithm, but generates multiple hypothesis or combinations of these rough segmentations as it remains unknown which have been labelled correctly. Thus, a set of image features are computed at both the level of the super-pixel and the larger region segments. Using training image data of ground-truthed, labelled urban scenes, learning the parameters to predict final labels operates at two stages: *i)* Grouping super-pixels is learned by estimating the likelihood that two super-pixels belong in the same region based on their features. The multiple segmentation hypotheses are then generated by varying the number of regions and the initialization of the algorithm. *ii)* The final labelling of the geometric classes of image segments is learned by computing the features for each region and labelling them with a geometric class based on likelihood functions (i.e., the likelihood that super-pixels have the same label and the confidence in each label). Once labelled in this fashion, the optimal likelihood functions are then learned through training (SI, Appendix).

With our images segmented and geometric classes labelled by this procedure, we applied the semantic labels to each pixel accordingly: ground, sky, building and trees. The percent of tree cover, ground, sky and building in an image were calculated as the total number of pixels belonging to that class divided by the total number of image pixels.

Since this method is well established in the computer vision field, we did not retain the pixel-level classification results. Due to this approach we were not able to visually inspect the image segmentations that the algorithm performed and report a pixel-wise misclassification statistic. We refer to Hoiem et al. (2005) and Naik et al. (2015) for benchmarked classification statistics of the algorithm. Nonetheless, in order to validate the robustness of this approach we took a random sample of 100 Boston city GSV images and derived two estimates of the percent of tree cover in an image by pixel masking to compare to the output of the learning

algorithm: *i)* we performed manual pixel masking by tracing all tree components in an image and summed the number of pixels falling inside and ; *ii)* we computed a single-feature binary excess green index Meyer et Neto (2008) which derives the proportion of green within an RGB image. Concerning the latter, similar single-feature methods have been used before to estimate vegetation presence in digital photographs (Li *et al.*, 2015; Yang *et al.*, 2009). Considering the former, we performed the manual pixel masking under two schemes: *i)* a conservative estimation where only tree species and only their clearly defined components were traced, while shrubs, small woody vegetation and distant, poorly defined trees were excluded and ; *ii)* a liberal estimation where tree-like, small woody vegetation was also included if it was clearly visible and, likewise, distant trees were included if we judged them very likely to be trees.

3.3.3 Modelling streetscape tree cover

Given an algorithm that quantifies the amount of area covered by trees in a 2D photograph, the remaining challenge we address is to relate such a value to a measure of real-world tree cover. Specifically, we test if and how well our metric of streetscape tree cover may estimate true percent tree canopy cover of the same area by modelling the relationship between them.

We derive the dependent variable of true percent canopy cover at each GSV sampling point FOV from a high resolution (3 ft.) and comprehensive land-cover map for New York developed by MacFaden *et al.* (2012). Derived from LiDAR data and multispectral imagery acquired in 2010, the map represents the most up to date and high resolution data on New York's tree canopy. We compute the percent canopy cover inside each i^{th} GSV sampling point FOV, at each j^{th} FOV-level:

Eq. 1

$$\%\, tree\ canopy\ cover_{i,j} = \frac{number\ of\ pixels\ classified\ as\ tree\ inside\ FOV_{i,j}}{total\ number\ of\ pixels\ inside\ FOV_{i,j}} \times 100$$

Simply measuring the tree cover from a 2D image poses two challenges in terms of predicting a real-world representation of it. First, the image representation compresses three dimensions into two (horizontal and vertical) and so a simple sum of same-classed pixels does not provide complete information on object depth or volume. This also means that trees that are occluded by other trees or objects can not be measured. Considering that this method is limited to streetscapes, this later effect is limited since urban street trees are typically not crowded and their general arrangement is one layer (row) of trees backed by buildings. Second, the amount of area covered by trees in an image will be highly dependent on the proximity of the tree(s) to the camera. Thus, the image tree cover is somewhat independent of their real-world size; all else equal, foliage that is closer to the camera will cover more of the image area. Both issues are a problem of perspective and location with respect to the camera at a given GSV sampling point.

We address these problems of perspective with the hypothesis that additional information about a scene can be gained from overlapping, neighbouring images which differ in their perspective and proximity to the same object. The amount of overlap between neighbouring images will depend on the road-to-image orientation since our image directions were fixed at a 90 east heading, while the road orientation varied (Fig. 3.1 D). We do not perform any stereoscopic interpretation explicitly, but by adding information from neighbouring images (i.e., the image-derived percent tree cover values), the real-world representation of a given scene may be approximated by an aggregation of all neighbouring GSV images which

capture a portion of that scene.

More formally, we assume a linear relationship between the scene information captured by a central GSV sampling point, hereafter termed the "node", and the contributions of its neighbouring GSV sampling points. We consider neighbour GSV points to be GSV sampling points on the same road segment as the node point and that are adjacent to the node in either direction. We estimated the average range of view for a typical GSV scene to be roughly 45 - 60 m by manually inspecting neighbouring GSV images. Given this range, we considered two neighbour points to either side of the node (four neighbours per GSV node point in total). We acknowledge that this parameter could be varied and tested in further applications. We establish a relationship between the real-world street tree cover and the GSV images of it:

Eq. 2

$$\beta_i = \sum \omega_{i,n} X_{i,n}$$

where, β_i is the real-world measure of tree cover for the given scene i, X is the percent tree cover in the GSV images for the node i and neighbouring n sampling points and ω is a weighting factor representing the relative contribution of each neighbour, X_i. Since the distance interval between GSV sampling points is not always constant, we may also normalize the contribution of each neighbour by dividing each neighbour term by its distance (δ) to the node point. Thus, expanding the equation and given that we include a total of four neighbouring points, with $-n$ neighbouring points below the node point and $+n$ neighbouring points above the node point, i:

Eq. 3

$$\beta_i = \frac{\omega_1 X_{i,-2}}{\delta_{i,-2}} + \frac{\omega_2 X_{i,-1}}{\delta_{i,-1}} + \omega_3 X_i + \frac{\omega_4 X_{i,1}}{\delta_{i,1}} + \frac{\omega_5 X_{i,2}}{\delta_{i,2}}$$

To determine the weighted contributions of each image in a node-neighbour series, we learn the weighting factors by solving the linear system of equations for ω:

Eq. 4

$$\begin{bmatrix} \beta_1 \\ \vdots \\ \beta_i \end{bmatrix} = \begin{vmatrix} \frac{X_{1,-2}}{\delta_{1,-2}} & \frac{X_{1,-1}}{\delta_{1,-1}} & X_1 & \frac{X_{1,1}}{\delta_{1,1}} & \frac{X_{1,2}}{\delta_{1,2}} \\ \vdots & \vdots & \vdots & \vdots & \vdots \\ \frac{X_{i,-2}}{\delta_{i,-2}} & \frac{X_{i,-1}}{\delta_{i,-1}} & X_i & \frac{X_{i,1}}{\delta_{i,1}} & \frac{X_{i,2}}{\delta_{i,2}} \end{vmatrix} \times \begin{bmatrix} \omega_1 \\ \omega_2 \\ \omega_3 \\ \omega_4 \\ \omega_5 \end{bmatrix}$$

Once the weighting factors are learned, they may then be plugged into equation 3 and standardized to compute the neighbour-weighted percent tree cover score at each GSV sampling point – the *streetscape tree cover*.

Finally, we model the relationship between our streetscape tree cover metric and the true percent tree canopy cover using multiple linear, least squares regression and cross-validate using 4-fold cross validation. In the regression models we also include the other semantic streetscape classes (*i.e.,* percent building, ground and sky) as additional predictor variables under the hypothesis that the relative proportions of these features in an urban scene can provide descriptive information on the spatial arrangement, location and, hence, size of trees.

We also test this relationship at the city district-levels of dynamic block, commu-

nity district, school district and borough. A dynamic block (also known as atomic polygon) is the smallest unit in the city geospatial data. We compute the total percent tree canopy cover per block unit at each district-level (i.e., percent canopy cover in a given district polygon from the vertical view) and the associated mean of streetscape tree cover for all GSV sampling points (i.e., street-level view) inside each block unit (polygon).

In order to minimize the multiple sources of systemic error when relating the streetscape tree cover metric from GSV images to the percent tree canopy cover, we perform a set of filtering steps prior to the regression analysis (SI, Appendix). All image analysis and processing, geospatial analyses and statistical modelling were performed in the R software environment (R Core Team, 2013), Matlab (MATLAB, 2015), C++ and Python programming language.

3.4 Results

3.4.1 Manual pixel comparison

The streetscape tree cover algorithm applied to single GSV images most closely correlated with our liberal scheme of manual pixel masking in the streetscape images (adjusted r-square = 0.98) (Fig. 3.2). Though still highly correlated, the simple, single-feature automated green mask method did not relate as well to our streetscape tree cover estimator (adjusted r-square = 0.79). The conservative manual tree masks also related very closely to our tree detector (adjusted r-square = 0.97).

3.4.2 Predicting urban tree canopy cover

The results showed that percent canopy cover derived from the landcover map is relatively low for any given location in New York City ; that is, the distribution of tree canopy cover was skewed to the left. For this reason, and to conform to the assumptions of homoscedasticity, we log-transformed the dependent variable of true canopy cover and used this semi-log structure in the final regression models.

Moreover, there was a high number of data points with low and fractional percent tree canopy cover values (e.g., between 0 and 1 or 2 and 3 % for example). These fractional differences are trivial, yet can amplify the importance of the data points when log-transformed. Therefore, we binned the response values by rounding them to the nearest integer.

Based on preliminary scatterplots and regression analysis, it was clear that the road-to-image orientation category 2 (E-W road orientation and parallel east camera heading) showed the strongest potential for predicting tree cover. We, henceforth, present and discuss results belonging to this category.

The relationships at all FOV-levels followed a nonlinear or curve-linear pattern, as would be predicted by the semi-log structure of the modelled relationship (i.e., the response variable of percent tree canopy cover is log-transformed and the predictor streetscape tree cover variable was untransformed). The best fitting regression models (i.e., the highest r-squared and lowest root mean squared error (RMSE)) were at the 25 m and 35 m FOV-levels, with the 35 m level performing slightly better (Fig. 3.3 & Table 3.1). At the smaller FOV-levels (15 and 25 m) there was a high amount of false negative errors – sampling points with greater than zero streetscape tree cover predicted, but no trees (0 % true canopy cover) in the associated FOV. Applying the neighbour-weighting procedure (Eqs. 2 & 3) significantly improved the predictive power of the streetscape tree cover estimations relative to using only an unweighted single node-GSV image-based value (Table 3.1).

Model residuals of the final regression models for the 35 m FOV had a mean close to 0 and followed a near-normal distribution, though the error variance was not perfectly constant. This was likely due partly to the high and skewed residual error at low, and in particular zero %, true canopy cover values where our predictor was detecting a range of tree cover values. The final regression model generalized well to the test data (Fig. 3.3 & Table 3.1), having comparable r-square and root

mean square error values (RMSE) between the training data (r^2 = 0.74, RMSE = 0.27) and the test data (r^2 = 0.73, RMSE = 0.28). When using the more rigorously filtered data subset that was used to learn the weighting factors, the model performance increased significantly (r^2 = 0.81, RMSE = 0.23).

Scaling the sampling units across district-levels resulted in an increasing predictive power of the method to estimate true canopy cover (Fig. 3.4 & Table S2, SI Appendix). We note that for these results we enforced a sample size cutoff value for each district-level (see SI, Appendix for further details). This is why, for example, the the Bronx borough is missing from that district-level at this time. Nonetheless, at the borough district-level, the results showed a very strong relationship between the mean streetscape tree cover and the total tree canopy cover for each borough (Fig. 3.4 & Table S2, SI Appendix). It must be noted however, that there were only three boroughs remaining after the filtering steps (SI, Appendix).

3.5 Discussion

Hand in hand with the growing availability and breadth of open digital data, this study has exampled how computer vision tools can be applied to quantify patterns of ecological, environmental and urban design importance. Specifically, a novel application of computer vision techniques to digital photographs of a city's streetscapes has shown significant potential to estimate the presence and amount of urban trees at high spatial resolutions with city-wide extent. We may define this quantification of street trees as the perceived tree cover. The multi-step image segmentation method estimated the image area covered by trees in GSV images with high throughput; the algorithm processed about one image per second on an Intel core i7 CPU with 12 cores. The streetscape tree cover method correlated very closely to the classifications performed by a human on a subset of images (see Fig. 2) and this comparison suggested that the algorithm was inclusive of small trees and tree-like plants as well as distant trees in the scene background. It also

correlated with a computationally simple, single-feature automated green mask estimator of tree or vegetation presence in an image, though not as well as with the manual pixel masks. This suggests that our computer vision-based method provides a realistic and accurate representation of tree presence and cover while being much less prone to false positives – not everything green is a tree.

A small number of studies have attempted to extrapolate tree presence and coverage from single 2D digital photographs (Li *et al.*, 2015; Yang *et al.*, 2009; Peper et McPherson, 2003; Schroeder, 1988). in both urban and natural settings to varying degrees of success. The majority have relied on manual inputs or site-specific conditions to acquire or process images, resulting in low throughput (Yang *et al.*, 2009; Peper et McPherson, 2003; Schroeder, 1988). Others have performed automated estimates of vegetation presence, but using non-discriminate, single-feature metrics (e.g., image greenness) and single-image representations of a scene (Li *et al.*, 2015). By applying state-of-the-art computer vision algorithms, we are able to quantify vegetation represented in images using multiple features and attribute definitive semantic labels to tree-associated pixels.

from 2D images remains, we attempted to partially correct the proximity-to-camera problem by including information from multiple, neighbouring and overlapping images. The method significantly increased the power of the streetscape tree cover metric to predict true canopy cover. In doing so, we have demonstrated a generalized model of perceived urban tree cover that does not require external inputs beyond the images themselves.

We found that when the streetscape images were aligned parallel to the street direction (i.e., the camera heading was the same as the street heading) the streetscape tree cover predictor operated best relative to the three other road-to-image orientations that we tested. This may be somewhat expected as this orientation generally results in a full view of street trees to either side of the road. In the case of New York City, this result somewhat hampered the analysis because most

streets in New York do not have an east-west heading. This is not a limitation of the method in itself however, but rather an artifact of our image sampling scheme. In future applications of this method we can acquire all images at this orientation by adjusting the camera heading when acquiring the images from Google. Alternatively, future applications can make use of GSV panoramas to model the full 360 degrees of the streetscape perceived tree cover.

3.5.1 Predicting tree canopy cover

The final model estimating true percent canopy cover from our streetscape tree cover method explained a substantial portion of the variation, indicated good prediction accuracy and generalized well to new data. To date, we are not aware of any other urban tree cover mapping methods that correlate so well with state-of-the-art high-resolution canopy cover mapping techniques while achieving such high throughput at the city scale. Moreover, this result can be considered conservative since the temporal mismatch between the GSV image data (*ca.* 2014) and the tree canopy landcover map (*ca.* 2010) was undoubtedly a source of systemic error cases, and thus unexplained variation. What's more, given the differing perspectives between long-range remote sensing (e.g., satellite imagery and aerial LiDAR) and our street-view photograph-based technique, we would not expect a perfect relationship between the two metrics. Our streetscape metric quantifies the vertical profile of urban trees while landcover mapping uses an overhead view and, thus, sees trees as surfaces or polygons on a horizontal plane

The results illustrated that this new ground-derived quantification of urban trees can be considered as a *perceived tree cover* estimate rather than canopy cover per se. Traditional methods like high-resolution landcover maps are fundamentally fixed as a measure of canopy cover. They are well-suited to compute the coarse-scale distribution and total extent of the tree canopy in a city because they represent trees as a contiguous horizontal layer of leaves covering a given area.

Our streetscape metric, on the other hand, is an equally valid measure of tree cover, but is likened to that which is perceived by people at ground-level. As such, it may be better suited to evaluate the spatial variation in tree cover, fine-scale distributions of urban trees and its relationship to other scene features like buildings. Importantly, it presents a quantification of the urban tree cover consistent with the human perspective ; simply put, what people in a city see and experience. While data limitations in this initial effort prevented an analysis of the full extent of New York city, we demonstrated the applicability of the method to rapidly estimate the total or average amount of perceived tree cover at different city unit sizes. Averaging streetscape tree cover values for different city district-levels correlated well with their true percent tree canopy cover and this correlation increased with district-level unit size (i.e., from the dynamic block level to the borough level). Given its ability for rapid and high throughput, the method represents a promising tool to examine environmental – social and economic patterns within and across cities.

The high resolution and scale that the streetscape tree cover metric achieves will enable a better understanding of the role that trees and vegetation may play in urban dynamics and human health. For example, many studies have evidenced a link between human health benefits and the presence of urban tree cover Nowak *et al.* (2014); Kardan *et al.* (2015); Richardson *et al.* (2013b). However, these studies have been defined by small sample sizes and are limited in their geographic scope to a single city or a few neighbourhoods within them. The ability to quickly quantify urban tree cover for multiple cities concurrently would allow researchers to determine whether the health benefits of urban trees are pervasive or, alternatively, what specific contexts they exist or are maximized in (e.g., biogeographic conditions, local policies and management practices or socioeconomic indicators). This method permits the analysis of urban tree cover and its relationships with local conditions or social factors at much finer scales than allowed before. Rela-

tionships between urban trees and the physical and social components of cities that were previously opaque, such as how income level and social status relates to tree presence and neighbourhood aesthetics, can be investigated in depth.

3.5.2 Limitations

Systemic errors existed in the data wherein in a range of our streetscape tree cover metric's values were associated with low percent canopy cover values, and in particular 0%. We hypothesize these errors were largely produced by cases in which trees were indeed present, but too small and isolated (e.g., small trees or fine-scale structural features of the tree's shape) to be detected by the landcover mapping methods (MacFaden *et al.*, 2012). In others cases, trees may be present but were occluded in the image FOV by other objects (e.g., buildings or other trees).

The values of the weighting factors changed depending on the training dataset used to compute them, indicating that they are sensitive to sample size, sample area and the errors associated with both. Though the weighting factor values fluctuated up to 10 % with changing sample data, their proportions relative to each other (i.e., neighbours) were consistent. Much through trial and error, we attempted to optimize the weighting factors towards building final predictive models which generalized the best. Future developments of this methodology may benefit from more sophisticated techniques to learn the weighting factors such as non-linear methods.

Regardless of those systemic error cases, the method does not completely compensate for the object proximity-to-camera problem and, hence, explain all of the variation in true tree cover. To fully account for the proximity effect, the model would require additional spatial information (e.g., tree location or, as surrogate inferential features, street width or distance to the sidewalk etc). Over-predicted values of true percent canopy cover were likely due to proximity-to-camera effects

that have not been fully accounted for or to the streetscape metric's detection of small vegetation not represented in the landcover mapping methodology. Under-predicted values of true percent canopy cover were likely due to occlusion effects. We also noticed that tree shadows may, in some cases, be a source of segmentation error, in that the estimator included some areas of tree shadows as trees in a few cases. In addition, the estimator appeared somewhat sensitive to under- and over-exposed areas of the image, with underexposed areas surrounding a tree being included as tree cover, while overexposed portions of trees being excluded at times. While a rich and extensive source of data on the world's cities, using GSV images also presents limitations with the most obvious being the coverage is limited to streetscapes. At present, the GSV API has limitations on the number of daily requests and not all sampling years are available since the program begun in 2007. What's more, for most cases the streetview images do correspond with days of the year in which the growing season is active in the given geographic area, yet there may exist some locations or cities to which there are exceptions.

3.5.3 Conclusions

Quantifying the amount and distribution of trees in cities has been an open challenge due to the fine-scale data required to discern the cluttered and complex spatial heterogeneity defining them. We have addressed this challenge by presenting a novel method of quantifying urban tree cover in city streetscapes using only open source data and software, while achieving very high throughput at the city extent. We validated our streetscape metric by illustrating its ability to estimate percent tree canopy cover with accuracies comparable, and in some cases superior, to established image analysis methods used in landscape ecology.

This new method may be interpreted as a unique measure of urban tree cover – *perceived urban tree cover* – rather than a replacement for high resolution tree canopy cover maps or detailed field surveys. Though not explicitly measured,

it contributes inherent information on verticality (tree height) which is not easily obtained through current long-range remote sensing techniques. Taking advantage of the growing library of open source urban image data, the streetscape tree cover metric achieves fine spatial grain at the entire city extent. Importantly, it quantifies urban tree cover from a viewpoint in which urban citizens see and experience the urban landscape, that is the streets.

3.6 Supplementary Materials – Appendix 0.3

Appendix 0.3.1 - 0.3.2: Additional details on the computer vision algorithms to predict percent tree cover in an GSV image, the filtering procedure used to remove streets and sampling points with errors and supplementary results with tables providing the full summary statistics of all final regression models and their sample sizes.

Appendix 0.3.3: Methodology for an exploratory analysis of predicting street tree biomass.

35 m Field of View			
[HTML]C0C0C0 [HTML]C0C0C0Statistic	[HTML]C0C0C0Training Set	[HTML]C0C0C0Test Set	Training Subset
[HTML]EFEFEFformula	PTCC in FOV ~ STC + √STC + PG + PB	PTCC in FOV ~ STC + √STC + PG + PB	PTCC in FOV ~ STC + √STC + PG + PB
[HTML]EFEFEFr-square	0.74	0.73	0.81
[HTML]EFEFEFadj.rsquare	0.74	0.73	0.81
[HTML]EFEFEFRMSE	0.27	0.281	0.233
[HTML]EFEFEFMSE	0.073	0.079	0.054
[HTML]EFEFEFdf	3104	1328	1622
[HTML]EFEFEF4-fold cross validation MS	0.0731	NA	0.054
[HTML]EFEFEFmean fitted canopy cover (log)	0.822	0.81	0.641
[HTML]EFEFEFmean predicted canopy cover (log)	0.822	0.8	0.641
[HTML]EFEFEFSD fitted canopy cover (log)	0.452	0.44	0.487
[HTML]EFEFEFSD predicted canopy cover(log)	0.526	0.52	0.539
[HTML]C0C0C0 [HTML]C0C0C0	[HTML]C0C0C015 m Field of View	[HTML]C0C0C025 m Field of View	45 m Field of View
Statistic	Training Set	Training Set	Training Set
[HTML]EFEFEFformula	PTCC in FOV ~ STC + √STC + PG + PB	PTCC in FOV ~ STC + √STC + PG + PB	PTCC in FOV ~ STC + √STC + PG + PB
[HTML]EFEFEFr-square	0.68	0.7	0.67
[HTML]EFEFEFadj.rsquare	0.68	0.7	0.67
[HTML]EFEFEFRMSE	0.375	0.322	0.281
[HTML]EFEFEFMSE	0.140625	0.103684	0.078961
[HTML]EFEFEFdf	3130	3147	3146

No-neighbour 35 m Field of View*	
[HTML]C0C0C0Statistic	[HTML]C0C0C0Training Set
[HTML]EFEFEFformula	PTCC in FOV ~ STC + √STC + PG + PB
[HTML]EFEFEFr-square	0.59
[HTML]EFEFEFadj.rsquare	0.59
[HTML]EFEFEFRMSE	0.34
[HTML]EFEFEFMSE	0.1156
[HTML]EFEFEFdf	3149

Tableau 3.1: Model summary statistics for each final regression model of streetscape tree cover *vs.* the true percent tree canopy cover. Statistics are shown separately for models using the training, test and a vigorously-filtered training subset (to remove systemic errors) datasets as well as for the preliminary models testing all other FOV-levels. The lower section shows results of a regression analysis using only the un-weighted image tree cover values of the node GSV sampling points at the 35 m FOV-level (i.e., based on a single GSV image and before applying the neighbour-weighted percent tree cover score procedure). The input variable abbreviations are: **PTCC**, percent tree canopy cover; **STC**, streetscape tree cover; **PG**, percent ground; **PB**, percent building.

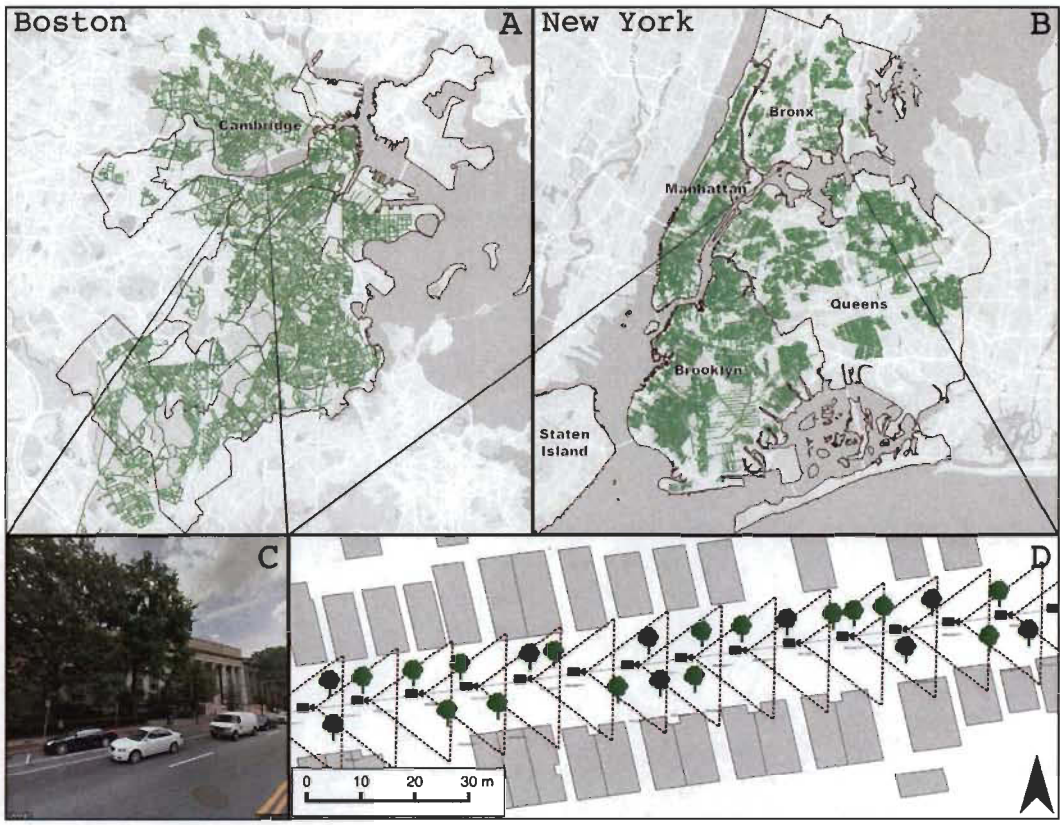

Figure 3.1: Map and examples of the GSV image sampling extent, distribution, images and sampling design. **A.** a map of the city of Boston showing the extent and distribution of the GSV sampling points (green circles). **B.** a map of the city of New York showing the extent and distribution of GSV sampling points (green circles). **C.** an example of one GSV sample image from Boston representing a streetscape scene given the image orientation parameters. **D** an example of a street segment (in this case, a east-west orientation) in New York city illustrating the GSV sampling point design wherein a sequence of neighbouring sampling points (black camera icons) are located approximately 15 m apart along the street and each have an associated field of view polygon (dashed lines; here showing just the 15 m FOV-level) with a 90° heading.

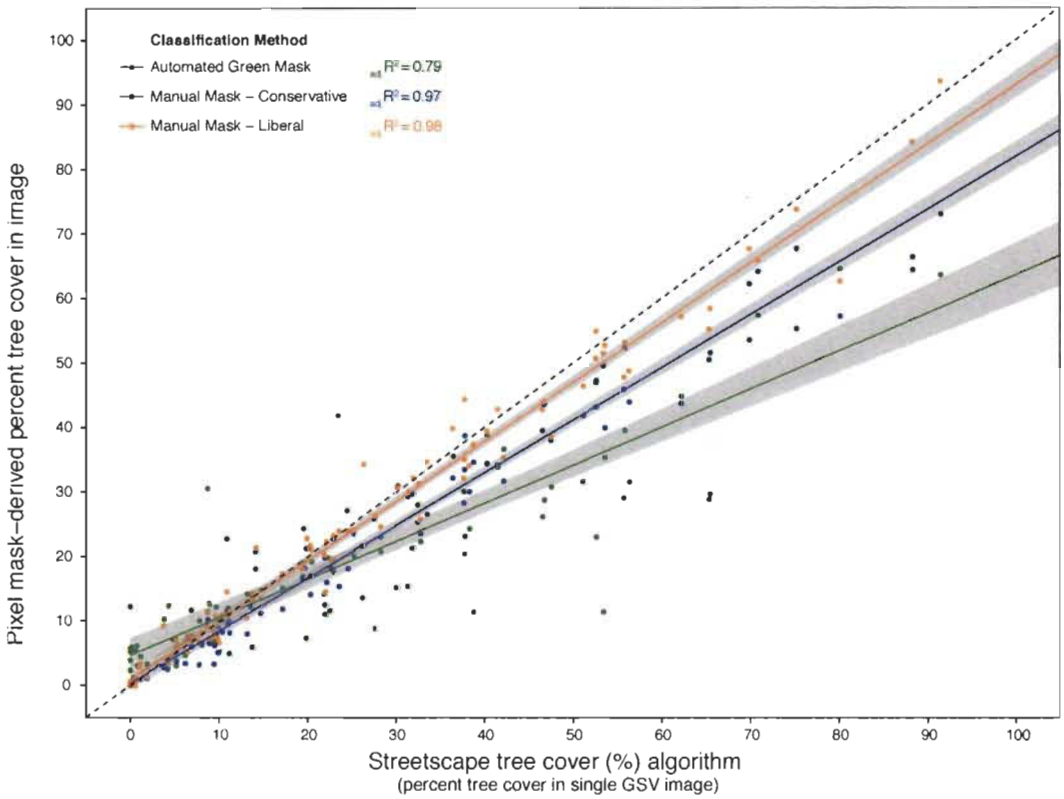

Figure 3.2: Scatter plot with fitted linear regression lines for the relationships between the percent tree cover for a single GSV image as estimated by the streetscape tree cover algorithm (x-axis) and as estimated by the three pixel-masking methods: automated green mask (green circles and line), conservative manual mask (blue circles and line) and liberal manual mask (orange circles and line). The adjusted r-square values of the regressions are shown in their matching colors. The shaded grey represent the 95 % confidence intervals.

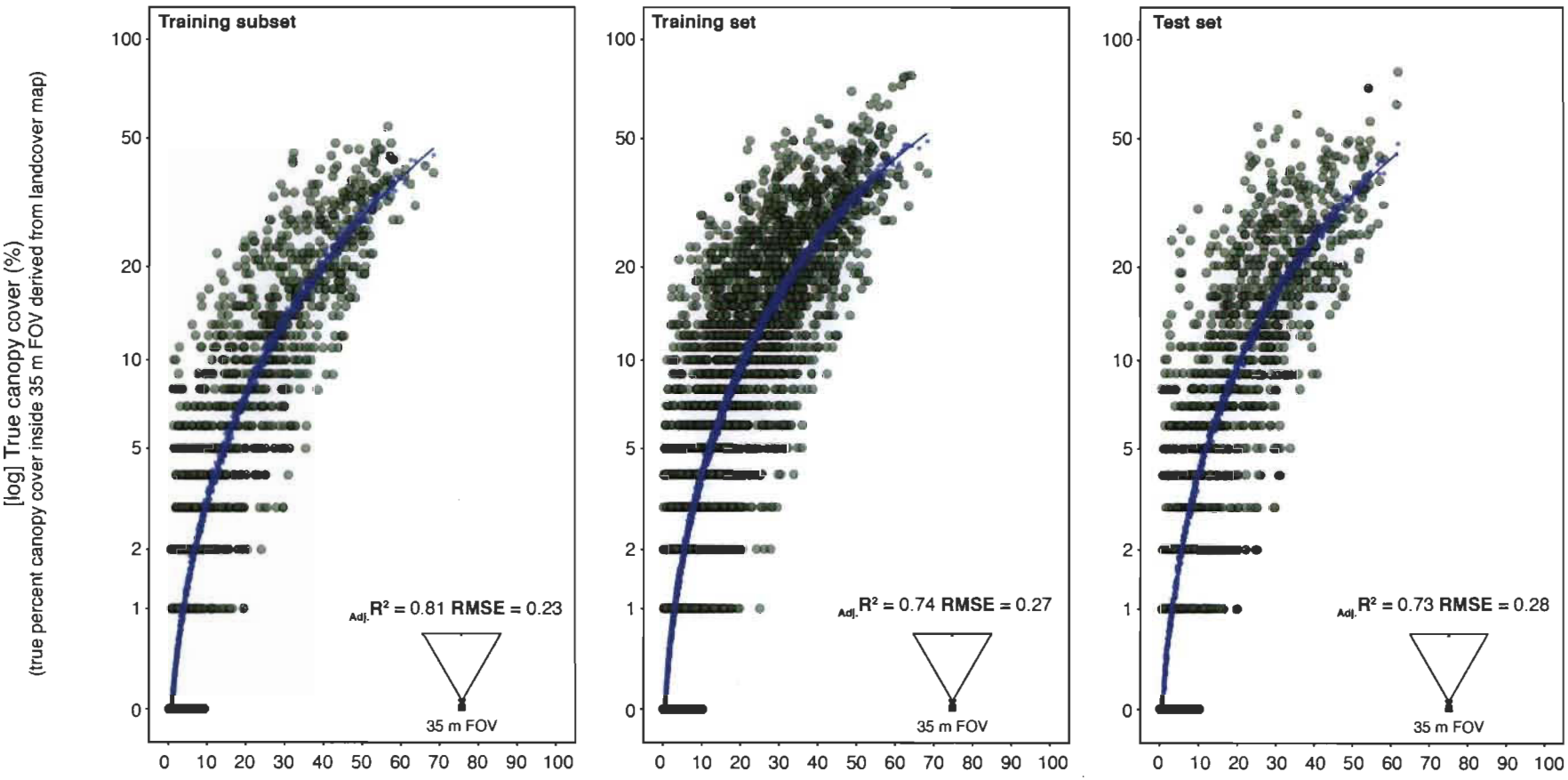
Training subset
Training set
Test set
Adj. R² = 0.81 RMSE = 0.23
Adj. R² = 0.74 RMSE = 0.27
Adj. R² = 0.73 RMSE = 0.28
35 m FOV
[log] True canopy cover (%)
(true percent canopy cover inside 35 m FOV derived from landcover map)
Streetscape tree cover (%)
(tree detection algorithm: neighbour-weighted percent tree cover in GSV images)

Figure 3.3: Relationship between the streetscape tree cover (x-axis) and the true percent tree canopy cover derived from a high resolution landcover map (y-axis displayed on a logarithmic scale) at the 35 m FOV-level for each dataset: the data subset used to learn the weighting factors (left panel), the training set using all data (centre panel) and the unseen test data (right panel). Small blue circles are the regression model's predicted values and the blue line is a smoothing line fit to the model's predicted values with a square-root polynomial. The adjusted r-square values and root mean squared-error values for the models are reported in the lower corner of each panel and Table 1.

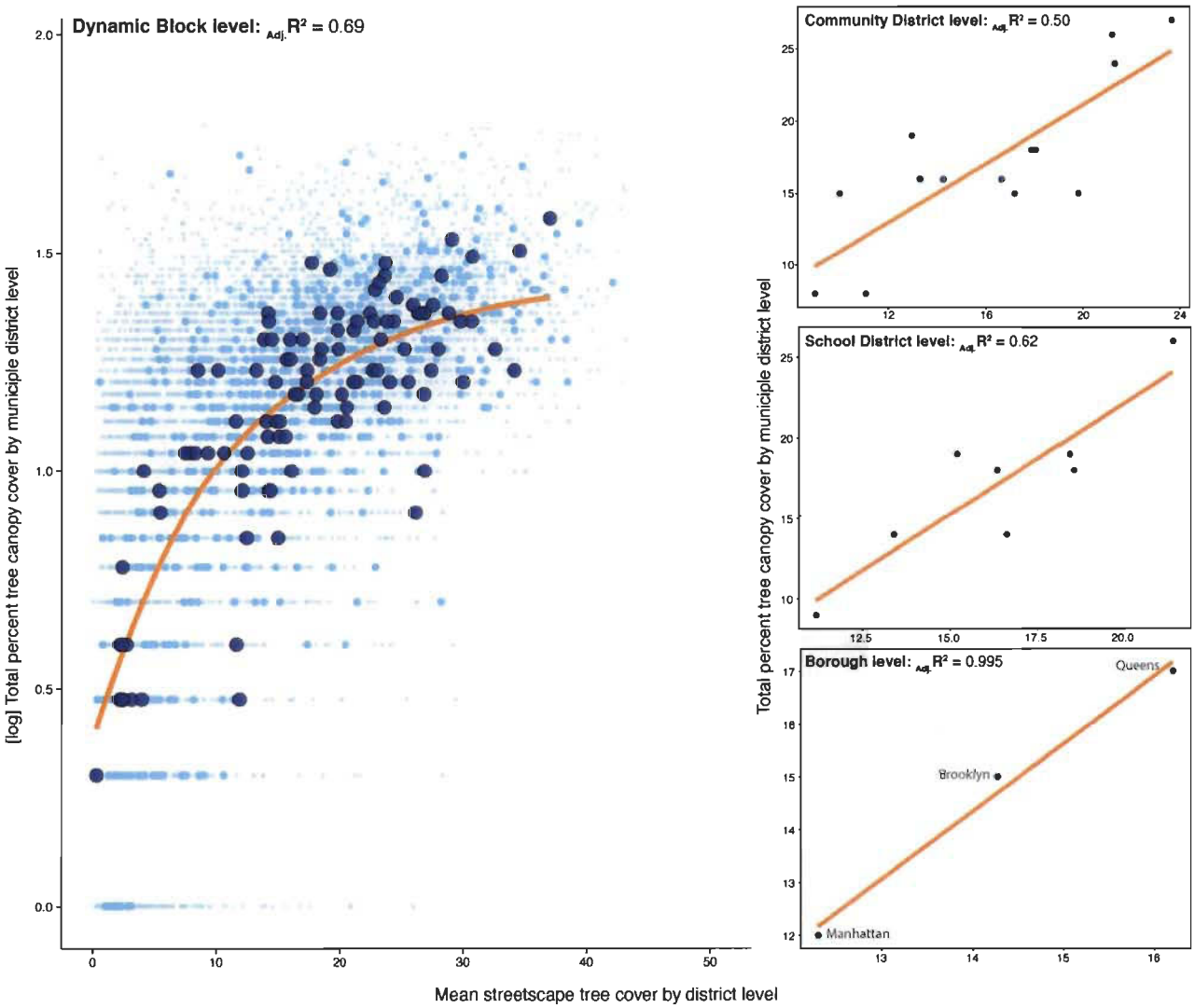
Dynamic Block level: Adj.R² = 0.69
[log] Total percent tree canopy cover by municiple district level
Mean streetscape tree cover by district level
Community District level: Adj.R² = 0.50
School District level: Adj.R² = 0.62
Borough level: Adj.R² = 0.995
Total percent tree canopy cover by municiple district level
Queens
Brooklyn
Manhattan

Figure 3.4: Relationship between the mean streetscape tree cover (x-axis) and the true percent tree canopy cover (y-axis) at different municipal district-levels of New York City: dynamic census block (large left panel; y-axis is displayed on a logarithmic scale), community district (top right panel), school district (centre right panel) and borough (lower right panel). The average unit size of each district-level is reported in Table S2 (SI, Appendix). For the dynamic block district level (left panel), the large blue circles correspond to data points retained after removing those not meeting the minimum count-per-block cutoff value (Table S2; SI, Appendix). The light-blue and smaller circles correspond to data points after increasing the minimum cutoff value (medium-sized, light blue) and all points with no cutoff (smallest, light blue). The regression model fits are shown for each level with the orange lines and the adjusted r-square values reported in the top left panel corners.

CONCLUSION

This work focussed on increasing our ability to quantify and describe the structure (spatial patterns and geometry) and dynamics (temporal patterns) of ecosystems at fine-grain resolutions with broad extents. Through it, I have uncovered generalizable patterns that shed new light on the interplay between species diversity and ecosystem functioning in terrestrial systems. I have also demonstrated novel applications of digital photography and image analysis to rapidly quantify, track and describe ecosystem features.

In Chapter 1 of this work...

I aimed to develop and present a new conceptual framework that could help reconcile the array of different EH - BD relationships that have been observed to date. The framework defines a quantitative and bounded gradient of landscape EH in order to enable cross-system comparisons of EH - BD dynamics. A statistically rigorous meta-analysis supported my hypothesis that that the direction of EH - BD relationships is contingent on the level of human footprint to which an ecosystem is subjected ; I termed this gradient of human footprint across terrestrial landscapes the *anthropocline*.

The results revealed that highly-modified and semi-natural ecosystems are characterized by a dominance of positive and negative EH-BD relationships respectively, whereas natural ecosystems show mixed responses – a general unimodal EH - BD relationship across the anthropocline gradient. When the relevant literature was viewed as a whole and the human footprint context considered, it was shown that natural ecosystems are typified, not by maximal or minimal, but by intermediate

levels of EH. Thus, a simple imperative was raised: increasing environmental heterogeneity is not always good.

After this work was completed Seiferling *et al.* (2014) several other studies made similar conclusions. It was suggested that the general shape of the EH - BD relationship is unimodal and driven by species - area relationships wherein high EH constrains species diversity due to the land area and geometry limits it imposes Allouche *et al.* (2012); Bar-Massada *et al.* (2012); Kadmon et Allouche (2007). The authors proposed that, given a finite space, more heterogeneous areas comprise less area per habitat type. Consequently, each habitat supports only smaller populations which, in turn, are prone to stochastic extinctions. The outcome of this area–heterogeneity tradeoff is manifested by a negative relationship between species abundance and heterogeneity, a positive relationship between extinction rates and heterogeneity, and a unimodal relationship between species richness and heterogeneity Bar-Massada et Wood (2014). Although the other studies did not quantify the level of human footprint represented in the data or models, it may be that the increasing EH associated with negative abundance and positive extinction effects is in fact human-driven (e.g., landscape modification and increasing pattern towards randomness as my framework dictates).

Allouche et al. (2012) also reported that, in specific systems, the shape of the relationship can be positive, negative, unimodal, or flat. Again, the level of human footprint associated with their study systems and data was not noted (i.e., where are they on the anthropocline?), but likely traversed the anthropocline gradient since it represented bird distribution data. In the case of the theoretical models the EH is simply a parameter following a distribution. Nonetheless, the finding that the shape of the EH - BD relationship can vary with specific systems or species is also in agreement with the framework and evidence I have presented here. In agreement, I found that natural areas are typified by intermediate EH

and mixed EH - BD responses.

Summarizing my results with those of the proceeding studies, we may conclude that natural systems are typified by mixed EH - BD responses which are most likely decided by species-specific properties. For example, species with high reproduction rates or with wide niches may be expected to show predominantly positive responses to increasing EH, whereas species with very narrow niches may be expected to show a predominantly negative response in a natural systems context Bar-Massada et Wood (2014). Beyond this, we must also acknowledge the implications of anthropogenic landscape modification as a source of EH. What other studies to date have left unacknowledged is that the level of human footprint may also predict the direction of species responses to EH ; na non-trivial conclusion considering that human landscape modification is now ubiquitous across the Earth. Specifically, it may extend the natural EH gradient limits in both directions (i.e., towards uniformity on the left and disorder on the right), leading to negative diversity effects as the system moves away from intermediate EH. Defining ecosystem structure and pattern in terms of empirical measures of complexity then seems preferable. Wherein natural systems are characterized by maximum complexity, any divergence from this optimal state, due to increased uniformity or disorder, results in a loss of complexity and a negative diversity response ; a general positive complexity - BD relationship.

In Chapter 2 of this work...

I switched perspectives from that of diversity as the response, to diversity as the driver of ecosystem dynamics and asked the question of whether the species diversity of forests' defining component – trees – has measurable effects on forest phenology. The results suggest that forest stand growing season length was primarily a product of the stand species composition and increased diversity lead

to the statistical averaging of species-specific phenologies – the portfolio effect. Thus, it appears that diverse overstory communities in European forests do not necessarily grow longer than the longest growing monocultures or low diversity communities.

The results also confirmed that forest phenology is not only an ecosystem response to climate, but also varies independent of climate. Specifically, I found that a substantial amount of intra-annual variation exists in the growing season length of forest stands independent of climatic and edaphic drivers and that this variation is primarily determined by the timing of fall senescence. In a novel finding, the results suggested that there was as much variation within a given bioclimatic region and forest type than there was across regions and forest types. Bioclimatic models have generally treated forested landscapes as uniformly-growing landcover, responding only to inter-annual climate variation. My findings reveal the necessity to quantify species-specific phenologies, particularly their autumn phenology, and incorporate them into terrestrial biosphere models.

Importantly, I also found that the understory community phenology was directly influenced by the overstory tree diversity. Understory communities growing under diverse tree canopies grew significantly longer than those growing under less-diverse canopies. Integrating these results with recent findings of my FunDivEUROPE colleagues, these results suggest that tree diversity may lead to increased light efficiencies that cascade from the overstory down to the understory. While evidence has illustrated that diverse stands attain higher packing densities and, hence, intercept more light at the canopy than less diverse stands, I suggest that increasing tree diversity also enhances understory light availability over the course of a growing season. I suggest that this diversity effect operates through complex and complimentary canopy structure, in both space and time, and in combination with the adaptive response of the understory plant community (i.e., understory

species composition, plasticity and turnover). However, more in depth study, particularly the explicit measurement and tracking of canopy structural traits, understory species composition and traits and high precision measures of below-canopy light availability, is required to confirm this hypothesis.

In Chapter 3 of this work...

I focussed on developing new computational tools to quantify environmental features from digital photographs. Specifically, I aimed to implement new metrics to map the distribution of trees and other vegetation in urban landscapes. The motivation for this work was to exploit new tools and data sources emerging from the "big data revolution" in order to overcome the limitations of traditional remote sensing (e.g., coarse spatio-temporal resolutions and high costs) or manual surveys (e.g., high labor and resource inputs and human error).

I tested the application of computer vision algorithms to quantify urban tree cover at the city street-level. I did so by utilizing the open-source image data of city streetscapes that is now abundant (Google Street View images). I found that a multi-step computer vision algorithm accurately segments and quantifies the percent of tree cover in streetscape images. With additional spatial modelling, I was then able to relate these single snapshots of an urban streetscape to the tree canopy cover in the area the images represent. The method is a significant advancement from previous efforts to quantify tree cover in photographs of urban scenes which used computationally simpler, single-feature metrics (i.e., counting the number of green pixels).

By making use of enormous datasets like Google Street View imagery and achieving automated rapid analysis with computer vision tools, we can quickly quantify ecosystem features at spatial and temporal scales rarely attainable before. As such, these tools will undoubtedly help to better understand ecosystem dynamics and

uncover new insights on how society interacts with and impacts the environment. This work has demonstrated a promising line of future research in the application of powerful machine learning and computer vision tools to rapidly assess and quantify environmental patterns.

Too much of the same thing, is not a good thing...(Alt. subsection title: Intermediate response hypothesis and maintaining a full portfolio) We learned from the results of *Chapter 1* that increasing environmental heterogeneity is not always good. The simplified paradigm that increasing EH represents an expansion of niche opportunities and, thus, increases diversity has been proven narrow and often incorrect. Recent evidence supports an updated hypothesis that natural systems tend towards optimizing system complexity Parrott (2010); Langton (1992); Levin (1992), equating to intermediate EH between states of uniform and random structure. Moreover, species diversity exhibits mixed responses to changing EH dependent on the system's initial state.

In a "chick or egg" causality dilemma, this intermediary and unimodal principle may not only explain a generalized EH - BD relationship, but also cascading effects of biodiversity on system processes and functioning. That is to say, we may also ask if a unimodal relationship holds true under the reciprocal perspective: species composition and diversity as a driver of system processes across a landscape. This would raise the question of whether increasing biodiversity across a landscape is always good or is ecological integrity maintained by maintaining a portfolio of diversity levels across a landscape; and if so, at what scales and relative proportions? These questions can not be fully addressed in the conclusion of this work, but if we use forest community phenology as a case study, we may gain some insights by reviewing my studies collectively (i.e., *Chapters 1 & 2.*

In the case of forest phenology, we saw that the overstory community growing sea-

son length is driven by species composition, such that increasing stand diversity likely has a statistical averaging effect on the length of the community growing season. On the other hand, monospecific stands exhibited, both, long and short-growing seasons depending on the species. Essentially a non-effect of tree diversity on growing season length if our hypothesis was to find a simple positive relationship. However, this non-effect of diversity on community phenology is not trivial and it should be highlighted that this suggests there is also no negative diversity effect. Thus, quantifying stand phenologies across a wide spatial extent, there exists a large patchwork of intra-regional variation in this key functional trait. It can be concluded that tree diversity moderates the phenological responses of tree communities, such that if we consider the full breadth of phenological types (i.e., the length of the growing season) a unimodal relationship may exist between community growing season lengths (if on the x-axis) and community species diversity (if on the y-axis).

Species diversity may promote multiple ecosystem functions (multi-functionality) since it represents a suite of the functional traits associated with each species. In the case of forest phenology, our *Chapter 2* results support this hypothesis. Likewise, recent large-scale studies and theoretical models have supported this idea; namely, diversity is positively related with multi-functionality, but specifically when moderate levels of functioning are required Van Der Plas *et al.* (2016); Allan *et al.* (2014). In line with my phenology results, van der Plas et al. (2016) concluded that a "jack-of-all-trades" effect, caused by the averaging of individual species effects on function, drives this observed pattern.

Yet the term "jack of all trades" attributes a singular importance to high species diversity or the enhancement of it, since it implies that high diversity assemblages may perform all the ecosystem functions its associated species represent; a sum of its parts so to speak. However, this diversity-centric perspective may ignore

scaling effects, as each individual in an assemblage may not act on its own so to speak. At least in the case of forest phenology, we discovered that tree diversity indeed leads to moderated community growing season lengths, but that the full breadth of phenological variation – a full portfolio – requires all levels of stand diversity to be represented. We still do not fully understand the implications of (forest) phenological heterogeneity on other system processes or feedbacks with it. However, if a management goal is to maintain the full portfolio of functional responses across a landscape (i.e., true multi-functionality) then it is also important to maintain a representative sample of low diversity communities just as it is to maintain high diversity communities.

Understanding how much and where diversity or EH is needed to maintain ecological integrity or generate resilient ecosystems is a complex task that ecologists are still struggling with. However, one can argue that it has been complicated by the use of disparate and unbounded EH measures and the singular promotion of biodiversity enhancement above all else. Clearly, in terms of conserving ecological integrity, the ideal is to preserve as much contiguous landscapes as possible in their pristine natural states. Given the current human population, our resource demands and technologies this is not realistic. Perhaps our research efforts should be devoted to developing tools to better quantify and define representative analogues of natural community types and assemblages, establish the bounded limits (i.e., size and relative proportions) of those areas in order to maintain a portfolio of ecosystem functions and better integrate this systems-level perspective into management policies.

Where to go next and promising explorations...

Particularly through the development and application of automated image-based metrics of environmental features, this work has identified several open and per-

tinent research questions as well as promising tools to develop and apply further.

First, tracking seasonal growth across forest types at fine spatial and temporal grain revealed intra-annual phenological variation that likely has important implications to several key ecosystem functions such as annual carbon sequestration. As such, this research has raised two pertinent questions that urge further study:

1. how does the heterogeneity in phenology exhibited by forest communities scale to the landscape level?
2. independent of climatic drivers, how much intra-annual phenological variation exists between trees of the same species?
3. what are the averaging functions that determine forest community phenology via the individual contributions of species-specific phenologies?

Beginning by answering these questions, we can work towards building more accurate biosphere models and a better understanding of how human and climate induced changes to temperate forests will affect critical the functions that maintain ecological ecosystem services.

Likewise, the high temporal resolution provided by the time-lapse imagery methods has provided new levels of data on the intra-annual growth patterns of forest vegetation communities, as well as insights into the top-down controls of canopy trees on the dynamics of communities growing below them. For example, the methods revealed that forests stands of different composition and diversity levels displayed seasonal growth patterns which appear to fall into a few distinct shapes (*SI Appendix — Conclusions* Fig. C1):

i) *smooth hump*, with a gradual green up phase, extended high green phase and a gradual offset phase;

ii) *skewed-left peak*, with a sharp green up phase, short high green phase and gradual offset and;

iii) *central peak*, with a sharp green up phase, short high green phase and sharp offset phase.

How these differing seasonal growth patterns of the forest overstory relate to their species composition, functional types and richness remains unexplored. Applying time series pattern recognition methods to these data should provide insights into the intrinsic mechanisms driving both species-specific and community-level phenology, help define phenological functional types and determine how tree species richness may effect intra-annual growth patterns. For example, does increased tree species richness act to moderate the growth patterns (i.e., smooth humps rather than sharp peaks) through statistical averaging effects and, in turn, is seasonal growth pattern related to stabilizing effects on system processes?

Another promising line of research that has emerged from these results relates to the hierarchical dynamics of tree diversity and crown structure on the growth patterns and composition of the plant communities growing below. While a positive effect of tree diversity on the growing season of understory communities was identified, there remains much to explore. I have suggested that this relationship is driven by a coupled canopy light interception – understory light availability balance in both space and time. Future research can be devoted to a closer examination of this relationship, including a thorough quantification of seasonal below-canopy light availability. For example, just as we extracted a time series of greenness from the time-lapse imagery, we can extract a time series of below-canopy luminance (*SI Appendix — Conclusions* Fig. C2) from the image parameters (exposure, shutter speed and aperture values). Quantifying specific features of the seasonality of understory light should shed further light on how canopy structure and tree richness determines the understory light environment in space and time. Certainly these results justify an effort to measure seasonal below-canopy light availability in a more direct and accurate manner such as the deployment of low cost light sensors

in the FunDivEUROPE plot network.

Furthermore, the results advocate examining how understory species richness, composition and functional types (e.g., growth form and life cycle) may interact with tree phenology. While there was no effect of tree species richness on understory richness, a preliminary look indicates that there may be a significant positive effect of mean annual understory light availability on the understory species richness (*SI Appendix — Conclusions* Fig. C2). Together with other environmental conditions, light availability may be a key parameter explaining overstory - understory diversity effects.

Second, the application of computer vision algorithms and standard digital photographs to measure, map and track environmental features represents a new line of remote sensing and research in ecology and social ecology. I demonstrated that computer vision techniques have the ability to describe and quantify tree cover in an image-represented scene. However, computer vision has the potential for much more. It is my aim to follow this line of research and work to apply computer vision to accurately quantify higher-level features such as tree functional (e.g., deciduous vs. coniferous) or taxonomic (species) type, height, canopy area and trunk width from standard 2D digital photographs like those of GSV.

Towards this end, an exploratory analysis using the New York City GSV dataset presented in *Chapter 3* already demonstrates the potential of computer vision models to estimate tree biomass in urban landscapes. I estimated the total aboveground biomass of all New York City street trees within each GSV sampling point FOV using a preliminary subset of the 2015 NYC Parks Street Tree Census Data NYC Parks (2016). By compiling a set of diameter-based allometric regression equations for estimating total aboveground biomass and applying them to each tree in the dataset, I computed a rough estimate of tree aboveground biomass [1].

These estimated street tree biomass values were then summed for all trees inside each GSV sampling point FOV and, replacing the percent tree canopy cover variable, were inputed as the response variable in the regression models described in *Chapter 3*.

Though the use of allometric equations to estimate urban tree biomass will be prone to error, the streetscape tree cover metric explained a substantial portion of the variation in the street tree biomass (*SI Appendix — Conclusions* Fig. C1). In fact, the method proved strikingly accurate at predicting street tree biomass when using the manually-clipped data subset. Granted, this data subset was relatively sparse ($n = 142$), however it also represents the cases in which the systemic errors were minimized the most through manual inspection and clipping. After all, such errors were frequent since the tree survey data only contains records for official city street trees. Hence, cases where non-surveyed trees or vegetation were present in an area but not measured were likely common. With higher quality biomass data of urban street trees we could expect even higher levels of predictive power from our streetscape-image method.

This early evidence that we may automatically derive accurate estimates of urban tree biomass from simple 2D digital photographs poses a very promising tool for numerous urban forestry applications. After all, tree biomass and volume are typically the most important statistics in forest management and also in relation to ecosystem services such as carbon sequestration. Having demonstrated its potential, a next step will be to to develop these computer vision techniques further by refining the algorithms and implementing new advancements in computer vision in order to automatically quantify, identify and map individual urban trees and to track tree health.

---

1. Full details on this methodology and the source of the allometric equations can be found in Appendix 3–B.

Of course, these methodologies need not be limited to urban systems. A promising research direction will be to test their abilities in the complex, crowded and often "blurry" domain of natural ecosystems ; a challenge computer vision researchers will likely be eager to engage. In particular, the power of machine learning and computer vision to model complex and non-linear patterns translates particularly well to complex natural systems and to the concept of ecological indicators Proulx et Parrott (2009) ; holistic measures of system functioning and integrity that often incorporate some intuitive or multi-dimensional aspects which, until now, only a trained human eye could determine.

BIBLIOGRAPHIE

Abdulkadir, A., Dossa, L. H., Lompo, D. J.-P., Abdu, N. et van Keulen, H. (2012). Characterization of urban and peri-urban agroecosystems in three West African cities. *International Journal of Agricultural Sustainability, 10*(4), 289–314. http://dx.doi.org/10.1080/14735903.2012.663559. Récupéré de http://www.tandfonline.com/doi/abs/10.1080/14735903.2012.663559

Abrams, P. A. (1995). Monotonic or unimodal diversity-productivity gradients: What does competition theory predict ? *Ecology, 76*(7), 2019–2027.

Adamsen, F. G., Pinter, P. J., Barnes, E. M., LaMorte, R. L., Wall, G. W., Leavitt, S. W. et Kimball, B. A. (1999). Measuring Wheat Senescence with a Digital Camera. *Crop Science, 39*(3), 719. http://dx.doi.org/10.2135/cropsci1999.0011183X003900030019x. Récupéré de https://www.crops.org/publications/cs/abstracts/39/3/CS0390030719

Ahmad, I., Naeem, A. M., Islam, M. et Nawaz, S. (2007). Weed classification using histogram maxima with threshold for selective herbicide applications. Dans *19th International Conference on Computer, Information and Systems Science and Engineering (CISSE 2007), Bangkok (Thailand)*, volume 19, p. 331À334.

Ahrends, H. E., Brügger, R., Stöckli, R., Schenk, J., Michna, P., Jeanneret, F., Wanner, H. et Eugster, W. (2008). Quantitative phenological observations of a mixed beech forest in northern Switzerland with digital photography. *Journal of Geophysical Research, 113*(G4), G04004. http://dx.doi.org/10.1029/2007JG000650. Récupéré de http://doi.wiley.com/10.1029/2007JG000650

Allan, E., Bossdorf, O., Dormann, C. F., Prati, D., Gossner, M. M., Tscharntke, T., Blüthgen, N., Bellach, M., Birkhofer, K., Boch, S., Böhm, S., Börschig, C., Chatzinotas, A., Christ, S., Daniel, R., Diekötter, T., Fischer, C., Friedl, T., Glaser, K., Hallmann, C., Hodac, L., Hölzel, N., Jung, K., Klein, A. M., Klaus, V. H., Kleinebecker, T., Krauss, J., Lange, M., Morris, E. K., Müller, J., Nacke, H., Pasalic, E., Rillig, M. C., Rothenwöhrer, C., Schall, P., Scherber, C., Schulze, W., Socher, S. A., Steckel, J., Steffan-Dewenter, I., Türke, M., Weiner, C. N., Werner, M., Westphal, C., Wolters, V., Wubet, T., Gockel, S., Gorke, M., Hemp, A., Renner, S. C., Schöning, I., Pfeiffer, S., König-Ries, B., Buscot, F., Linsenmair, K. E., Schulze, E.-D., Weisser, W. W. et Fischer, M. (2014). Interannual variation in land-use intensity enhances grassland multidiversity. *Proceedings of the National Academy of Sciences of the United States of America*, *111*(1), 308–13. http://dx.doi.org/10.1073/pnas.1312213111. Récupéré de http://lup.lub.lu.se/search/record/4319033

Allouche, O., Kalyuzhny, M., Moreno-Rueda, G., Pizarro, M. et Kadmon, R. (2012). Area–heterogeneity tradeoff and the diversity of ecological communities. *Proceedings of the National Academy of Sciences*, *109*(43), 17495–17500.

Amarasekare, P. (2003). Competitive coexistence in spatially structured environments: a synthesis. *Ecology Letters*, *6*(12), 1109–1122. http://dx.doi.org/10.1046/j.1461-0248.2003.00530.x. Récupéré de http://dx.doi.org/10.1046/j.1461-0248.2003.00530.x

Anderson, M. et Braak, C. T. (2003). Permutation tests for multi-factorial analysis of variance. *Journal of Statistical Computation and Simulation*, *73*(2), 85–113. http://dx.doi.org/10.1080/00949650215733. Récupéré de http://www.tandfonline.com/doi/abs/10.1080/00949650215733

Augspurger, C. K. (2008). Early spring leaf out enhances growth

and survival of saplings in a temperate deciduous forest. *Oecologia*, *156*(2), 281–286. Récupéré de http://www.scopus.com/inward/record.url?eid=2-s2.0-43049094350{&}partnerID=40{&}md5=1fe3c1b86d06d302a816dbe9f74f42c0

Augspurger, C. K. (2013). Reconstructing patterns of temperature, phenology, and frost damage over 124 years: Spring damage risk is increasing. *Ecology*, *94*(1), 41–50. Récupéré de http://www.scopus.com/inward/record.url?eid=2-s2.0-84876143445{&}partnerID=40{&}md5=05a3a77cecc2eb8d0f04e722fcbf4e8f

Augspurger, C. K. et Bartlett, E. A. (2003). Differences in leaf phenology between juvenile and adult trees in a temperate deciduous forest. *Tree Physiology*, *23*(8), 517–525.

Baeten, L., Verheyen, K., Wirth, C., Bruelheide, H., Bussotti, F., Finer, L., Jaroszewicz, B., Selvi, F., Valladares, F., Allan, E., Ampoorter, E., Auge, H., Avacariei, D., Barbaro, L., Barnoaiea, I., Bastias, C. C., Bauhus, J., Beinhoff, C., Benavides, R., Benneter, A., Berger, S., Berthold, F., Boberg, J., Bonal, D., Bruggemann, W., Carnol, M., Castagneyrol, B., Charbonnier, Y., Checko, E., Coomes, D., Coppi, A., Dalmaris, E., Danila, G., Dawud, S. M., de Vries, W., De Wandeler, H., Deconchat, M., Domisch, T., Duduman, G., Fischer, M., Fotelli, M., Gessler, A., Gimeno, T. E., Granier, A., Grossiord, C., Guyot, V., Hantsch, L., Hättenschwiler, S., Hector, A., Hermy, M., Holland, V., Jactel, H., Joly, F. X., Jucker, T., Kolb, S., Koricheva, J., Lexer, M. J., Liebergesell, M., Milligan, H., Muller, S., Muys, B., Nguyen, D., Nichiforel, L., Pollastrini, M., Proulx, R., Rabasa, S., Radoglou, K., Ratcliffe, S., Raulund-Rasmussen, K., Seiferling, I., Stenlid, J., Vesterdal, L., von Wilpert, K., Zavala, M. A., Zielinski, D. et Scherer-Lorenzen, M. (2013). A novel comparative research platform designed to determine the functional significance of tree species diversity

in European forests. *Perspectives in Plant Ecology, Evolution and Systematics*, *15*(5), 281–291.

Bakker, N., Dubbeling, M., Gündel, S., Sabel Koschella, U. et de Zeeuw, H. (2000). *Growing cities, growing food: urban agriculture on the policy agenda. A reader on urban agriculture*. DSE.

Balvanera, P. et Aguirre, E. (2006). Tree diversity, environmental heterogeneity, and productivity in a Mexican tropical dry forest. *Biotropica*, *38*(4), 479–491.

Bar-Massada, A. (2015). Immigration rates and species niche characteristics affect the relationship between species richness and habitat heterogeneity in modeled meta-communities. *PeerJ*, *3*, e832. http://dx.doi.org/10.7717/peerj.832. Récupéré de https://peerj.com/articles/832

Bar-Massada, A. et Wood, E. M. (2014). The richness-heterogeneity relationship differs between heterogeneity measures within and among habitats. *Ecography*, *37*(6), 528–535. http://dx.doi.org/10.1111/j.1600-0587.2013.00590.x

Bar-Massada, A., Wood, E. M., Pidgeon, A. M. et Radeloff, V. C. (2012). Complex effects of scale on the relationships of landscape pattern versus avian species richness and community structure in a woodland savanna mosaic. *Ecography*, *35*(5), 393–411. http://dx.doi.org/10.1111/j.1600-0587.2011.07097.x. Récupéré de http://dx.doi.org/10.1111/j.1600-0587.2011.07097.x

Barnosky, A. D., Hadly, E. A., Bascompte, J., Berlow, E. L., Brown, J. H., Fortelius, M., Getz, W. M., Harte, J., Hastings, A., Marquet, P. A., Martinez, N. D., Mooers, A., Roopnarine, P., Vermeij, G., Williams, J. W., Gillespie, R., Kitzes, J., Marshall, C., Matzke, N., Mindell, D. P., Revilla, E. et Smith, A. B. (2012). Approaching a state shift in Earth/'s biosphere. *Nature*, *486*(7401), 52–58. Récupéré de http://dx.doi.org/10.1038/nature11018

Bater, C. W., Coops, N. C., Wulder, M. A., Nielsen, S. E., McDermid, G. et Stenhouse, G. B. (2011). Design and installation of a camera network across an elevation gradient for habitat assessment. *Instrumentation Science & Technology*, *39*(3), 231–247. http://dx.doi.org/10.1080/10739149.2011.564700

Bennett, L. T., Judd, T. S. et Adams, M. A. (2000). Close-Range Vertical Photography for Measuring Cover Changes in Perennial Grasslands. *Journal of Range Management*, *53*(6), 634. http://dx.doi.org/10.2307/4003159. Récupéré de http://www.jstor.org/stable/4003159?origin=crossref

Breiman, L. (2001). Random Forests. *Machine Learning*, *45*(1), 5–32. http://dx.doi.org/10.1023/A:1010933404324. Récupéré de http://link.springer.com/article/10.1023/A{%}3A1010933404324

Cardinale, B. J., Duffy, J. E., Gonzalez, A., Hooper, D. U., Perrings, C., Venail, P., Narwani, A., Mace, G. M., Tilman, D., Wardle, D. A., Kinzig, A. P., Daily, G. C., Loreau, M., Grace, J. B., Larigauderie, A., Srivastava, D. S. et Naeem, S. (2012). Biodiversity loss and its impact on humanity. *Nature*, *486*(7401), 59–67. http://dx.doi.org/10.1038/nature11148. Récupéré de http://dx.doi.org/10.1038/nature11148

Ceballos, G., Ehrlich, P. R., Barnosky, A. D., García, A., Pringle, R. M. et Palmer, T. M. (2015). Accelerated modern human–induced species losses: Entering the sixth mass extinction. *Science Advances*, *1*(5). Récupéré de http://advances.sciencemag.org/content/1/5/e1400253.abstract

Chmielewski, F.-M. et Rotzer, T. (2001). Phenological maps of Europe. *Climate Research*, *18*(November), 249–257.

Churkina, G., Schimel, D., Braswell, B. H. et Xiao, X. (2005). Spatial analysis of growing season length control over net ecosystem exchange. *Glo-*

bal Change ..., *11*, 1777–1787. http://dx.doi.org/10.1111/j.1365-2486.2005.01012.x. Récupéré de http://onlinelibrary.wiley.com/doi/10.1111/j.1365-2486.2005.001012.x/full

Crimmins, M. et Crimmins, T. (2008). Monitoring Plant Phenology Using Digital Repeat Photography. *Environmental Management*, *41*(6), 949–958. http://dx.doi.org/10.1007/s00267-008-9086-6. Récupéré de http://dx.doi.org/10.1007/s00267-008-9086-6

Dickinson, J. L., Zuckerberg, B. et Bonter, D. N. (2010). Citizen Science as an Ecological Research Tool: Challenges and Benefits. *Annual Review of Ecology, Evolution, and Systematics*, *41*, 149–172. Récupéré de http://www.jstor.org/stable/27896218

Diez, J. M., Ibáñez, I., Miller-Rushing, A. J., Mazer, S. J., Crimmins, T. M., Crimmins, M. a., Bertelsen, C. D. et Inouye, D. W. (2012). Forecasting phenology: from species variability to community patterns. *Ecology letters*, *15*(6), 545–53. http://dx.doi.org/10.1111/j.1461-0248.2012.01765.x. Récupéré de http://www.ncbi.nlm.nih.gov/pubmed/22433120

Dragoni, D., Schmid, H. P., Wayson, C. A., Potter, H., Grimmond, C. S. B. et Randolph, J. C. (2011). Evidence of increased net ecosystem productivity associated with a longer vegetated season in a deciduous forest in south-central Indiana, USA. *Global Change Biology*, *17*(2), 886–897. http://dx.doi.org/10.1111/j.1365-2486.2010.02281.x

Dufour, A., Gadallah, F., Wagner, H. H., Guisan, A. et Buttler, A. (2006). Plant species richness and environmental heterogeneity in a mountain landscape: Effects of variability and spatial configuration. *Ecography*, *29*(4), 573–584. Récupéré de http://www.scopus.com/

inward/record.url?eid=2-s2.0-33845597335{&}partnerID=40{&}md5=3a555300e0356694f34d5ddab324bc4d

El-Faki, M. S., Zhang, N. et Peterson, D. E. (2000). Factors affecting color-based weed detection. *Transactions of the ASAE*, *43*(4), 1001–1009. http://dx.doi.org/10.13031/2013.2968. Récupéré de http://elibrary.asabe.org/abstract.asp??JID=3{&}AID=2968{&}CID=t2000{&}v=43{&}i=4{&}T=1

Endler, J. A. (1993). The Color of Light in Forests and Its Implications. *Ecological Monographs*, *63*(1), 1–27. http://dx.doi.org/10.2307/2937121. Récupéré de http://doi.wiley.com/10.2307/2937121

Fahrig, L., Baudry, J., Brotons, L., Burel, F. G., Crist, T. O., Fuller, R. J., Sirami, C., Siriwardena, G. M. et Martin, J. L. (2011). Functional landscape heterogeneity and animal biodiversity in agricultural landscapes. *Ecology Letters*, *14*(2), 101–112. http://dx.doi.org/10.1111/j.1461-0248.2010.01559.x

Fath, B. D., Jørgensen, S. E., Patten, B. C. et Straškraba, M. (2004). Ecosystem growth and development. *BioSystems*, *77*(1), 213–228.

Felzenszwalb, P. F. et Huttenlocher, D. P. (2004). Efficient Graph-Based Image Segmentation. *International Journal of Computer Vision*, *59*(2), 167–181. http://dx.doi.org/10.1023/B:VISI.0000022288.19776.77. Récupéré de http://link.springer.com/10.1023/B:VISI.0000022288.19776.77

Franklin, J. F. et Van Pelt, R. (2004). Spatial Aspects of Structural Complexity in Old-Growth Forests. *Journal of Forestry*, *102*(3), 22–28. Récupéré de http://www.ingentaconnect.com/content/saf/jof/2004/00000102/00000003/art00008

Fridley, J. D. (2012). Extended leaf phenology and the autumn niche in deciduous

forest invasions. *Nature*, *485*(7398), 359–U105. http://dx.doi.org/10.1038/nature11056

Fuller, R. A. et Gaston, K. J. (2009). The scaling of green space coverage in European cities. *Biology letters*, *5*(3), 352–5. http://dx.doi.org/10.1098/rsbl.2009.0010. Récupéré de http://rsbl.royalsocietypublishing.org/content/5/3/352

Gillespie, A. R., Kahle, A. B. et Walker, R. E. (1987). Color enhancement of highly correlated images. II. Channel ratio and "chromaticity" transformation techniques. *Remote Sensing of Environment*, *22*(3), 343–365. http://dx.doi.org/10.1016/0034-4257(87)90088-5. Récupéré de http://linkinghub.elsevier.com/retrieve/pii/0034425787900885

Glaeser, E. L., Kominers, S. D., Luca, M. et Naik, N. (2015). Big Data and Big Cities : The Promises and limitations of improved measures of urban life. *NBER Working Paper*. http://dx.doi.org/10.3386/w21778

Google Inc. (2014). Google Street View Image API. Récupéré de https://developers.google.com/maps/documentation/streetview/intro?hl=en

Graham, E. A., Riordan, E. C., Yuen, E. M., Estrin, D. et Rundel, P. W. (2010). Public Internet-connected cameras used as a cross-continental ground-based plant phenology monitoring system. *Global Change Biology*, *16*(11), 3014–3023.

Granados, J. A., Graham, E. A., Bonnet, P., Yuen, E. M. et Hamilton, M. (2013). EcoIP: An open source image analysis toolkit to identify different stages of plant phenology for multiple species with pan–tilt–zoom cameras. *Ecological Informatics*, *15*(0), 58–65. http://dx.doi.org/http://dx.doi.org/10.1016/j.ecoinf.2013.03.002. Récupéré de http://www.sciencedirect.com/science/article/pii/S157495411300023X

Grossiord, C., Granier, A., Ratcliffe, S., Bouriaud, O., Bruelheide, H., Checko, E., Forrester, D. I., Dawud, S. M., Finer, L., Pollastrini, M., Scherer-Lorenzen, M., Valladares, F., Bonal, D. et Gessler, A. (2014). Tree diversity does not always improve resistance of forest ecosystems to drought. *Proceedings of the National Academy of Sciences*, *111*(41), 14812–14815. http://dx.doi.org/10.1073/pnas.1411970111. Récupéré de http://www.pnas.org/content/111/41/14812{%}5Cnhttp://www.ncbi.nlm.nih.gov/pubmed/25267642{%}5Cnhttp://www.pnas.org.are.uab.cat/content/111/41/14812

Hector, A. et Loreau, M. (2000). Large-scale biodiversity experiments. *Encyclopedia of Biodiversity*, *4*, 583–589. http://dx.doi.org/10.1016/B978-0-12-384719-5.00228-8

Hoiem, D., Efros, A. et Hebert, M. (2005). Geometric context from a single image. Dans *Tenth IEEE International Conference on Computer Vision (ICCV'05) Volume 1*, volume 1, 654–661 Vol. 1. IEEE. http://dx.doi.org/10.1109/ICCV.2005.107. Récupéré de http://ieeexplore.ieee.org/articleDetails.jsp?arnumber=1541316

Homer, C., Dewitz, J., Fry, J., Coan, M., Hossain, N., Larson, C., Herold, N., McKerrow, A., VanDriel, J. N. et Wickham, J. (2007). Completion of the 2001 national land cover database for the counterminous United States. *Photogrammetric Engineering and Remote Sensing*, *73*(4), 337.

Homer, C. G., Dewitz, J. A., Yang, L., Jin, S., Danielson, P., Xian, G., Coulston, J., Herold, N. D., Wickham, J. D. et Megown, K. (2015). Completion of the 2011 National Land Cover Database for the conterminous United States-Representing a decade of land cover change information. *Photogrammetric Engineering and Remote Sensing*, *81*(5), 345–354.

Hubbell, S. P. (2001). No Title. *The Unified Neutral Theory of Biodiversity and Biogeography.*

Isbell, F. I., Polley, H. W. et Wilsey, B. J. (2009). Biodiversity, productivity and the temporal stability of productivity: patterns and processes. *Ecology letters*, *12*(5), 443–51. http://dx.doi.org/10.1111/j.1461-0248.2009.01299.x. Récupéré de http://www.ncbi.nlm.nih.gov/pubmed/19379138

Ishii, H. et Asano, S. (2010). The role of crown architecture, leaf phenology and photosynthetic activity in promoting complementary use of light among coexisting species in temperate forests. *Ecological Research*, *25*(4), 715–722. http://dx.doi.org/10.1007/s11284-009-0668-4

Jackson, R. B., Lechowicz, M. J., Li, X. et Mooney, H. A. (2001). Phenology, growth, and allocation in global terrestrial productivity. *Terrestrial Global Productivity*, 61–82.

Jenkins, J. C., Chojnacky, D. C., Heath, L. S. et Birdsey, R. A. (2003). National-scale biomass estimators for United States tree species. *Forest Science*, *49*(1), 12–35.

Jennions, M. D. et Moller, A. P. (2002). Publication bias in ecology and evolution: an empirical assessment using the 'trim and fill' method. *Biological Reviews of the Cambridge Philosophical Society*, *77*(2), 211–222. http://dx.doi.org/10.1017/S1464793101005875. Récupéré de http://journals.cambridge.org/abstract{_}S1464793101005875

Jeong, S. et Medvigy, D. (2014). Macroscale prediction of autumn leaf coloration throughout the continental United States. *Global Ecology and Biogeography.*

Johnson, M. P., Frost, N. J., Mosley, M. W. J., Roberts, M. F. et Hawkins, S. J. (2003). The area-independent effects of habitat complexity on biodiversity vary

between regions. *Ecology Letters*, *6*(2), 126–132. Récupéré de http://www.scopus.com/inward/record.url?eid=2-s2.0-0037314738{&}partnerID=40{&}md5=41048fd215a9934b2f848a96c254416e

Jucker, T., Bouriaud, O., Avacaritei, D., Danila, I., Duduman, G., Valladares, F. et Coomes, D. a. (2014). Competition for light and water play contrasting roles in driving diversity-productivity relationships in Iberian forests. *Journal of Ecology*, *102*, 1202–1213. http://dx.doi.org/10.1111/1365-2745.12276

Jucker, T., Bouriaud, O. et Coomes, D. A. (2015). Crown plasticity enables trees to optimize canopy packing in mixed-species forests. *Functional Ecology*, n/a–n/a. http://dx.doi.org/10.1111/1365-2435.12428. Récupéré de http://doi.wiley.com/10.1111/1365-2435.12428

Kadmon, R. et Allouche, O. (2007). Integrating the effects of area, isolation, and habitat heterogeneity on species diversity: A unification of island biogeography and niche theory. *American Naturalist*, *170*(3), 443–454. Récupéré de http://www.scopus.com/inward/record.url?eid=2-s2.0-34548183780{&}partnerID=40{&}md5=b3dfffb57f3c5f244b8f228631a69500

Kardan, O., Gozdyra, P., Misic, B., Moola, F., Palmer, L. J., Paus, T. et Berman, M. G. (2015). Neighborhood greenspace and health in a large urban center. *Scientific reports*, *5*, 11610. http://dx.doi.org/10.1038/srep11610. Récupéré de http://www.nature.com/srep/2015/150709/srep11610/full/srep11610.html

Keesing, F., Belden, L. K., Daszak, P., Dobson, A., Harvell, C. D., Holt, R. D., Hudson, P., Jolles, A., Jones, K. E., Mitchell, C. E., Myers, S. S., Bogich, T. et Ostfeld, R. S. (2010). Impacts of biodiversity on the emergence and transmission of infectious diseases. *Nature*, *468*(7324),

647–652. Récupéré de http://dx.doi.org/10.1038/nature09575http://www.nature.com/nature/journal/v468/n7324/abs/nature09575.html{#}supplementary-information

Kerr, J. T. (2001). Butterfly species richness patterns in Canada: Energy, heterogeneity, and the potential consequences of climate change. *Conservation Ecology*, *5*(1), XXIX–XXX.

Kerr, J. T. et Packer, L. (1997). Habitat heterogeneity as a determinant of mammal species richness in high-energy regions. *Nature*, *385*(6613), 252–254. Récupéré de http://www.scopus.com/inward/record.url?eid=2-s2.0-0030620651{&}partnerID=40{&}md5=7de7f385b2b0d5ef65f751165377f715

Kovalenko, K., Thomaz, S. et Warfe, D. (2012). Habitat complexity: approaches and future directions. *Hydrobiologia*, *685*(1), 1–17. http://dx.doi.org/10.1007/s10750-011-0974-z. Récupéré de http://dx.doi.org/10.1007/s10750-011-0974-z

Kudo, G., Ida, T. Y. et Tani, T. (2008). Linkages between phenology, pollination, photosynthesis, and reproduction in deciduous forest understory plants. *Ecology*, *89*(2), 321–331. http://dx.doi.org/10.1890/06-2131.1

Kühn, I. et Klotz, S. (2006). Urbanization and homogenization – Comparing the floras of urban and rural areas in Germany. *Biological Conservation*, *127*(3), 292–300. http://dx.doi.org/http://dx.doi.org/10.1016/j.biocon.2005.06.033. Récupéré de http://www.sciencedirect.com/science/article/pii/S0006320705003605

Kumar, S., Simonson, S. E. et Stohlgren, T. J. (2009). Effects of spatial heterogeneity on butterfly species richness in Rocky Mountain Na-

tional Park, CO, USA. *Biodiversity and Conservation*, *18*(3), 739–763. Récupéré de http://www.scopus.com/inward/record.url?eid=2-s2.0-60449112979{&}partnerID=40

Kuussaari, M., Bommarco, R., Heikkinen, R. K., Helm, A., Krauss, J., Lindborg, R., Öckinger, E., Pärtel, M., Pino, J., Rodà, F., Stefanescu, C., Teder, T., Zobel, M. et Steffan-Dewenter, I. (2009). Extinction debt: a challenge for biodiversity conservation. *Trends in Ecology & Evolution*, *24*(10), 564–571. http://dx.doi.org/http://dx.doi.org/10.1016/j.tree.2009.04.011. Récupéré de http://www.sciencedirect.com/science/article/pii/S0169534709001918

Laanisto, L., Tamme, R., Hiiesalu, I., Szava-Kovats, R., Gazol, A. et Pärtel, M. (2013). Microfragmentation concept explains non-positive environmental heterogeneity–diversity relationships. *Oecologia*, *171*(1), 217–226. http://dx.doi.org/10.1007/s00442-012-2398-5. Récupéré de http://link.springer.com/10.1007/s00442-012-2398-5

Langton, C. G. (1992). Life at the edge of chaos. *Artificial life II*, *10*, 41–91.

Legendre, P. et Legendre, L. (1998). Numerical ecology. Developments in environmental modeling, 20. *Numerical ecology: Developments in environmental modelling 20*.

Levin, L. A., Sibuet, M., Gooday, A. J., Smith, C. R. et Vanreusel, A. (2010). The roles of habitat heterogeneity in generating and maintaining biodiversity on continental margins: An introduction. *Marine Ecology*, *31*(1), 1–5. Récupéré de http://www.scopus.com/inward/record.url?eid=2-s2.0-77950991037{&}partnerID=40{&}md5=423a535dd17343b48e261f445ab52479

Levin, S. A. (1992). The problem of pattern and scale in ecology: the Robert H. MacArthur award lecture. *Ecology*, *73*(6), 1943–1967.

Li, X., Zhang, C., Li, W., Ricard, R., Meng, Q. et Zhang, W. (2015). Assessing street-level urban greenery using Google Street View and a modified green view index. *Urban Forestry & Urban Greening*, *14*(3), 675–685. http://dx.doi.org/10.1016/j.ufug.2015.06.006. Récupéré de http://www.sciencedirect.com/science/article/pii/S1618866715000874

Liang, L., Schwartz, M. et Fei, S. (2012). Photographic assessment of temperate forest understory phenology in relation to springtime meteorological drivers. *International Journal of Biometeorology*, *56*(2), 343–355. http://dx.doi.org/10.1007/s00484-011-0438-1. Récupéré de http://dx.doi.org/10.1007/s00484-011-0438-1

Liaw, A. et Wiener, M. (2002). Classification and regression by randomForest. *R news*, *2*(3), 18–22.

Lopez, O. R., Farris-Lopez, K., Montgomery, R. A. et Givnish, T. J. (2008). Leaf phenology in relation to canopy closure in southern Appalachian trees. *American Journal of Botany*, *95*(11), 1395–1407. http://dx.doi.org/10.3732/ajb.0800104

Lothian, A. (1999). Landscape and the philosophy of aesthetics: is landscape quality inherent in the landscape or in the eye of the beholder? *Landscape and Urban Planning*, *44*(4), 177–198. http://dx.doi.org/10.1016/S0169-2046(99)00019-5. Récupéré de http://www.sciencedirect.com/science/article/pii/S0169204699000195

Lovasi, G. S., Quinn, J. W., Neckerman, K. M., Perzanowski, M. S. et Rundle, A. (2008). Children living in areas with more street trees have lower prevalence of

asthma. *Journal of epidemiology and community health*, *62*(7), 647–9. http://dx.doi.org/10.1136/jech.2007.071894. Récupéré de http://jech.bmj.com/content/62/7/647.short

Lukina, E. V., Stone, M. L. et Raun, W. R. (1999). Estimating vegetation coverage in wheat using digital images. *Journal of Plant Nutrition*, *22*(2), 341–350. http://dx.doi.org/10.1080/01904169909365631. Récupéré de http://www.tandfonline.com/doi/abs/10.1080/01904169909365631

Lundholm, J. T. (2009). Plant species diversity and environmental heterogeneity: Spatial scale and competing hypotheses. *Journal of Vegetation Science*, *20*(3), 377–391. Récupéré de http://www.scopus.com/inward/record.url?eid=2-s2.0-67650084358{&}partnerID=40{&}md5=9653a8078e8d8536da1ed4ddf16a9f8c

Luscier, J. D., Thompson, W. L., Wilson, J. M., Gorham, B. E. et Dragut, L. D. (2006). Using digital photographs and object-based image analysis to estimate percent ground cover in vegetation plots. *Frontiers in Ecology and the Environment*, *4*(8), 408–413. http://dx.doi.org/10.1890/1540-9295(2006)4[408:UDPAOI]2.0.CO;2. Récupéré de http://doi.wiley.com/10.1890/1540-9295(2006)4[408:UDPAOI]2.0.CO;2

MacArthur, R. H. W. et Wilson, E. O. (1967). The theory of island biogeography. *Princeton University Press, Monogr. Popul. Biol*, *1*, 202.

MacFaden, S. W., O'Neil-Dunne, J. P., Royar, A. R., Lu, J. W. et Rundle, A. G. (2012). High-resolution tree canopy mapping for New York City using LIDAR and object-based image analysis. *Journal of Applied Remote Sensing*, *6*(1), 063567–1. http://dx.doi.org/10.1117/1.JRS.6.063567. Récupéré de http://remotesensing.spiedigitallibrary.org/article.aspx?articleid=1358118

MATLAB. (2015). *version 8.5.0.197613 (R2015a)*. Natick, Massachusetts: The MathWorks Inc.

McHale, M. R., Burke, I. C., Lefsky, M. A., Peper, P. J. et McPherson, E. G. (2009). Urban forest biomass estimates: is it important to use allometric relationships developed specifically for urban trees? *Urban Ecosystems*, *12*(1), 95–113. http://dx.doi.org/10.1007/s11252-009-0081-3. Récupéré de http://link.springer.com/10.1007/s11252-009-0081-3

McKinney, M. (2008). Effects of urbanization on species richness: A review of plants and animals. *Urban Ecosystems*, *11*(2), 161–176. http://dx.doi.org/10.1007/s11252-007-0045-4. Récupéré de http://dx.doi.org/10.1007/s11252-007-0045-4

McPherson, G., Nowak, D., Heisler, G., Grimmond, S., Souch, C., Grant, R. et Rowntree, R. (1997). Quantifying urban forest structure, function, and value: the Chicago Urban Forest Climate Project. *Urban Ecosystems*, *1*(1), 49–61. http://dx.doi.org/10.1023/A:1014350822458. Récupéré de http://link.springer.com/article/10.1023/A{%}3A1014350822458

Mellin, C., Parrott, L., Andreffouet, S., Bradshaw, C. J. A., MacNeil, M. A. et Caley, M. J. (2012). Multi-scale marine biodiversity patterns inferred efficiently from habitat image processing. *Ecological Applications*, *22*(3), 792–803. http://dx.doi.org/10.1890/11-2105.1. Récupéré de http://www.esajournals.org/doi/abs/10.1890/11-2105.1

Meyer, G. E. et Neto, J. C. (2008). Verification of color vegetation indices for automated crop imaging applications. *Computers and Electronics in Agriculture*, *63*(2), 282–293.

Miller, T. R., Minteer, B. A. et Malan, L. C. (2011). The new conser-

vation debate: The view from practical ethics. *Biological Conservation*, *144*(3), 948–957. Récupéré de http://www.scopus.com/inward/record.url?eid=2-s2.0-79951814059{&}partnerID=40{&}md5=d25b9f971702fae06ee13a98207c7a17

Morisette, J. T., Richardson, A. D., Knapp, A. K., Fisher, J. I., Graham, E. A., Abatzoglou, J., Wilson, B. E., Breshears, D. D., Henebry, G. M., Hanes, J. M. et Liang, L. (2009). Tracking the rhythm of the seasons in the face of global change: phenological research in the 21st century. *Frontiers in Ecology and the Environment*, *7*(5), 253–260. http://dx.doi.org/10.1890/070217. Récupéré de http://doi.wiley.com/10.1890/070217

Muller, R. N. et Bormann, F. H. (1976). Role of Erythronium americanum Ker. in Energy Flow and Nutrient Dynamics of a Northern Hardwood Forest Ecosystem. *Science (New York, N.Y.)*, *193*(4258), 1126–8. http://dx.doi.org/10.1126/science.193.4258.1126. Récupéré de http://www.ncbi.nlm.nih.gov/pubmed/17792752

Naeem, S. (2002). Biodiversity: Biodiversity equals instability ? *Nature*, *416*(6876), 23–24. Récupéré de http://dx.doi.org/10.1038/416023a

Naik, N., Kominers, S. D., Raskar, R., Glaeser, E. L. et Hidalgo, C. A. (2015). Do People Shape Cities, or Do Cities Shape People ? The Co-evolution of Physical, Social, and Economic Change in Five Major U.S. Cities. *National Bureau of Economic Research Working Paper Series, No. 21620.* http://dx.doi.org/10.3386/w21620. Récupéré de http://www.nber.org/papers/w21620{%}5Cnhttp://www.nber.org/papers/w21620.pdf

Naik, N., Philipoom, J., Raskar, R. et Hidalgo, C. (2014a). Streetscore – Predicting the Perceived Safety of One Million Streetscapes. Dans *2014 IEEE Conference on Computer Vision and Pattern Recognition Workshops*, 793–799. IEEE. http:

//dx.doi.org/10.1109/CVPRW.2014.121. Récupéré de http://ieeexplore.ieee.org/articleDetails.jsp?arnumber=6910072

Naik, N., Philipoom, J., Raskar, R. et Hidalgo, C. (2014b). Streetscore – Predicting the Perceived Safety of One Million Streetscapes. Dans *2014 IEEE Conference on Computer Vision and Pattern Recognition Workshops*, 793–799. IEEE. http://dx.doi.org/10.1109/CVPRW.2014.121. Récupéré de http://ieeexplore.ieee.org/lpdocs/epic03/wrapper.htm?arnumber=6910072

Nicolis, G. et Prigogine, I. (1977). *Self-organization in nonequilibrium systems*, volume 191977. Wiley, New York.

Niemelä, J. (1999). Ecology and urban planning. *Biodiversity and Conservation*, *8*(1), 119–131.

Noss, R. F. (1990). Indicators for Monitoring Biodiversity: A Hierarchical Approach. *Conservation Biology*, *4*(4), 355–364. http://dx.doi.org/10.1111/j.1523-1739.1990.tb00309.x. Récupéré de http://dx.doi.org/10.1111/j.1523-1739.1990.tb00309.x

Nowak, D. J., Hirabayashi, S., Bodine, A. et Greenfield, E. (2014). Tree and forest effects on air quality and human health in the United States. *Environmental Pollution*, *193*, 119–129.

NYC Parks (2016). *New York City Department of Parks & Recreation Preliminary 2015 Street Tree Census Data, as of January 2016.* Rapport technique, New York City Department of Parks & Recreation, New York, New York, USA.

Olea, P. P. et Mateo-Tomas, P. (2013). Assessing Species Habitat Using Google Street View: A Case Study of Cliff-Nesting Vultures. *PLOS ONE*, *8*(1), e54582.

Otsu, N. (1975). A threshold selection method from gray-level histograms. *Automatica*, *11*(285-296), 23–27.

Palmer, M. W. (1994). Variation in species richness: Towards a unification of hypotheses. *Folia Geobotanica et Phytotaxonomica*, *29*(4), 511–530.

Palmer, M. W. et White, P. S. (1994). Scale dependence and the species-area relationship. *American Naturalist*, *144*(5), 717–740.

Parrott, L. (2010). Measuring ecological complexity. *Ecological Indicators*, *10*(6), 1069–1076. Récupéré de http://www.sciencedirect.com/science/article/pii/S1470160X10000567

Peper, P. J. et McPherson, E. G. (2003). Evaluation of four methods for estimating leaf area of isolated trees. *Urban Forestry & Urban Greening*, *2*(1), 19–29. http://dx.doi.org/10.1078/1618-8667-00020. Récupéré de http://www.sciencedirect.com/science/article/pii/S1618866704700205

Pretzsch, H. (2014). Canopy space filling and tree crown morphology in mixed-species stands compared with monocultures. *Forest Ecology and Management*, *327*, 251–264. http://dx.doi.org/10.1016/j.foreco.2014.04.027. Récupéré de http://www.sciencedirect.com/science/article/pii/S0378112714002667

Proulx, R. et Parrott, L. (2009). Structural complexity in digital images as an ecological indicator for monitoring forest dynamics across scale, space and time. *Ecological Indicators*, *9*(6), 1248–1256. Récupéré de http://www.scopus.com/inward/record.url?eid=2-s2.0-67349225179{&}partnerID=40{&}md5=ecf991a5e3bb47dc5727d3c66772e060

Proulx, R., Roca, I. T., Cuadra, F. S., Seiferling, I. et Wirth, C. (2014). A novel photographic approach for monitoring the structural heterogeneity and diversity of grassland ecosystems. *Journal of Plant Ecology*, *7*(6), 518–525. http://dx.

doi.org/10.1093/jpe/rtt065. Récupéré de http://jpe.oxfordjournals.org/content/7/6/518.short

Przeszlowska, A., Trlica, M. J. et Weltz, M. A. (2006). Near-Ground Remote Sensing of Green Area Index on the Shortgrass Prairie. *Rangeland Ecology & Management*, *59*(4), 422–430. http://dx.doi.org/10.2111/05-059R1.1. Récupéré de http://linkinghub.elsevier.com/retrieve/pii/S155074240650048X

R Core Team (2013). *R: A Language and Environment for Statistical Computing*. R Foundation for Statistical Computing, Vienna, Austria

Richardson, A. D., Black, T. A., Ciais, P., Delbart, N., Friedl, M. A., Gobron, N., Hollinger, D. Y., Kutsch, W. L., Longdoz, B., Luyssaert, S., Migliavacca, M., Montagnani, L., Munger, J. W., Moors, E., Piao, S., Rebmann, C., Reichstein, M., Saigusa, N., Tomelleri, E., Vargas, R. et Varlagin, A. (2010). Influence of spring and autumn phenological transitions on forest ecosystem productivity. *Philosophical transactions of the Royal Society of London. Series B, Biological sciences*, *365*(1555), 3227–46. http://dx.doi.org/10.1098/rstb.2010.0102. Récupéré de http://rstb.royalsocietypublishing.org/content/365/1555/3227.short

Richardson, A. D., Braswell, B. H., Hollinger, D. Y., Jenkins, J. P. et Ollinger, S. V. (2009a). Near-surface remote sensing of spatial and temporal variation in canopy phenology. *Ecological Applications*, *19*(6), 1417–1428. http://dx.doi.org/10.1890/08-2022.1. Récupéré de http://doi.wiley.com/10.1890/08-2022.1

Richardson, A. D., Braswell, B. H., Hollinger, D. Y., Jenkins, J. P. et Ollinger, S. V. (2009b). Near-surface remote sensing of spatial and temporal variation in canopy phenology. *Ecological Applications*, *19*(6), 1417–1428. http://dx.doi.org/1029/2007JG000650. Récupéré de http://www.

scopus.com/inward/record.url?eid=2-s2.0-69449089117{&}partnerID=40{&}md5=dfc6d769401b51e7ba6305a74eb03874

Richardson, A. D., Keenan, T. F., Migliavacca, M., Ryu, Y., Sonnentag, O. et Toomey, M. (2013a). Climate change, phenology, and phenological control of vegetation feedbacks to the climate system. *Agricultural and Forest Meteorology*, *169*, 156–173. http://dx.doi.org/10.1016/j.agrformet.2012.09.012. Récupéré de http://www.sciencedirect.com/science/article/pii/S0168192312002869

Richardson, E. A., Pearce, J., Mitchell, R. et Kingham, S. (2013b). Role of physical activity in the relationship between urban green space and health. *Public health*, *127*(4), 318–24. http://dx.doi.org/10.1016/j.puhe.2013.01.004. Récupéré de http://www.sciencedirect.com/science/article/pii/S003335061300005X

Rocchini, D., Balkenhol, N., Carter, G. A., Foody, G. M., Gillespie, T. W., He, K. S., Kark, S., Levin, N., Lucas, K., Luoto, M., Nagendra, H., Oldeland, J., Ricotta, C., Southworth, J. et Neteler, M. (2010). Remotely sensed spectral heterogeneity as a proxy of species diversity: Recent advances and open challenges. *Ecological Informatics*, *5*(5), 318–329. Récupéré de http://www.scopus.com/inward/record.url?eid=2-s2.0-77956878537{&}partnerID=40{&}md5=3af9c2a06727ab6417c674dd2e2dd4e6

Roscher, C., Schumacher, J., Baade, J., Wilcke, W., Gleixner, G., Weisser, W. W., Schmid, B. et Schulze, E.-D. (2004). The role of biodiversity for element cycling and trophic interactions: an experimental approach in a grassland community. *Basic and Applied Ecology*, *5*(2), 107–121. http://dx.doi.org/http://dx.doi.org/10.1078/1439-1791-00216. Récupéré de http://www.sciencedirect.com/science/article/pii/S1439179104701644

Rousselet, J., Imbert, C.-E., Dekri, A., Garcia, J., Goussard, F., Vincent, B., Denux, O., Robinet, C., Dorkeld, F. et Roques, A. (2013). Assessing Species Distribution Using Google Street View: A Pilot Study with the Pine Processionary Moth. *PLOS ONE*, *8*(10), e74918.

Sapijanskas, J., Paquette, A., Potvin, C., Kunert, N. et Loreau, M. (2014). Tropical tree diversity enhances light capture through crown plasticity and spatial and temporal niche differences. *Ecology*, *9*(95), 2479–2492. Récupéré de http://www.esajournals.org/doi/abs/10.1890/13-1366.1

Scherer-Lorenzen, M. (2013). The functional role of biodiversity in the context of global change. *Forests and Global Change*, 195–238. Récupéré de http://books.google.com/books?hl=en{&}lr={&}id=FU9kAgAAQBAJ{&}oi=fnd{&}pg=PA195{&}dq=The+functional+role+of+biodiversity+in+the+context+of+global+change{&}ots=fNaonpr8Vb{&}sig=B0jS2IbW8ogDvv0sfXgHmtRa8H8

Schroeder, H. W. (1986). Estimating park tree densities to maximize landscape esthetics. *Journal of environmental management*, *23*(4), 325–333. Récupéré de http://cat.inist.fr/?aModele=afficheN{&}cpsidt=8381648

Schroeder, H. W. (1988). Visual impact of hillside development: Comparison of measurements derived from aerial and ground-level photographs. *Landscape and Urban Planning*, *15*(1-2), 119–126. http://dx.doi.org/10.1016/0169-2046(88)90020-5. Récupéré de http://www.sciencedirect.com/science/article/pii/0169204688900205

Seiferling, I., Proulx, R. L. et Wirth, C. (2014). Disentangling the environmental-heterogeneity-species-diversity relationship along a gradient of human footprint. *Ecology*, *95*(8), 2084–2095.

Seiferling, I. S., Proulx, R., Peres-Neto, P. R., Fahrig, L. et Messier, C. (2012). Measuring protected-area isolation and correlations of isolation with land-use intensity and protection status. *Conservation biology : the journal of the Society for Conservation Biology*, *26*(4), 610–8. http://dx.doi.org/10.1111/j.1523-1739.2011.01674.x. Récupéré de http://www.ncbi.nlm.nih.gov/pubmed/21488956

Shannon, C. E. (1948). A Mathematical Theory of Communication. *Bell System Technical Journal*, *27*(3), 379–423. http://dx.doi.org/10.1002/j.1538-7305.1948.tb01338.x. Récupéré de http://ieeexplore.ieee.org/lpdocs/epic03/wrapper.htm?arnumber=6773024

Simpson, E. H. (1949). Measurement of diversity. *Nature*, *163*(4148), 688. Récupéré de http://www.scopus.com/inward/record.url?eid=2-s2.0-33344464667{&}partnerID=40{&}md5=0ddde401055192e649f13658380c8031

Siroky, D. S. (2009). Navigating Random Forests and related advances in algorithmic modeling. *Statistics Surveys*, *3*, 147–163. Récupéré de http://projecteuclid.org/euclid.ssu/1257431567

Smith, T. W. et Lundholm, J. T. (2012). Environmental geometry and heterogeneity-diversity relationships in spatially explicit simulated communities. *Journal of Vegetation Science*, *23*(4), 732–744. http://dx.doi.org/10.1111/j.1654-1103.2011.01380.x. Récupéré de http://doi.wiley.com/10.1111/j.1654-1103.2011.01380.x

Sonnentag, O., Hufkens, K., Teshera-Sterne, C., Young, A. M., Friedl, M., Braswell, B. H., Milliman, T., OaKeefe, J. et Richardson, A. D. (2012). Digital repeat photography for phenological research in forest ecosystems. *Agricultural and Fo-*

rest Meteorology, *152*(0), 159–177. Récupéré de http://www.sciencedirect.com/science/article/pii/S0168192311002851

Stohlgren, T., Coughenour, M., Chong, G., Binkley, D., Kalkhan, M., Schell, L., Buckley, D. et Berry, J. (1997). Landscape analysis of plant diversity. *Landscape Ecology*, *12*(3), 155–170. http://dx.doi.org/10.1023/A:1007986502230. Récupéré de http://dx.doi.org/10.1023/A{%}3A1007986502230

Tamme, R., Hiiesalu, I., Laanisto, L., Szava-Kovats, R. et Partel, M. (2010). Environmental heterogeneity, species diversity and co-existence at different spatial scales. *Journal of Vegetation Science*, *21*(4), 796–801. Récupéré de http://www.scopus.com/inward/record.url?eid=2-s2.0-77954329653{&}partnerID=40{&}md5=7f7d949e66bc90777160a0b30d24ba79

Tews, J., Brose, U., Grimm, V., Tielborger, K., Wichmann, M. C., Schwager, M. et Jeltsch, F. (2004). Animal species diversity driven by habitat heterogeneity/diversity: The importance of keystone structures. *Journal of Biogeography*, *31*(1), 79–92. Récupéré de http://www.scopus.com/inward/record.url?eid=2-s2.0-1642523451{&}partnerID=40{&}md5=cc5fbbcc02c8ee777c90a5fe4f0ff29b

Thayer, R. L. et Atwood, B. G. (1978). Plants, complexity, and pleasure in urban and suburban environments. *Environmental Psychology and Nonverbal Behavior*, *3*(2), 67–76. http://dx.doi.org/10.1007/BF01135604. Récupéré de http://link.springer.com/10.1007/BF01135604

Thompson, I., Mackey, B., McNulty, S. et Mosseler, A. (2009). Forest resilience, biodiversity, and climate change. Dans *A synthesis of the biodiversity/resilience/stability relationship in forest ecosystems. Secretariat of the Convention on Biological Diversity, Montreal. Technical Series*, volume 43.

Tilman, D. (1999). The ecological consequences of changes in biodiversity: a search for general principles 101. *Ecology*, *80*(5), 1455–1474. http://dx.doi.org/10.1890/0012-9658(1999)080[1455:TECOCI]2.0.CO;2. Récupéré de http://www.esajournals.org/doi/abs/10.1890/0012-9658(1999)080{%}5B1455:TECOCI{%}5D2.0.CO;2

Tilman, D. et May, R. M. (1994). Habitat destruction and the extinction debt. *Nature*, *371*(6492), 65. Récupéré de http://search.ebscohost.com/login.aspx?direct=true{&}db=a9h{&}AN=9409231447{&}site=ehost-live

Trichon, V., Walter, J.-M. N. et Laumonier, Y. (1998). Identifying spatial patterns in the tropical rain forest structure using hemispherical photographs. *Plant Ecology*, *137*(2), 227–244. http://dx.doi.org/10.1023/A:1009712925343. Récupéré de http://link.springer.com/10.1023/A:1009712925343

Tuanmu, M. N., Vina, A., Bearer, S., Xu, W. H., Ouyang, Z. Y., Zhang, H. M. et Liu, J. G. (2010). Mapping understory vegetation using phenological characteristics derived from remotely sensed data. *Remote Sensing of Environment*, *114*(8), 1833–1844. http://dx.doi.org/10.1016/j.rse.2010.03.008

U.S. Geological Survey (USGS) (2009). High Resolution Orthoimagery from ADS40 Sensor ; 0.3 m resolution. Récupéré de http://earthexplorer.usgs.gov

Valladares, F., Skillman, J. B. et Pearcy, R. W. (2002). Convergence in light capture efficiencies among tropical forest understory plants with contrasting crown architectures: a case of morphological compensation. *American journal of botany*, *89*(8), 1275–84. http://dx.doi.org/10.3732/ajb.89.8.1275. Récupéré de http://www.amjbot.org/cgi/content/long/89/8/1275

Van Der Plas, F., Manning, P., Allan, E., Scherer-Lorenzen, M., Verheyen, K.,

Wirth, C., Zavala, M. A., Hector, A., Ampoorter, E., Baeten, L., Barbaro, L., Bauhus, J., Benavides, R., Benneter, A., Berthold, F., Bonal, D., Bouriaud, O., Bruelheide, H., Bussotti, F., Carnol, M., Castagneyrol, B., Charbonnier, Y., Coomes, D., Coppi, A., Bastias, C. C., Muhie Dawud, S., De Wandeler, H., Domisch, T., Finer, L., Gessler, A., Granier, A., Grossiord, C., Guyot, V., Hättenschwiler, S., Jactel, H., Jaroszewicz, B., Joly, F.-X., Jucker, T., Koricheva, J., Milligan, H., Muller, S., Muys, B., Nguyen, D., Pollastrini, M., Raulund-Rasmussen, K., Selvi, F., Stenlid, J., Valladares, F., Vesterdal, L., Zielínski, D. et Fischer, M. (2016). Jack-of-all-trades effects drive biodiversity-ecosystem multifunctionality relationships in European forests. *Nature communications*, *7*, 11109. http://dx.doi.org/10.1038/ncomms11109. Récupéré de http://www.nature.com/ncomms/2016/160324/ncomms11109/full/ncomms11109.html

Vartanian, M., Nijland, W., Coops1, N. C., Bater, C., Wulder, M. A. et Stenhouse, G. (2014). Assessing the Impact of Field of View on Monitoring Understory and Overstory Phenology Using Digital Repeat Photography. *Canadian Journal of Remote Sensing*, *40*(2), 85–91.

Vellend, M., Verheyen, K., Jacquemyn, H., Kolb, A., Van Calster, H., Peterken, G. et Hermy, M. (2006). Extinction debt of forest plants persists for more than a century following habitat fragmentation. *Ecology*, *87*(3), 542–548. http://dx.doi.org/10.1890/05-1182. Récupéré de http://dx.doi.org/10.1890/05-1182

Walther, G.-R., Post, E., Convey, P., Menzel, A., Parmesan, C., Beebee, T. J. C., Fromentin, J.-M., Hoegh-Guldberg, O. et Bairlein, F. (2002). Ecological responses to recent climate change. *Nature*, *416*(6879), 389–395. http://dx.doi.org/10.1038/416389a. Récupéré de http://www.nature.com/doifinder/10.1038/416389a

Wang, N., Zhang, N., Dowell, F. E., Sun, Y. et Peterson, D. E. (2001). Design of an optical weed sensor using plant spectral characteristics. *Transactions of the ASAE*, *44*(2), 409. http://dx.doi.org/10.13031/2013.4673. Récupéré de http://elibrary.asabe.org/abstract.asp??JID=3{&}AID=4673{&}CID=t2001{&}v=44{&}i=2{&}T=1

Wang, Q., Tenhunen, J., Nguyen, Q. D., Reichstein, M., Otieno, D., Granier, A. et Pilegarrd, K. (2005). Evaluation of seasonal variation of MODIS derived leaf area index at two European deciduous broadleaf forest sites. *Remote Sensing of Environment*, *96*(3-4), 475–484. http://dx.doi.org/10.1016/j.rse.2005.04.003

Wania, A., Kühn, I. et Klotz, S. (2006). Plant richness patterns in agricultural and urban landscapes in Central Germany—spatial gradients of species richness. *Landscape and Urban Planning*, *75*(1), 97–110.

Wenhua Mao, W., Yiming Wang, Y. et Yueqing Wang, Y. (2003). Real-time Detection of Between-row Weeds Using Machine Vision. Dans *2003, Las Vegas, NV July 27-30, 2003*, p. 1., St. Joseph, MI. American Society of Agricultural and Biological Engineers. http://dx.doi.org/10.13031/2013.15381. Récupéré de http://elibrary.asabe.org/abstract.asp?JID=5{&}AID=15381{&}CID=lnv2003{&}T=1

White, M. A., Thornton, P. E. et Running, S. W. (1997). A continental phenology model for monitoring vegetation responses to interannual climatic variability. *Global biogeochemical cycles*, *11*(2), 217–234.

Woebbecke, D. M., Meyer, G. E., Von Bargen, K. et Mortensen, D. A. (1995). Color Indices for Weed Identification Under Various Soil, Residue, and Lighting Conditions. *Transactions of the ASAE*, *38*(1), 259–269. http://dx.

doi.org/10.13031/2013.27838. Récupéré de http://elibrary.asabe.org/abstract.asp??JID=3{&}AID=27838{&}CID=t1995{&}v=38{&}i=1{&}T=1

Xian, G., Homer, C., Dewitz, J., Fry, J., Hossain, N. et Wickham, J. (2011). The change of impervious surface area between 2001 and 2006 in the conterminous United States. *Photogrammetric Engineer*, *77*(8), 758–762.

Yang, C.-C., Prasher, S. O., Landry, J.-A. et Ramaswamy, H. S. (2003). Development of an Image Processing System and a Fuzzy Algorithm for Site-Specific Herbicide Applications. *Precision Agriculture*, *4*(1), 5–18. http://dx.doi.org/10.1023/A:1021847103560. Récupéré de http://link.springer.com/10.1023/A:1021847103560

Yang, J., Zhao, L., Mcbride, J. et Gong, P. (2009). Can you see green? Assessing the visibility of urban forests in cities. *Landscape and Urban Planning*, *91*(2), 97–104. http://dx.doi.org/10.1016/j.landurbplan.2008.12.004. Récupéré de http://www.sciencedirect.com/science/article/pii/S0169204608002314

.1 Chapter 1 — Appendices

.1.1 Literature review and data extraction

To test our hypothesis, a literature review of all peer-reviewed scientific papers to date (n = 430), which empirically tested for a relationship between EH and species diversity, was performed. Through this literature review, relevant study parameters were extracted from the literature to form the database (Table TabAOne; also see supplied Excel file for full raw dataset). A record (i.e., line in the database) was created for each reported overall EH-BD relationship type (i.e., positive, negative, non-significant or unimodal) between a measure of environmental heterogeneity and a measure of biodiversity, which then constituted the EH-BD relationship direction variable. All other study parameters that applied to the record where then amended to it.

.1.2 Additional explanatory variable effects on the EH-BD relationship direction

Beyond the ecosystem category and spatial scale variables (see main manuscript text), no other significant excesses or rarities were identified for the relative frequencies of RDs in any of the other explanatory variables (taxonomic group and model type; Fig. FigA1, panels A & B). The results (Fig. FigA1) illustrate that the pattern of RD relative frequencies across their ecosystem category levels was consistent for the taxonomic group and model type variables. That is, when the relative frequency of positive relationships increases or decreases moving from one level to the next, so to does the negative RD type.

.1.3 Treatment of polynomial model results

Cases of non-linear modeling and unimodal EH-BD relationships were present in the literature (n=26). This represented only a small fraction of all EH-BD relationships (3%) and a complete re-analysis excluding these records made no detectable difference on any of the results presented. In an aim to include as many studies and

records as possible however, we examined each of these 26 relationships and their studies in detail. When the study authors concluded the relationship in question was generally positive (i.e., left tailed; that is species richness increased linearly with EH and only leveled at the extreme high or low values of EH), we recorded the relationship as "positive". When the study concluded the relationship in question was generally negative (i.e., right tailed; that is species richness decreased with EH, but the curve was concave or convex to the origin), we recorded the relationship as "negative". All others records, in which a figure or adequate description was not provided or when the relationship had both positive and negative trends (i.e., unimodal), were not included in the final analysis (n = 4).

LIST OF APPENDIX CHAPTER 1 TABLES

Table S1- 1: All study parameters, explanatory variables and the effect variable that were extracted from the reviewed literature to form the database. For each record parameter or extracted variable, the table provides it's definition, the number of levels it has and, where relevant, the parameters used to define the levels. The bracketed numbers beside the variable level descriptions are the number of occurrences in the database.

Extracted Variable	Definition	Levels	Level Parameters
Record Number	Identification number of the study record.	various (870)	NA
Authors	Authors of the study article for each record	various	NA
Article Title	Article title of the study the record is extracted from.	various	NA
Year of Publication	Publication year of the article that the record is extracted from.	1961 - 2011	NA
Country of Study Location	Country the sampling was performed in.	various (39)	NA
Geographical Coordinates of Study Site(s)	Geographic coordinates or geo-political description of the study area.	various	NA
Ecosystem category/ Level - Categorical	The level of human modification to the study area (extent). If the human footprint includes 2 or more differing landuse types, or it is comprised of some natural landcover and some exploited landcover, then it falls into the semi-natural category.	highly-modified (83) strictly natural (264) semi-natural (523)	see description and definitions in the main text
Spatial Extent - Categorical	Total sampling spatial extent that the record statistic was derived from. This can include the total area encompassing sampling points or sampling blocks that are separated by un-sampled space.	local (176) mesoscale (467) continental+ (187)	local < 9.99 km2 mesoscale = 10 - 99 999 km2 continental+ > 100 001 km2
Spatial Extent - Continuous (km2)	The spatial extent in continuous (square kilometer units).	3.92*10-6 - 2.47*107 km2	NA
Sampling Coverage of the Spatial Extent	The sampling coverage of the studies' entire spatial extent. Is complete coverage when the entire extent was sampled or partial coverage when the extent was partially sampled separated (i.e., samples are separated by unsampled space).	complete (297) partial (523) NA (50)	NA
Spatial Grain - Categorical	The spatial area of the sampling points within the extent used to derive the EH measure for the sampling extent, to which then enter the model of the recorded statistic.	fine-scale (276) mesoscale (177) large-scale (416)	fine-scale < 9.9*103 m2 mesoscale = 10*103 - 9.9*105 m2 lareg-scale > 10*105 m2
Spatial Grain - Continuous (m2)	The spatial grain in continuous and explicit form (square meter units).	1.13*10-2 - 2.7*109 m2	NA
Spatial Resolution - Categorical	The spatial resolution of the study sampling design based on cross-matching the categorical spatial extent and spatial grain levels	fine (276) mesoscale (177) coarse-scale (416)	fine: grain < extent mesoscale: grain = extent coarse-scale: grain > extent

Table S1- 0: continued...

Extracted Variable	Definition	Levels	Level Parameters
Ecosystem	The ecosystem and/or landcover type that dominates the study sampling extent for each record.	alpine (201), bedrock (3), chaparral (68), coastal (45), cropland (280), desert (17), forest (646), grassland (403), mosaic (313), pasture (166), plantation (23), riparian (5), shrubland (63), tundra (44), urban (192), wetland (55)	NA
Sampling Mode (remotely-sensed vs ground-based)	The colleciton mode of the EH data for the record.	ground-based (215) remotely-sensed (590) remotely-sensed & ground-based (65)	ground-based: any record where EH and BD data is collected by manned observations; remotely-sensed: any record where data is collected by remote sensors; remotely-sensed and ground-based: any record where the data is collected by both of above.
Spatial EH vs. Temporal EH	Indicates whether the EH variable denotes spatial variability or temporal variability of the environmental feature measured.	spatial (831) temporal (39)	NA
Abiotic EH vs Biotic EH	Indicates whether the record's EH variable is a measure of an abiotic feature (e.g., elevation, soil texture, precipitation, temperature) or a biotic feature (e.g., vegetation structure, plant species richness, landcover classes).	abiotic (350) biotic (468) abiotic & biotic (52)	NA

Table S1- -1: continued...

Extracted Variable	Definition	Levels	Level Parameters
Measure of EH	The metric used to quantifying the spatial or temporal heterogeneity/variability of the measured environmental feature.	complexity metric (41) diversity metric (91), heterogeneity/fragmentation metric (162) percent cover (58) range (197) variability (e.g., standard deviation) (341)	NA
Taxonomic Group (plant vs. animal)	The study organism representing the record's measure of biodiversity.	plant (466) animal (405)	NA
Taxonomic Sub-Group	Further division of the taxanomic groupings.	amphibians (17), arthropods (74), birds (105), fish (18), other invertebrates (36), mammals (43), microbial (4), plant (480), reptiles (17), vertebrates mixed (81)	NA
Measure of Biodiversity	The metric used to quantify biodiversity in each record.	diversity metrics (53) evenness (4) range size rarity (1) rarefaction (12) richness (789) slope of species area curve (11)	NA
Multi-variate vs. Single Variable EH-BD Model	Indicates whether the statistic reported for each record is based on a single EH variable and EH-BD correlation or is A) a model result from a variable that integrates two or more environmental variables, at least one of which is a measure of EH (e.g., a regression model using a PCA axis as its independent variable) or B) a multi-variate analysis (e.g., multiple regression) where at least one of the independent variables entered in the model is a measure of EH.	uni-variate (723) multi-variate (147)	NA

Table S1- -2: continued...

Extracted Variable	Definition	Levels	Level Parameters
Correlation or Regression Model	The type of statistical model the record's reported statistic was produced from and from which the relationship direction was derived.	various correlation (399) regression (390) ANOVA (16) ANCOVA (4) AIC goodness of fit (6) Akaike criterian (3)	NA
Correlation Statistic Type	The reported model statistic	r-value (207) r2-value (146) other or un-extractable for EH variable (517)	NA
Reported Correlation Statistic	The reported value of the model statistic, representing the EH-BD relationship.	various	NA
Overall EH-BD Relationship Direction	The overall direction of the model result and, thus, EH-BD relationship. Moreover the relationship direction always refers to the effect of the environmental heterogeneity variable where possible. In cases where only one variable in a multi-variate model represents EH, then the variable's partial r^2 or weight or F-value is extracted when possible.	positive (547) negative (93) non-significant (190) not necessarily related (40)	see description of how the overall relationship direction was derived in the Methods section of the main text.
Study Sample Size (n)	The sample size for the model statistic reported in the record.	4 - 10926	NA

LIST OF APPENDIX CHAPTER 1 FIGURES

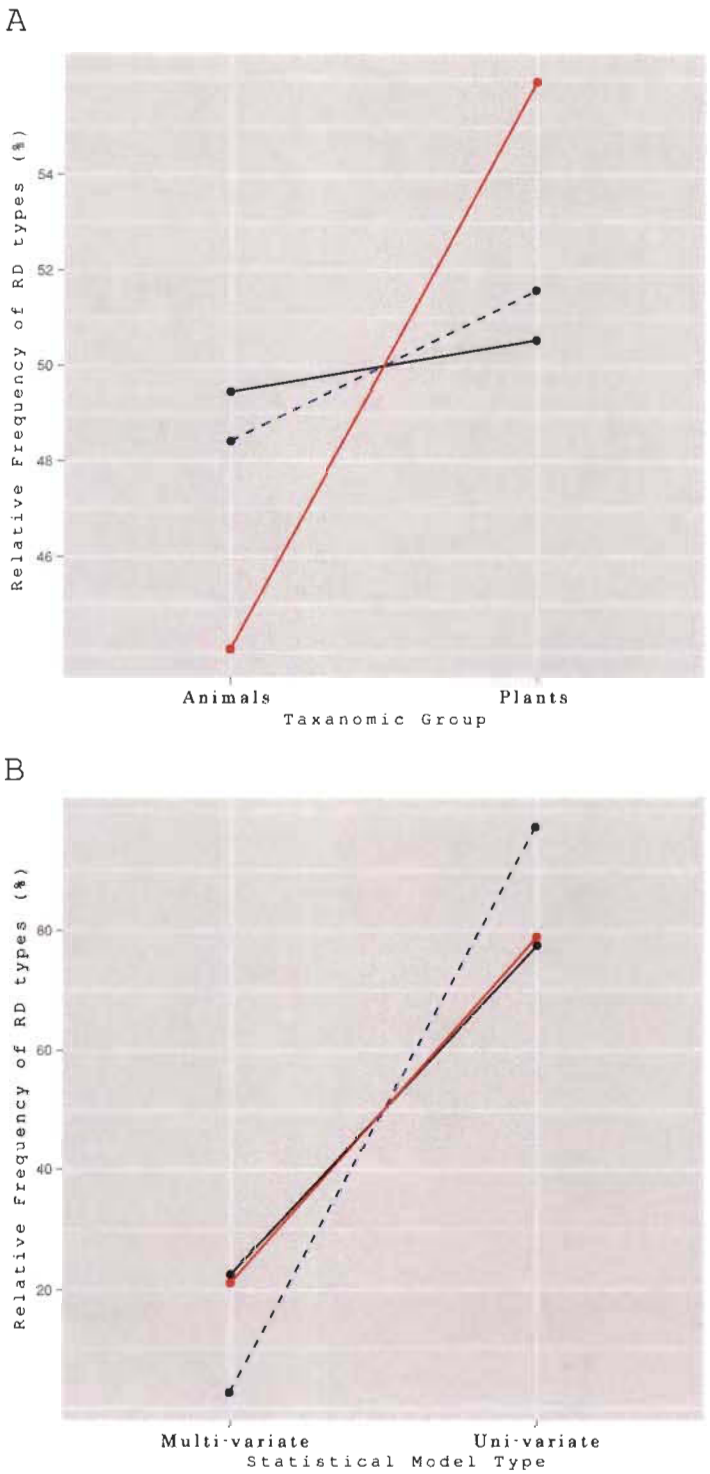

Figure S1 - 1: Relative frequency of EH-BD relationship direction (RD) types across the levels of A) taxonomic group and B) statistical model type. No significant differences from randomized frequency values were found for these two variables.

.1.4 Data-source references

1. Anderson J.M. (1978). A method to quantify soil-microhabitat complexity and its application to a study of soil animal species diversity. Soil Biology and Biochemistry, 10, 77-78.
2. Anderson K.L. & Leopold D.J. (2002). The role of canopy gaps in maintaining vascular plant diversity at a forested wetland in New York State. Journal of the Torrey Botanical Society, 129, 238-250.
3. Anderson T.M., McNaughton S.J. & Ritchie M.E. (2004). Scale-dependent relationships between the spatial distribution of a limiting resource and plant species diversity in an African grassland ecosystem. Oecologia, 139, 277-287. Atauri J.A. & De Lucio J.V. (2001). The role of landscape structure in species richness distribution of birds, amphibians, reptiles and lepidopterans in Mediterranean landscapes. Landscape Ecology, 16, 147-159.
4. Bakker C., Blair J.M. & Knapp A.K. (2003). Does resource availability, resource heterogeneity or species turnover mediate changes in plant species richness in grazed grasslands? Oecologia, 137, 385-391.
5. Balvanera P. & Aguirre E. (2006). Tree diversity, environmental heterogeneity, and productivity in a Mexican tropical dry forest. Biotropica, 38, 479-491.
6. Bino G., Levin N., Darawshi S., Van Der Hal N., Reich-Solomon A. & Kark S. (2008). Accurate prediction of bird species richness patterns in an urban environment using Landsat-derived NDVI and spectral unmixing. International Journal of Remote Sensing, 29, 3675-3700.
7. Bohning-Gaese K. (1997). Determinants of avian species richness at different spatial scales. Journal of Biogeography, 24, 49-60.
8. Brose U. (2003a). Bottom-up control of carabid beetle communities in early successional wetlands: Mediated by vegetation structure or plant diversity?

Oecologia, 135, 407-413.

9. Brose U. (2003b). Regional diversity of temporary wetland carabid beetle communities: A matter of landscape features or cultivation intensity ? Agriculture, Ecosystems and Environment, 98, 163-167.
10. Bruun H.H., Moen J. & Angerbjorn A. (2003). Environmental correlates of meso-scale plant species richness in the province of Härjedalen, Sweden. Biodiversity and Conservation, 12, 2025-2041.
11. Burnett M.R., August P.V., Brown Jr J.H. & Killingbeck K.T. (1998). The influence of geomorphological heterogeneity on biodiversity: I. A patch-scale perspective. Conservation Biology, 12, 363-370.
12. Chust G., Pretus J.L., Ducrot D., Bedos A. & Deharveng L. (2003). Response of Soil Fauna to Landscape Heterogeneity: Determining Optimal Scales for Biodiversity Modeling. Conservation Biology, 17, 1712-1723.
13. Cousin J.A. & Phillips R.D. (2008). Habitat complexity explains species-specific occupancy but not species richness in a Western Australian woodland. Australian Journal of Zoology, 56, 95-102.
14. Currie D.J. & Paquin V. (1987). Large-scale biogeographical patterns of species richness of trees. Nature, 329, 326-327.
15. Davies K.F., Chesson P., Harrison S., Inouye B.D., Melbourne B.A. & Rice K.J. (2005). Spatial heterogeneity explains the scale dependence of the native-exotic diversity relationship. Ecology, 86, 1602-1610.
16. Desilets P. & Houle G. (2005). Effects of resource availability and heterogeneity on the slope of the species-area curve along a floodplain-upland gradient. Journal of Vegetation Science, 16, 487-496.
17. Deutschewitz K., Lausch A., Kühn I. & Klotz S. (2003). Native and alien plant species richness in relation to spatial heterogeneity on a regional scale in Germany. Global Ecology and Biogeography, 12, 299-311.

18. Dufour A., Gadallah F., Wagner H.H., Guisan A. & Buttler A. (2006). Plant species richness and environmental heterogeneity in a mountain landscape: Effects of variability and spatial configuration. Ecography, 29, 573-584.

19. Durães R. & Loiselle B.A. (2004). Inter-scale relationship between species richness and environmental heterogeneity: A study case with antbirds in the Brazilian Atlantic forest. ORNITOLOGIA NEOTROPICAL 15, 127 - 135.

20. Eadie J.M. & Keast A. (1984). Resource heterogeneity and fish species diversity in lakes. Canadian Journal of Zoology, 62, 1689-1695.

21. Eriksson B.K., Rubach A. & Hillebrand H. (2006). Biotic habitat complexity controls species diversity and nutrient effects on net biomass production. Ecology, 87, 246-254.

22. Everson D.A. & H. Boucher D. (1998). Tree species-richness and topographic complexity along the riparian edge of the Potomac River. Forest Ecology and Management, 109, 305-314.

23. Ewers R.M., Didham R.K., Wratten S.D. & Tylianakis J.M. (2005). Remotely sensed landscape heterogeneity as a rapid tool for assessing local biodiversity value in a highly modified New Zealand landscape. Biodiversity and Conservation, 14, 1469-1485.

24. Fava F., Parolo G., Colombo R., Gusmeroli F., Della Marianna G., Monteiro A.T. & Bocchi S. (2010). Fine-scale assessment of hay meadow productivity and plant diversity in the European Alps using field spectrometric data. Agriculture, Ecosystems and Environment, 137, 151-157.

25. Fischer J.R. & Paukert C.P. (2009). Effects of sampling effort, assemblage similarity, and habitat heterogeneity on estimates of species richness and relative abundance of stream fishes. Canadian Journal of Fisheries and Aquatic Sciences, 66, 277-290.

26. Fraser R.H. (1998). Vertebrate species richness at the mesoscale: relative roles of energy and heterogeneity. Global Ecology and Biogeography Letters, 7, 215-220.

27. Freestone A.L. & Harrison S. (2006). Regional enrichment of local assemblages is robust to variation in local productivity, abiotic gradients, and heterogeneity. Ecology Letters, 9, 95-102.

28. Gaba S., Chauvel B., Dessaint F., Bretagnolle V. & Petit S. (2010). Weed species richness in winter wheat increases with landscape heterogeneity. Agriculture, Ecosystems and Environment, 138, 318-323.

29. Goetz S., Steinberg D., Dubayah R. & Blair B. (2007). Laser remote sensing of canopy habitat heterogeneity as a predictor of bird species richness in an eastern temperate forest, USA. Remote Sensing of Environment, 108, 254-263.

30. Gough L., Shaver G.R., Carroll J., Royer D.L. & Laundre J.A. (2000). Vascular plant species richness in Alaskan arctic tundra: The importance of soil pH. Journal of Ecology, 88, 54-66.

31. Gould W. (2000). Remote sensing of vegetation, plant species richness, and regional biodiversity hotspots. Ecological Applications, 10, 1861-1870.

32. Graham J.H., Krzysik A.J., Kovacic D.A., Duda J.J., Freeman D.C., Emlen J.M., Zak J.C., Long W.R., Wallace M.P., Chamberlin-Graham C., Nutter J.P. & Balbach H.E. (2009). Species richness, equitability, and abundance of ants in disturbed landscapes. Ecological Indicators, 9, 866-877.

33. Gratwicke B. & Speight M.R. (2005). The relationship between fish species richness, abundance and habitat complexity in a range of shallow tropical marine habitats. Journal of Fish Biology, 66, 650-667.

34. Harner R.F. & Harper K.T. (1976). The Role of Area, Heterogeneity, and

Favorability in Plant Species Diversity of Pinyon-Juniper Ecosystems. Ecology, 57, 1254-1263.

35. Harrison S., Safford H.D., Grace J.B., Viers J.H. & Davies K.F. (2006). Regional and local species richness in an insular environment: Serpentine plants in California. Ecological Monographs, 76, 41-56.

36. Heikkinen R.K. & Neuvonen S. (1997). Species richness of vascular plants in the subarctic landscape of northern finland: Modelling relationships to the environment. Biodiversity and Conservation, 6, 1181-1201.

37. Hofer G., Wagner H.H., Herzog F. & Edwards P.J. (2008). Effects of topographic variability on the scaling of plant species richness in gradient dominated landscapes. Ecography, 31, 131-139.

38. Honkanen M., Roberge J.M., Rajasärkkä A. & Mönkkönen M. (2010). Disentangling the effects of area, energy and habitat heterogeneity on boreal forest bird species richness in protected areas. Global Ecology and Biogeography, 19, 61-71.

39. Honnay O., Hermy M. & Coppin P. (1999). Effects of area, age and diversity of forest patches in Belgium on plant species richness, and implications for conservation and reforestation. Biological Conservation, 87, 73-84.

40. Honnay O., Piessens K., Van Landuyt W., Hermy M. & Gulinck H. (2003). Satellite based land use and landscape complexity indices as predictors for regional plant species diversity. Landscape and Urban Planning, 63, 241-250.

41. Jimenez I., Distler T. & Jorgensen P.M. (2009). Estimated plant richness pattern across northwest South America provides similar support for the species-energy and spatial heterogeneity hypotheses. Ecography, 32, 433-448.

42. Johnson M.P., Frost N.J., Mosley M.W.J., Roberts M.F. & Hawkins S.J. (2003). The area-independent effects of habitat complexity on biodiversity

vary between regions. Ecology Letters, 6, 126-132.

43. Johnson M.P. & Simberloff D.S. (1974). Environmental determinants of island species numbers in the British Isles. Journal of Biogeography, 1, 149-154.

44. Kerr J.T. (2001). Butterfly species richness patterns in Canada: Energy, heterogeneity, and the potential consequences of climate change. Conservation Ecology, 5.

45. Kerr J.T. & Packer L. (1997). Habitat heterogeneity as a determinant of mammal species richness in high-energy regions. Nature, 385, 252-254.

46. Kerr J.T., Southwood T.R.E. & Cihlar J. (2001). Remotely sensed habitat diversity predicts butterfly species richness and community similarity in Canada. Proceedings of the National Academy of Sciences of the United States of America, 98, 11365-11370.

47. Koh C.N., Lee P.F. & Lin R.S. (2006). Bird species richness patterns of northern Taiwan: Primary productivity, human population density, and habitat heterogeneity. Diversity and Distributions, 12, 546-554.

48. Kohn D.D. & Walsh D.M. (1994). Plant species richness - The effect of island size and habitat diversity. Journal of Ecology, 82, 367-377.

49. Koivisto M.E. & Westerbom M. (2010). Habitat structure and complexity as determinants of biodiversity in blue mussel beds on sublittoral rocky shores. Marine Biology, 157, 1463-1474.

50. Kostylev V.E., Erlandsson J., Mak Y.M. & Williams G.A. (2005). The relative importance of habitat complexity and surface area in assessing biodiversity: Fractal application on rocky shores. Ecological Complexity, 2, 272-286.

51. Kumar S., Simonson S.E. & Stohlgren T.J. (2009). Effects of spatial heterogeneity on butterfly species richness in Rocky Mountain National Park, CO, USA. Biodiversity and Conservation, 18, 739-763.

52. Kumar S., Stohlgren T.J. & Chong G.W. (2006). Spatial heterogeneity influences native and nonnative plant species richness. Ecology, 87, 3186-3199.

53. Lassau S.A. & Hochuli D.F. (2005). Wasp community responses to habitat complexity in Sydney sandstone forests. Austral Ecology, 30, 179-187.

54. Lassau S.A. & Hochuli D.F. (2007). Associations between wasp communities and forest structure: Do strong local patterns hold across landscapes? Austral Ecology, 32, 656-662.

55. Lassau S.A. & Hochuli D.F. (2008). Testing predictions of beetle community patterns derived empirically using remote sensing. Diversity and Distributions, 14, 138-147.

56. Leniere A. & Houle G. (2006). Response of herbaceous plant diversity to reduced structural diversity in maple-dominated (Acer saccharum Marsh.) forests managed for sap extraction. Forest Ecology and Management, 231, 94-104.

57. Levin N., Shmida A., Levanoni O., Tamari H. & Kark S. (2007). Predicting mountain plant richness and rarity from space using satellite-derived vegetation indices. Diversity and Distributions, 13, 692-703.

58. Linder H.P. (1991). Environmental correlates of patterns of species richness in the south-western Cape Province of South Africa. Journal of Biogeography, 18, 509-518.

59. Lobo J.M., Castro I. & Moreno J.C. (2001). Spatial and environmental determinants of vascular plant species richness distribution in the Iberian Peninsula and Balearic Islands. Biological Journal of the Linnean Society, 73, 233-253.

60. Loneragan W.A. & Del Moral R. (1984). The influence of microrelief on community structure of subalpine meadows. Bulletin - Torrey Botanical Club, 111, 209-216.

61. Lucas K.L. & Carter G.A. (2008). The use of hyperspectral remote sensing to assess vascular plant species richness on Horn Island, Mississippi. Remote Sensing of Environment, 112, 3908-3915.

62. Lundholm J.T. & Larson D.W. (2003). Relationships between spatial environmental heterogeneity and plant species diversity on a limestone pavement. Ecography, 26, 715-722.

63. Mandl N.A., Kessler M. & Gradstein S.R. (2009). Effects of environmental heterogeneity on species diversity and composition of terrestrial bryophyte assemblages in tropical montane forests of Southern Ecuador. Plant Ecology and Diversity, 2, 313-321.

64. Marini L., Prosser F., Klimek S. & Marrs R.H. (2008). Water-energy, landcover and heterogeneity drivers of the distribution of plant species richness in a mountain region of the European Alps. Journal of Biogeography, 35, 1826-1839.

65. McMahon B.J., Purvis G. & Whelan J. (2008). The influence of habitat heterogeneity on bird diversity in Irish farmland. Biology and Environment, 108, 1-8.

66. Moody A. & Meentemeyer R.K. (2001). Environmental factors influencing spatial patterns of shrub diversity in chaparral, Santa Ynez Mountains, California. Journal of Vegetation Science, 12, 41-52.

67. Moora M., Öpik M., Zobel K. & Zobel M. (2009). Understory plant diversity is related to higher variability of vegetative mobility of coexisting species. Oecologia, 159, 355-361. Moreno-Rueda G. & Pizarro M. (2007). The relative influence of climate, environmental heterogeneity, and human population on the distribution of vertebrate species richness in south-eastern Spain. Acta Oecologica, 32, 50-58.

68. Moreno-Rueda G. & Pizarro M. (2009). Relative influence of habitat hete-

rogeneity, climate, human disturbance, and spatial structure on vertebrate species richness in Spain. Ecological Research, 24, 335-344.

69. Moser D., Zechmeister H.G., Plutzar C., Sauberer N., Wrbka T. & Grabherr G. (2002). Landscape patch shape complexity as an effective measure for plant species richness in rural landscapes. Landscape Ecology, 17, 657-669.

70. Muller C., Berger G. & Glemnitz M. (2004). Quantifying geomorphological heterogeneity to assess species diversity of set-aside arable land. Agriculture, Ecosystems and Environment, 104, 587-594.

71. Nagendra H., Rocchini D., Ghate R., Sharma B. & Pareeth S. (2010). Assessing plant diversity in a dry tropical forest: comparing the utility of Landsat and IKONOS satellite images. Remote Sens., 2, 478-496.

72. Nichols W.F., Killingbeck K.T. & August P.V. (1998). The influence of geomorphological heterogeneity on biodiversity: II. A landscape perspective. Conservation Biology, 12, 371-379.

73. Nielsen U.N., Osler G.H.R., Campbell C.D., Neilson R., Burslem D.F.R.P. & van der Wal R. (2010). The enigma of soil animal species diversity revisited: The role of small-scale heterogeneity. PLoS ONE, 5.

74. Nilsson C., Grelsson G., Johansson M. & Sperens U. (1989). Patterns of plant species richness along riverbanks. Ecology, 70, 77-84.

75. Oindo B.O. (2002). Predicting mammal species richness and abundance using multi-temporal NDVI. Photogrammetric Engineering and Remote Sensing, 68, 623-629.

76. Oindo B.O., De By R.A. & Skidmore A.K. (2000). Interannual variability of NDVI and bird species diversity in Kenya. ITC Journal, 2, 172-180.

77. Oindo B.O. & Skidmore A.K. (2002). Interannual variability of NDVI and species richness in Kenya. International Journal of Remote Sensing, 23, 285-298.

78. Oldeland J., Wesuls D., Rocchini D., Schmidt M. & Jürgens N. (2010). Does using species abundance data improve estimates of species diversity from remotely sensed spectral heterogeneity? Ecological Indicators, 10, 390-396.

79. Olofsson J., De Mazancourt C. & Crawley M.J. (2008). Spatial heterogeneity and plant species richness at different spatial scales under rabbit grazing. Oecologia, 156, 825-834.

80. Oster M., Cousins S.A.O. & Eriksson O. (2007). Size and heterogeneity rather than landscape context determine plant species richness in semi-natural grasslands. Journal of Vegetation Science, 18, 859-868.

81. Palmer M.W. (1991). Patterns of species richness among North Carolina hardwood forests: Tests of two hypotheses. J. Veg. Sci., 2, 361-366.

82. Palmer M.W., Earls P.G., Hoagland B.W., White P.S. & Wohlgemuth T. (2002). Quantitative tools for perfecting species lists. Environmetrics, 13, 121-137.

83. Parviainen M., Luoto M. & Heikkinen R.K. (2010). NDVI-based productivity and heterogeneity as indicators of plant-species richness in boreal landscapes. Boreal Environment Research, 15, 301-318.

84. Pausas J.G., Carreras J., Ferré A. & Font X. (2003). Coarse-scale plant species richness in relation to environmental heterogeneity. Journal of Vegetation Science, 14, 661-668.

85. Pereira J.A.A., Oliveira-Filho A.T. & Lemos-Filho J.P. (2007). Environmental heterogeneity and disturbance by humans control much of the tree species diversity of Atlantic montane forest fragments in SE Brazil. Biodiversity and Conservation, 16, 1761-1784.

86. Petersen M.J. & Courtney G.W. (2010). Landscape heterogeneity and the confluence of regional faunas promote richness and structure community

assemblage in a tropical biodiversity hotspot. Journal of Insect Conservation, 14, 181-189.

87. Pollock M.M., Naiman R.J. & Hanley T.A. (1998). Plant species richness in riparian wetlands-a test of biodiversity theory. Ecology, 79, 94-105.

88. Replansky T. & Bell G. (2009). The relationship between environmental complexity, species diversity and productivity in a natural reconstructed yeast community. Oikos, 118, 233-239.

89. Ribas C.R., Schoereder J.H., Pic M. & Soares S.M. (2003). Tree heterogeneity, resource availability, and larger scale processes regulating arboreal ant species richness. Austral Ecology, 28, 305-314.

90. Richard M., Bernhardt T. & Bell G. (2000). Environmental heterogeneity and the spatial structure of fern species diversity in one hectare of old-growth forest. Ecography, 23, 231-245.

91. Richerson P.J. & Lum K.L. (1980). Patterns of plant species diversity in California: Relation to weather and topography. American Naturalist, 116, 504-536.

92. Rocchini D., He K.S., Oldeland J., Wesuls D. & Neteler M. (2010). Spectral variation versus species β-diversity at different spatial scales: A test in African highland savannas. Journal of Environmental Monitoring, 12, 825-831.

93. Rocchini D., Ricotta C. & Chiarucci A. (2007). Using satellite imagery to assess plant species richness: The role of multispectral systems. Applied Vegetation Science, 10, 325-331.

94. Rocchini D., Wohlgemuth T., Ghisleni S. & Chiarucci A. (2008). Spectral rarefaction: Linking ecological variability and plant species diversity. Community Ecology, 9, 169-176.

95. Rogers G. & Overton J. (2000). Regional patterns of plant species richness in southern New Zealand. New Zealand Journal of Botany, 38, 609-627.

96. Roschewitz I., Gabriel D., Tscharntke T. & Thies C. (2005). The effects of landscape complexity on arable weed species diversity in organic and conventional farming. Journal of Applied Ecology, 42, 873-882.

97. Roth R.R. (1976). Spatial Heterogeneity and Bird Species Diversity. Ecology, 57, 773-782.

98. Schmitz M., Platt W. & DeCoster J. (2002). Substrate heterogeneity and number of plant species in Everglades savannas (Florida, USA). Plant Ecology, 160, 137-148.

99. Schneider K.N. & Winemiller K.O. (2008). Structural complexity of woody debris patches influences fish and macroinvertebrate species richness in a temperate floodplain-river system. Hydrobiologia, 610, 235-244.

100. Shi J., Ma K., Wang J., Zhao J. & He K. (2010). Vascular plant species richness on wetland remnants is determined by both area and habitat heterogeneity. Biodiversity and Conservation, 19, 1279-1295.

101. Shochat E., Abramsky Z. & Pinshow B. (2001). Breeding bird species diversity in the Negev: Effects of scrub fragmentation by planted forests. Journal of Applied Ecology, 38, 1135-1147.

102. Smith H.G., Dänhardt J., Lindström Ã. & Rundlöf M. (2010). Consequences of organic farming and landscape heterogeneity for species richness and abundance of farmland birds. Oecologia, 162, 1071-1079.

103. Southwood T.R.E., Brown V.K. & Reader P.M. (1979). The relationships of plant and insect diversities in succession. Biological Journal of the Linnean Society, 12, 327-348.

104. Symonds M.R.E. & Johnson C.N. (2008). Species richness and evenness in Australian birds. American Naturalist, 171, 480-490.

105. Taboada A., Tárrega R., Calvo L., Marcos E., Marcos J.A. & Salgado J.M. (2010). Plant and carabid beetle species diversity in relation to forest type

and structural heterogeneity. European Journal of Forest Research, 129, 31-45.

106. Tales E. & Berrebi R. (2007). Controls of local young-of-the-year fish species richness in flood plain water bodies: Potential effects of habitat heterogeneity, productivity and colonisation-extinction events. Ecology of Freshwater Fish, 16, 144-154.

107. Therriault T.W. & Kolasa J. (2000). Explicit links among physical stress, habitat heterogeneity and biodiversity. Oikos, 89, 387-391.

108. Thuiller W., F. Midgley G., Rougeti M. & M. Cowling R. (2006). Predicting patterns of plant species richness in megadiverse South Africa. Ecography, 29, 733-744.

109. Weibull A.C., Bengtsson J. & Nohlgren E. (2000). Diversity of butterflies in the agricultural landscape: Role of farming system and landscape heterogeneity. Ecography, 23, 743-750.

110. Zelený D., Li C.-F. & Chytrý M. (2010). Pattern of local plant species richness along a gradient of landscape topographical heterogeneity: result of spatial mass effect or environmental shift ? Ecography, 33, 578-589.

.2 Chapter 2 — Appendices

.2.1 FunDivEUROPE study design

In doing so, we divided the the data into training and test sets using a 70-30 % split and randomly sampling without replacement (Table S1, Appendix). With the training sets, w

This study was conducted across a network of permanent forest plots, spanning the primary bioclimatic gradient of the European continent and representing the major European forest types: boreal forests in Finland, hemi-boreal forests in Poland, beech forests in Germany, mountainous beech forests in Romania, thermophilous deciduous forests in Italy and Mediterranean-mixed forests in Spain (`http://www.fundiveurope.eu`). All plots were established in mature forest stands that differed primarily by tree species richness (stochastic or management driven) while variation in other environmental factors and management history was minimized as much as possible. As such, while regions differed strongly from one another in terms of climate, the 30 X 30 m plots within each region shared similar elevation, topography and soil quality. At each region, 30 X 30 m permanent plots with different combinations of locally dominant tree species were established in 2011 (as detailed in: Baeten et al. Baeten *et al.* (2013)). Plots range in target tree species richness from 1 to 3 in Finland, 1 to 4 in Romania, Germany and Spain and 1 to 5 in Italy and Poland. Each species is represented in all species richness levels, and whenever possible each species combination was replicated at least twice (59 of 91 combinations were replicated ; Table S1). In total, the network comprises 209 plots and 16 target species, several of which were present at more than one region (*e.g.*, *Picea abies*, *Pinus sylvestris* and *Fagus sylvatica*). The species pool includes conifers, deciduous broadleaves and evergreen broadleaves (for a full species' list see Table S2). Plots were also selected such that mixtures are similar in their species relative abundances (i.e. high evenness) and the presence of non-target species was minimal (*i.e.*, $< 5\%$ of the total basal area).

.2.2 Camera hardware, installation and sampling period

Within 5 m from the southern side of each study plot, one camera was installed on a large (DBH > 10cm) and visually healthy tree, to which the trunk was perpendicular to (*i.e.,* forms a 90° angle with) the ground slope. The cameras were installed at a height of 2m on the tree side and oriented towards the magnetic North. The final, specific location of the mounting tree was a matter of visual judgement ; within the camera's field of view, there were no major visual obstructions within 5m from the camera and the field of view captured a representative view of the plot's target species mixture (i.e., species richness level) and a side-view, vertical profile of the stand structure (*i.e.,* understory, midstory and overstory strata). The camera was fastened to the tree securely and the angle of view was be adjusted with backing materials.

The cameras were RGB digital cameras with intervalometers (Model 8.0 WSCT01, Wingscapes, Alabaster, AL, USA). The cameras were were programmed to take JPEG images (2592 X 1944 pixels). The camera parameters were set to automatic white balance, aperture-priority of f/2.8, ISO 200, and a focal length of 35 mm. During each sampling period (*i.e.,* growing season) the cameras acquired a single image three times daily (9 am, 12 pm and 3 pm local time) for the length of the growing season. Depending on the region, cameras were installed as early as April and were left acquiring images as late as January.

In 2012, cameras were installed in all plots of the German, Polish, Romanian, Italian and Spanish regions ; the image sampling seasonal extent varied by region, with cameras being installed in April and removed in October to December depending on the region. In all regions the cameras were removed well after fall senescence, but in some regions understory leaf flushing was already in progress when the cameras were installed. In 2013, cameras were again installed at the German region in April and at the Finnish region in May. After collecting images

for the full length of the 2013 growing season, cameras were then removed in November, 2013.

During image post-processing, three regions of interest (ROI) were manually delineated for each image time-series (*i.e.,* each plot): understory, midstory and overstory or canopy. We then used the binary excess green index described by Meyer and Neto Meyer et Neto (2008) to calculate the proportion of green within each ROI for each image in a time-series. The size (pixel coordinates) of any particular stratum ROI was determined as the largest unobstructed field of view of the stratum in question and, hence, varied across plots. In agreement with previous research (27), although ROI size varied, it did not have an effect on the excess green metric time-series and, hence, the detection of phenological events from it.

.2.3 Community phenology and growing season estimation

Digital repeat photography is fast becoming an important long-term data source for phenological research given its established benefits over traditional human-observed vegetation monitoring (*i.e.,* logistical, continuity, objectivity and cost advantages). Moreover, recent developments in image analysis techniques have illustrated that time-lapse photographic datasets can yield highly accurate estimates of the timing of key phenological events (*e.g.,* leaf flushing, start of growing season and end of season senescence), across a variety of ecosystem types and at spatio-temporal resolutions rarely achieved by satellite image datasets Sonnentag *et al.* (2012); Richardson *et al.* (2009b); Meyer et Neto (2008); Bater *et al.* (2011). The traditional methods of either manual surveying or aerial remote sensing to track and quantify understory growth and phenology have been extremely limited due to the associated logistical challenges (*e.g.,* labor intensity and the multiplicity of species and heterogeneous spatial distribution of understory species) or the interference of overstory canopies, respectively Tuanmu *et al.* (2010). While the use of in-situ digital photography remains in its early development and uti-

lization stages, a handful of studies have proven it a relatively robust method to capture forest understory green-up and other key above-ground plant phenological events Bater *et al.* (2011); Vartanian *et al.* (2014); Liang *et al.* (2012); Crimmins et Crimmins (2008); Graham *et al.* (2010).

Images from commercial-grade digital cameras represent combined brightness levels from three color channels spanning overlapping wavelength ranges of the visible electromagnetic spectrum. The Red-green-blue (RGB) color channel information from digital images can be separately extracted and summarized through color indices such as excess green Sonnentag *et al.* (2012). Thus, color indices accentuate a particular color feature of the photographed environment such as plant greenness. Calculated across image scenes captured at recurring time intervals (*e.g.*, hourly, daily, weekly), a time-series of a greenness index may be employed as a proxy of plant biomass development and seasonal growth.

To minimize redundancy and variation caused by diurnal light intensity changes and sun-angle, we used only images captured at 12:00 local time. Considering that each region of interest (ROI) defines a stratum in the forest stand, inclusive of all plant biomass visible from the camera's viewpoint, and that individual trees are not classified in the image scene, these time-series of greenness values can be plotted to estimate the period of active plant growth. To then identify the seasonal trends in growth for each ROI in each plot, we applied a smoothing spline function to each time-series and, subsequently, applied the first derivative of the smoothing function to determine start of season (SOS) and end of season (EOS) dates White *et al.* (1997). Finally, we defined the resulting growing season lengths (GSL) of the plot ROI or strata as the number of days between the SOS and EOS. We performed all image and time-series analyses in MATLAB version 2009a (MathWorks, 2009 ; Natick, USA).

.2.4 Regions of interest (ROI) and effect of the field of view

Vartanian *et al.* Vartanian *et al.* (2014) showed that when estimating biomass and seasonal growth trends from image-based color metrics, broad field of view images perform in a similar manner when compared to images captured using a narrow field of view. They found that no statistically significant difference existed between image-derived estimates of biomass growth from broad and narrow fields of view. As the authors noted, larger areas can be sampled and phenological status of an increased number of individuals is possible using broad field of view data, in turn allowing for more efficient data collection. We also found no significant effect of ROI size in relation to the image-derived greenness values and phenophases extracted from them.

.2.5 Predictor variables of interest

The primary predictor variable of interest across the plot network was the Shannon diversity of tree species Shannon (1948) to characterize tree species diversity in each forest stand. The advantage of this commonly used diversity index is that it not only takes into account species richness but also the species evenness of the forest stand; likely a key factor seeing that the GSL estimates from the images are likely influenced by the species' relative abundances inside the plot. The index is based on the probability that an individual picked at random from an infinitely large community will be a certain species. The more uncertainty one has about the species of a randomly selected individual, the higher the diversity of the community. The Shannon diversity index (H') is defined as follows:

$$H' = \sum_{i=1}^{n} p_i ln p_i$$

where, p_i is the number of individuals of each tree species i in the plot, and n is the total number of species in the stand.

As plant species phenology is, in part, the timing of an event in relation to environmental conditions, chiefly ground and air temperature dynamics, we examined the effect of geographic location (latitude) and exogenous environmental factors on the timing of growing season length. As such we included, mean annual temperature, mean annual precipitation, mean diurnal temperature range and exposition as predictor variables in our statistical models. We also initially included and tested several additional site and environmental variables such as soil type, ground cover and management level but excluded them from any further statistical analysis after they showed no perceivable correlations with our response variables. Climate data was sourced from `www.worldclim.org` and was as a spatial resolution of 1 X 1 km; admittedly coarse for any local or microclimate variation in temperature and precipitation. We also included mean age of canopy trees as a predictor variable of interest. All site and stand characteristics variables were recorded at the time of plot establishment by the FunDivEUROPE field technicians and to which further details can be found in Baeten et al. Baeten *et al.* (2013).

.2.6 Image exposure as a proxy for below-canopy seasonal light availability

In a *post-hoc* and preliminary effort to further test the hypothesis that the below-canopy light availability may play a role in driving understory phenology, we calculated rough but temporally high resolution estimate of below-canopy light availability and heterogeneity at the plot-level from the camera exposure values of the time-series images during the period of peak canopy closure (*i.e.,* July and August). Although image exposure values represent an uncalibrated and co-

arse measure of localized light intensity, and thus availability for photosynthetic absorption, it was included as a potential predictor of GSL in the RF models. Exposure is the amount of light per unit area (the image plane illuminance times the exposure time) reaching the camera sensor, as determined by shutter speed, lens aperture and scene luminance. Thus, since exposure is an inverse measure of scene luminance, we extracted the exposure value of each 12:00 pm image for each plot time-lapse sequence, computed their inverse and use these values as an estimate of generalized below-canopy (the cameras were approximately 1 m above the ground) scene illumination or light availability. This provided a daily chronology of illumination in each plot for the growing season. Of course, such values are highly dependent on weather conditions, however we suggest sky conditions would be relatively uniform across the study regions on a given day and any local variation between plots would be minimized through averaging across the growing season or would simply contribute to some level of unavoidable "noise". We then computed the mean understory light availability for various phases of the growing season (start of season: May - June; mid or peak of season: July - August ; end of season: September - October ; and the entire growing season). We also computed the standard deviation of understory light availability for each of these phases of the growing season. We further suggest, that SD of understory light availability may capture, to some degree, the temporal and spatial heterogeneity in understory light conditions as a more heterogenous below-canopy light environment would likely vary more over time than a homogenous one ; again, this metric would also be influenced by daily variations in sky conditions. We acknowledge that this proxy metric of understory light availability has not been validated to date, and present the results tentatively. However, we also suggest that given that we find significant effects of this predictor variable on our key phenological response variables, at least in part, suggests it operates as a rough estimate of understory light conditions and should be explored further as such.

.2.7 Statistical Analysis: random forests of regression trees

The random forest algorithm implements two powerful approaches: bagging and boosting, where bagging consists of using a bootstrap sample of the data to train the regression tree. A random subset of one-third of the observations (with replacement) is used at each bootstrap run for growing a regression tree while the remaining (out-of-bag) observations are used for validation. Each regression tree is gown until each sub-partition contains a small but fixed number of observations. Boosting consists of using only a random subset of the predictor variables at each split in the regression tree. Boosting reduces dependence between similarly important (collinear) variables and prevents over-fitting Siroky (2009). Finally, random forests contains a cross-validation method to calculate the model bias using the out-of-bag observations.

To build the RFs, we used the *randomForest* package in R Liaw et Wiener (2002) and constructed models for each of the three stand strata (*i.e.,* ROIs): overstory, midstory and understory. For regression trees, as we implement here, the random forests package provides two measures of predictor variable importance: 1) the mean decrease in the accuracy of predictions in the out of bag samples when a given variable is excluded from the model (%IncMSE), hereafter termed variable MSE-importance ; and 2) a measure of the total decrease in node impurity that results from splits over that variable and averaged over all trees (IncNodePurity), hereafter termed variable node purity.

Most statistical procedures for regression and classification measure variable importance indirectly by selecting variables using criteria such as statistical significance and Akaike's Information Criterion. The approach taken in RF is different. For each tree in the forest, there is a misclassification rate for the out-of-bag observations. To assess the importance of a specific predictor variable, the values of the variable are randomly permuted for the out-of-bag observations, and then the

modified out-of-bag data are passed down the tree to get new predictions. The difference between the misclassification rate for the modified and original out-of-bag data, divided by the standard error, is a measure of the importance of the variable. The technique was developed by Breiman Breiman (2001). The first step in measuring the variable importance in a data set $\mathcal{D}_n = \{(X_i, Y_i)\}_{i=1}^n$ is to fit a random forest to the data. During the fitting process the out-of-bag error for each data point is recorded and averaged over the forest (errors on an independent test set can be substituted if bagging is not used during training). To measure the importance of the *j-th* feature after training, the values of the *j-th* feature are permuted among the training data and the out-of-bag error is again computed on this perturbed data set. The importance score for the j-th feature is computed by averaging the difference in out-of-bag error before and after the permutation over all trees. The score is normalized by the standard deviation of these differences. Features which produce large values for this score are ranked as more important than features which produce small values. The node purity value can be interpreted as follows: at each split of a tree, the algorithm calculates how much this split reduces node impurity. For regression trees, this is the difference between the residual sum of squares before and after the split. This is then summed over all splits for that variable and over all trees. As the node purity increases, the conditional distribution of the response is more concentrated around particular points.

A cross-validated rsquare value can also be computed for each RF model as:

$$R^2_{CV} = 1 - \frac{\sum_i (y_i - \hat{y})^2}{\sum_i (y_i - \bar{y})^2}$$

That is, we compute the mean-squared error of the original out-of-bag predictions ($\hat{y}$) and divide those by the variance of the original observations. Thus, in this form it is possible for RF models to produce cross-validated rsquare values greater than 100 or less than 0; in the later case, if the predictions are no better than random.

In our application of the RF algorithm we applied the following parameters:

$ntree = 10000$, $mtry = 3$, $ndsize = 5$

,where *ntree* is the number of regression trees constructed per model, *mtry* is the number of variables randomly selected at each node and *ndsize* is the minimum node size used.

.2.8 Evergreen bias

A methodological limitation of the image-based estimation of phenology lies with the issue of estimating the phenophases of evergreen species, including their relative contributions to phenology. Evergreen monocultures tended to display the highest standard deviations of EOS between plots of the same species (Table S2). Seasonal green up and down patterns were, in fact, unimodal (*i.e.,* a clear seasonal green- up and down growth pattern is produced) and mathematically discernible for evergreen plots. Moreover, previous studies employing similar time-lapse photographic methods have also demonstrated their capacity to capture phenological trends in boreal evergreen stands Bater *et al.* (2011). However, since the greenness baseline (*i.e.,* the dormant season will be different for evergreen vs. deciduous species, wherein evergreen species start and end the growing season green), the leaf flushing and senescence phases are much less pronounced than those of deciduous species or communities. As such the image-derived SOS and EOS dates become sensitive to variations in the slopes of the fitted seasonal curves since they are calculated as derivatives. We acknowledged this potential form of "noise" or evergreen bias, by sequentially filtering out plots containing an increasing proportion

of evergreen tree species and then performing our statistical analysis (*i.e.,* building the RF models) with each of these subsets. The expectation was that, with successive filtering out of plots with evergreen trees, any relationships between EOS and the predictor variables should become evident or stronger.

.2.9 Supplementary results

Start of season invariability

The time-lapse photography approach to tracking forest phenology is not without limitations. One such limitation may be its apparent insensitivity to the SOS green-up. Our results showed little variation (ca. 3-5 days; Table S3) in SOS between tree species (*i.e.,* monoculture plots) or assemblages (*i.e.,* mixed-species plots) and this result held true for the understory communities as well. The majority of plant phenological studies, on the other hand, have focussed on SOS as the principle phenophase of interest, specifically the timing of spring leaf flushing. For forest systems, theory dictates that there is strong selection pressure to maximize light capture in the spring when it is most available across all forest strata Diez *et al.* (2012); Augspurger (2008). As such, the SOS phenophase is expected to respond to environmental factors and to differ between species. Alternatively, there is no general consensus on the mechanisms driving the autumn phenology events of temperate forests, indicating not that it is irrelevant, but simply not well understood.

More recent studies employing image-derived phenologies have shown that autumn senescence in temperate forests exhibits higher levels of interspecific variation within a year than the typical mean senescence date across years Jeong et Medvigy (2014). Moreover, at least for the case of understory saplings, long leaf lifespan is achieved mainly by delaying leaf senescence in autumn rather than by early spring leaf flushing Lopez *et al.* (2008). It may be that spring phenology, and the race to exploit the spring light window, is primarily initiated by temperature (*i.e.,* attaining a growing degree day threshold) and thus varies across years with

climate conditions and not necessarily between species; that is, the earliest leafing species always wins the race to exploit the light window, but the race can begin at different times from year to year.

LIST OF APPENDIX CHAPTER 2 TABLES

Table S2- 1: Summary statistics for the FunDivEUROPE project permanent forest plots (region names are abbreviated using the first three letters of the country). Plot descriptors include elevation (m.a.s.l.), slope (categorical; 1 — 3 in order of increasing steepness), aspect, soil depth (cm), aboveground biomass (AGB; $MgC/_{ha}$), basal area ($m^2/_{ha}$), quadratic mean stem diameter (QMD; cm), number of stems, species richness (SR) and species composition (species names are abbreviated using the first two letter of the genus and species name; for species full names see Table S2.

Site	Plot	Elevation	Slope	Aspect	Soil depth	AGB	Basal area	QMD	Stems	SR	Composition
FIN	FIN01	87	1	None	80	64.4	26.9	21.1	69	2	PICA.PINS
FIN	FIN02	138	1	None	80	46.7	17.8	19.8	52	2	PICA.BETP
FIN	FIN03	139	1	None	80	38.5	14.6	20.4	40	2	PICA.BETP
FIN	FIN04	138	1	None	80	50.6	20.1	20.5	55	2	PICA.BETP
FIN	FIN05	114	2	S	70	51.0	19.7	22.2	46	2	PINS.BETP
FIN	FIN06	112	1	N	80	86.1	32.3	21.6	79	1	PICA
FIN	FIN07	120	1	None	80	47.3	17.1	17.9	61	1	BETP
FIN	FIN08	120	1	None	80	44.2	15.7	19.3	48	1	BETP
FIN	FIN09	119	1	None	80	58.1	24.4	21.6	60	1	PINS
FIN	FIN10	134	1	None	80	68.4	27.2	21.7	66	1	PICA
FIN	FIN11	124	2	W	80	34.9	15.6	15.7	73	1	BETP
FIN	FIN12	233	1	None	80	54.0	27.0	14.4	149	3	PICA.PINS.BETP
FIN	FIN13	219	2	NW	70	37.7	18.9	15.5	90	2	PINS.BETP
FIN	FIN14	101	1	S	80	37.4	16.6	18.9	53	1	PINS
FIN	FIN15	97	1	None	80	47.0	19.3	19.1	61	2	PINS.BETP
FIN	FIN16	143	1	None	80	62.9	25.8	21.2	66	1	PINS
FIN	FIN17	139	2	SE	70	58.3	24.8	21.4	62	2	PICA.PINS
FIN	FIN18	110	1	None	80	68.7	28.8	19.6	86	1	PICA
FIN	FIN19	130	2	N	80	70.7	27.6	23.3	58	2	PICA.PINS
FIN	FIN20	119	1	None	80	77.3	29.2	22.7	65	2	PICA.BETP
FIN	FIN21	135	2	NE	80	37.2	16.0	19.1	50	1	PINS
FIN	FIN22	126	1	None	80	55.5	25.7	16.9	103	2	PICA.PINS
FIN	FIN23	122	1	None	80	64.8	27.8	18.8	90	1	PICA
FIN	FIN24	151	2	E	70	44.5	23.3	12.5	170	2	PICA.BETP
FIN	FIN25	136	1	N	80	72.5	30.3	17.8	110	3	PICA.PINS.BETP
FIN	FIN26	108	1	SE	80	61.6	25.2	20.0	72	3	PICA.PINS.BETP
FIN	FIN27	119	1	N	80	43.2	20.1	16.3	87	2	PICA.PINS
FIN	FIN28	111	2	NW	80	52.7	21.5	19.5	65	2	PINS.BETP
GER	GER01	423	2	SW	NA	156.1	30.6	33.1	32	1	FAGS
GER	GER02	390	1	N	NA	141.0	29.2	34.0	29	1	FAGS
GER	GER03	323	1	N	NA	227.6	37.7	28.3	54	2	ACEP.FRAE
GER	GER04	273	1	N	NA	332.1	51.1	34.2	50	1	FRAE
GER	GER05	337	1	N	NA	196.3	43.1	28.7	60	1	QUEP
GER	GER06	284	1	E	NA	283.3	58.5	33.1	61	2	FAGS.QUEP
GER	GER07	480	1	N	NA	72.7	29.9	19.4	91	1	PICA
GER	GER08	329	1	N	NA	101.0	42.1	22.3	97	1	PICA
GER	GER09	372	1	SE	NA	105.2	35.1	15.8	162	3	FAGS.ACEP.FRAE
GER	GER10	381	2	E	NA	113.8	25.2	20.8	67	3	FAGS.ACEP.FRAE
GER	GER11	458	1	N	NA	278.9	39.2	36.9	33	2	FAGS.FRAE
GER	GER12	383	1	N	NA	148.1	31.2	39.4	23	2	FAGS.QUEP
GER	GER13	301	1	N	NA	218.9	41.6	39.2	31	3	ACEP.FRAE.QUEP
GER	GER14	324	1	N	NA	100.6	31.4	27.4	48	2	PICA.FAGS
GER	GER15	378	2	N	NA	164.0	42.7	31.9	48	2	PICA.FRAE
GER	GER16	331	2	NE	NA	181.4	47.0	38.7	36	3	PICA.FAGS.QUEP
GER	GER17	365	1	E	NA	109.7	25.9	23.9	52	2	FAGS.ACEP
GER	GER18	494	1	N	NA	267.9	45.6	30.5	56	2	ACEP.FRAE
GER	GER19	407	1	NE	NA	132.6	29.5	36.0	26	3	FAGS.ACEP.QUEP

Table S2- 2: Table con't...

GER	GER20	325	1	E	NA	122.6	28.6	22.8	63	3	FAGS.FRAE.QUEP
GER	GER21	392	1	N	NA	147.7	27.8	39.9	20	4	FAGS.ACEP.FRAE.QUEP
GER	GER22	383	1	N	NA	185.9	38.7	25.2	70	2	FAGS.FRAE
GER	GER23	378	1	N	NA	186.9	45.6	32.3	50	3	PICA.FAGS.QUEP
GER	GER24	418	2	S	NA	94.7	18.3	31.6	21	3	FAGS.ACEP.FRAE
GER	GER25	368	1	N	NA	133.5	28.9	29.1	39	3	FAGS.ACEP.QUEP
GER	GER26	392	2	N	NA	112.7	30.5	28.2	44	3	FAGS.ACEP.FRAE
GER	GER27	469	1	N	NA	272.8	38.3	40.3	27	4	FAGS.ACEP.FRAE.QUEP
GER	GER28	283	1	N	NA	108.6	21.0	27.8	31	2	ACEP.FRAE
GER	GER29	401	2	N	NA	206.1	41.6	33.3	43	3	FAGS.FRAE.QUEP
GER	GER30	415	3	E	NA	64.0	15.6	23.7	32	2	FAGS.QUEP
GER	GER31	459	1	N	NA	189.1	31.7	39.8	23	2	FAGS.FRAE
GER	GER32	388	1	E	NA	275.6	47.9	33.1	50	3	FAGS.ACEP.FRAE
GER	GER33	391	1	N	NA	196.6	39.1	31.2	46	4	PICA.FAGS.ACEP.FRAE
GER	GER34	353	3	N	NA	172.9	35.2	24.4	68	3	PICA.FAGS.FRAE
GER	GER35	331	1	N	NA	270.6	54.2	46.3	29	2	FAGS.QUEP
GER	GER36	305	1	N	NA	81.3	15.8	27.5	24	2	PICA.FRAE
GER	GER37	430	2	SE	NA	166.7	30.8	34.3	30	4	FAGS.ACEP.FRAE.QUEP
GER	GER38	496	1	N	NA	307.2	52.2	47.1	27	3	FAGS.ACEP.FRAE
ITA	ITA01	443	2	NW	80	82.8	24.8	20.3	69	2	QUEP.QUEC
ITA	ITA02	470	2	NE	80	100.9	24.2	26.4	40	4	QUEI.QUEP.QUEC.OSTC
ITA	ITA03	416	2	NW	80	69.6	21.3	16.8	86	2	QUEI.OSTC
ITA	ITA04	397	2	NE	80	108.4	27.9	24.3	54	1	QUEP
ITA	ITA05	422	2	NW	80	99.9	27.3	18.5	91	3	QUEI.QUEP.OSTC
ITA	ITA06	393	1	N	30	119.6	34.4	15.2	170	1	QUEI
ITA	ITA07	402	3	W	70	78.0	30.0	20.2	84	1	CASS
ITA	ITA08	383	3	N	30	59.5	21.3	12.6	154	2	QUEI.OSTC
ITA	ITA09	429	2	N	50	124.6	34.1	16.2	148	3	QUEI.QUEC.OSTC
ITA	ITA10	438	2	NE	50	106.7	28.6	23.2	61	3	QUEI.QUEP.CASS
ITA	ITA11	379	2	NW	50	97.2	29.6	17.9	106	4	QUEI.QUEP.CASS.OSTC
ITA	ITA12	445	2	N	70	68.9	29.3	18.6	97	1	CASS
ITA	ITA13	479	2	W	80	107.1	29.6	19.8	86	2	QUEC.CASS
ITA	ITA14	444	2	NW	80	97.7	27.1	20.8	72	3	QUEI.QUEC.CASS
ITA	ITA16	417	2	NW	70	88.0	23.6	24.8	44	1	QUEI
ITA	ITA17	395	2	SW	80	84.1	22.0	23.6	45	2	QUEI.QUEP
ITA	ITA18	425	2	NE	80	135.4	30.2	21.9	72	4	QUEI.QUEP.QUEC.OSTC
ITA	ITA19	478	2	NE	80	108.2	23.6	28.2	34	2	QUEC.OSTC
ITA	ITA20	508	2	NE	80	94.7	29.0	18.7	95	3	QUEI.QUEP.QUEC
ITA	ITA21	464	2	NW	70	103.2	33.4	27.4	51	2	QUEI.CASS
ITA	ITA22	410	3	NW	80	133.9	38.6	21.7	94	4	QUEI.QUEC.CASS.OSTC
ITA	ITA23	523	2	NE	80	86.4	25.1	21.1	65	4	QUEI.QUEP.QUEC.CASS
ITA	ITA24	416	2	SW	80	194.0	38.6	29.5	51	2	QUEI.QUEC
ITA	ITA25	355	2	N	70	77.7	22.9	13.5	144	3	QUEI.CASS.OSTC
ITA	ITA26	406	1	NW	50	77.8	26.8	17.5	100	3	QUEP.QUEC.CASS
ITA	ITA27	421	2	N	70	101.1	30.3	20.3	84	1	QUEP
ITA	ITA28	418	3	N	70	50.8	18.7	19.6	56	2	QUEP.CASS
ITA	ITA29	471	2	NE	80	87.5	22.1	22.7	49	3	QUEP.QUEC.OSTC
ITA	ITA30	389	2	NE	70	91.9	25.0	22.4	57	2	CASS.OSTC
ITA	ITA31	269	2	N	50	89.6	26.0	15.9	118	1	OSTC

Table S2- 2: Table con't...

ITA	ITA32	429	2	E	70	92.7	26.1	17.3	100	4	QUEI.QUEC.CASS.OSTC
ITA	ITA33	519	2	NE	50	62.0	23.6	17.1	92	4	QUEI.QUEP.QUEC.CASS
ITA	ITA34	480	3	NE	70	63.5	21.7	14.8	114	4	QUEI.QUEP.QUEC.CASS.OSTC
ITA	ITA36	436	2	NE	50	77.5	25.6	19.5	77	3	QUEP.QUEC.CASS
POL	POL01	182	1	N	80	100.2	34.7	33.2	36	1	PICA
POL	POL02	157	1	N	80	96.6	29.8	30.8	36	1	CARB
POL	POL03	163	1	N	80	93.4	33.2	32.1	37	1	PICA
POL	POL04	171	1	N	80	205.1	51.7	33.8	52	3	PICA.BETP.QUER
POL	POL05	176	1	N	80	116.4	31.5	25.0	58	2	CARB.QUER
POL	POL06	190	1	N	80	109.5	36.5	25.0	67	3	PICA.BETP.CARB
POL	POL07	190	1	N	80	141.1	38.3	34.4	37	4	PICA.BETP.CARB.QUER
POL	POL08	180	1	N	80	98.5	32.9	31.1	39	2	BETP.CARB
POL	POL09	195	1	N	80	100.6	31.1	35.7	28	2	PICA.CARB
POL	POL10	145	1	N	80	164.2	33.5	31.8	38	2	CARB.QUER
POL	POL11	185	1	N	80	108.7	33.0	26.2	55	2	BETP.CARB
POL	POL12	160	1	N	80	87.2	28.4	34.7	27	1	CARB
POL	POL13	160	1	N	80	83.7	24.4	28.2	35	3	BETP.CARB.QUER
POL	POL14	150	1	N	80	120.5	38.2	35.3	35	4	PICA.PINS.CARB.QUER
POL	POL15	184	1	N	80	127.5	34.0	30.8	41	3	PICA.CARB.QUER
POL	POL16	186	1	N	80	130.4	32.9	30.7	40	2	PICA.QUER
POL	POL17	155	1	N	80	111.0	37.6	29.1	51	4	PICA.PINS.BETP.CARB
POL	POL18	160	1	N	80	178.5	55.0	30.9	66	3	PINS.CARB.QUER
POL	POL19	175	1	N	80	134.3	46.9	33.5	48	2	PICA.PINS
POL	POL20	173	1	N	80	141.9	32.1	24.8	60	2	CARB.QUER
POL	POL21	170	1	N	80	142.1	51.5	27.0	81	1	PINS
POL	POL22	160	1	N	80	198.2	60.6	39.3	45	3	PICA.PINS.QUER
POL	POL23	170	1	N	80	122.5	42.3	32.8	45	3	PICA.PINS.CARB
POL	POL24	170	1	N	80	130.2	38.3	26.8	61	3	PINS.CARB.QUER
POL	POL25	171	1	N	80	107.8	38.5	28.1	56	2	PINS.CARB
POL	POL26	165	1	N	80	94.4	31.4	24.1	62	2	BETP.CARB
POL	POL27	175	1	N	80	141.4	40.6	35.9	36	4	PICA.PINS.CARB.QUER
POL	POL28	170	1	N	80	169.7	51.4	33.0	54	2	PICA.BETP
POL	POL29	155	1	N	80	125.1	36.7	29.6	48	3	PINS.BETP.QUER
POL	POL30	140	1	N	80	110.1	37.4	26.9	59	4	PICA.PINS.BETP.CARB
POL	POL31	150	1	N	80	127.6	38.8	30.1	49	4	PICA.BETP.CARB.QUER
POL	POL32	177	1	N	80	103.1	31.7	22.0	75	4	PICA.PINS.BETP.QUER
POL	POL33	184	1	N	80	92.7	32.8	30.3	41	3	PINS.BETP.CARB
POL	POL34	189	1	N	80	91.6	27.8	25.3	50	4	PINS.BETP.CARB.QUER
POL	POL35	188	1	N	80	121.2	37.4	31.9	42	5	PICA.PINS.BETP.CARB.QUER
POL	POL36	160	1	N	80	114.6	31.4	28.6	44	3	BETP.CARB.QUER
POL	POL37	145	1	N	80	117.7	39.1	31.9	44	5	PICA.PINS.BETP.CARB.QUER
POL	POL38	165	1	N	80	124.8	41.0	27.3	63	3	PINS.BETP.CARB
POL	POL39	170	1	N	80	128.1	35.7	28.3	51	4	PINS.BETP.CARB.QUER
POL	POL40	175	1	N	80	155.2	55.9	35.4	51	1	PINS
POL	POL41	200	1	N	80	143.7	42.9	28.1	62	4	PICA.PINS.BETP.QUER
POL	POL42	177	1	N	80	96.5	34.5	31.8	39	4	PICA.PINS.BETP.CARB
POL	POL43	186	1	N	80	104.0	33.2	31.2	39	3	PICA.PINS.QUER
ROM	ROM01	838	2	SW	80	123.3	39.2	34.8	37	1	PICA
ROM	ROM02	865	2	SW	80	150.5	51.8	34.1	51	1	PICA

Table S2- 2: Table con't...

ROM	ROM03	869	2	SW	80	240.0	54.0	33.0	57	3	PICA.FAGS.ACEP
ROM	ROM05	1019	2	SW	70	206.3	64.0	41.3	43	2	PICA.ABIA
ROM	ROM06	1045	2	SE	80	216.4	52.7	34.4	51	2	FAGS.ACEP
ROM	ROM07	1062	2	SE	80	215.7	75.6	33.3	78	1	ABIA
ROM	ROM0B	1028	2	E	80	228.5	62.3	33.1	65	4	PICA.ABIA.FAGS.ACEP
ROM	ROM09	984	2	SE	80	284.8	61.2	45.4	34	2	PICA.FAGS
ROM	ROM10	968	2	SE	80	182.8	57.6	38.7	44	3	PICA.ABIA.ACEP
ROM	ROM11	805	2	NE	80	180.8	45.8	43.3	28	3	PICA.ABIA FAGS
ROM	ROM12	799	2	NE	80	187.7	44.5	38.7	34	2	PICA.FAGS
ROM	ROM13	812	2	NE	80	207.1	38.0	37.5	31	1	FAGS
ROM	ROM14	909	2	SE	70	158.0	36.6	36.8	31	2	FAGS.ACEP
ROM	ROM15	930	3	SE	30	88.3	28.9	28.4	41	1	ACEP
ROM	ROM16	972	2	SE	80	130.1	39.9	29.6	52	1	ACEP
ROM	ROM17	1047	2	NW	30	202.5	69.7	34.0	69	2	PICA.ABIA
ROM	ROM1B	1012	2	N	70	228.5	68.7	35.6	62	3	PICA.ABIA.FAGS
ROM	ROM19	951	2	N	80	230.4	53.6	37.0	45	2	ABIA.FAGS
ROM	ROM20	869	2	N	70	186.0	43.1	39.9	31	3	ABIA.FAGS.ACEP
ROM	ROM21	718	2	W	70	177.5	48.4	32.6	52	3	PICA.FAGS.ACEP
ROM	ROM22	843	2	NE	80	152.4	49.9	28.8	69	3	PICA.ABIA.FAGS
ROM	ROM23	894	2	SW	80	237.3	71.3	44.7	41	1	ABIA
ROM	ROM24	919	2	NW	80	214.3	58.5	33.4	60	2	ABIA.FAGS
ROM	ROM25	1030	2	NE	70	180.7	50.8	29.9	65	3	ABIA.FAGS.ACEP
ROM	ROM26	782	2	NE	80	186.2	39.3	30.3	49	1	FAGS
ROM	ROM27	738	2	NE	80	111.4	33.7	31.9	38	2	PICA.ACEP
ROM	ROM28	655	1	None	70	143.2	44.2	38.0	35	2	ABIA.FAGS
ROM	ROM29	893	2	SW	80	198.9	54.0	33.0	57	4	PICA.ABIA.FAGS.ACEP
SPA	SPA01	1224	2	NE	20	57.7	26.1	18.3	89	2	PINS.QUEF
SPA	SPA02	1238	1	SW	20	24.2	12.9	14.1	74	3	PINS.QUEF.PINN
SPA	SPA03	1228	2	SW	20	52.3	22.1	27.7	33	2	QUEF.PINN
SPA	SPA04	1286	1	None	50	74.8	29.1	30.9	35	2	PINS.QUEF
SPA	SPA05	1283	1	NW	70	48.8	22.2	19.5	67	2	PINS.QUEF
SPA	SPA06	1306	2	NE	30	66.7	26.1	25.5	46	2	QUEF.PINN
SPA	SPA07	1291	2	NE	30	26.2	12.8	23.3	27	2	PINS.PINN
SPA	SPA08	1207	2	SW	20	67.1	26.8	16.1	118	2	QUEF.PINN
SPA	SPA09	1211	2	S	20	71.6	30.6	12.5	223	1	QUEF
SPA	SPA10	1270	2	SE/S	70	42.1	17.5	12.7	125	1	QUEF
SPA	SPA11	1187	2	SE	20	24.7	10.3	13.1	69	1	QUEF
SPA	SPA12	1073	2	NE	NA	119.2	39.3	25.2	71	1	PINN
SPA	SPA13	1010	2	W	20	30.8	13.3	14.6	71	3	QUEF.QUEI.PINN
SPA	SPA14	999	2	W	20	28.8	13.1	17.5	49	2	QUEI.PINN
SPA	SPA15	980	2	W	20	34.8	15.6	20.9	41	1	PINN
SPA	SPA16	1032	2	NW	30	34.2	13.8	17.5	52	2	QUEI.PINN
SPA	SPA17	960	1	None	20	85.7	33.6	18.8	109	1	PINN
SPA	SPA18	1403	1	None	70	115.9	52.0	31.0	62	1	PINS
SPA	SPA19	1310	1	None	50	67.8	34.2	24.7	64	1	PINS
SPA	SPA20	1311	1	None	20	81.3	42.1	26.1	71	1	PINS
SPA	SPA21	1404	1	N	70	50.5	24.4	20.1	69	2	PINS.PINN
SPA	SPA22	1325	1	None	20	92.6	40.9	25.2	74	2	PINS.PINN
SPA	SPA23	1388	2	NE	50	45.9	22.2	21.1	57	2	PINS.PINN

Table S2- 2: Table con't...

SPA	SPA24	1377	1	SW	50	53.9	23.2	19.2	72	4	PINS.QUEF.QUEI.PINN
SPA	SPA25	1314	2	NE	20	57.5	22.1	22.7	49	3	PINS.QUEF.PINN
SPA	SPA26	1387	2	N	30	45.0	17.1	19.6	51	4	PINS.QUEF.QUEI.PINN
SPA	SPA27	1322	1	NW	20	59.9	23.0	18.5	77	3	QUEF.QUEI.PINN
SPA	SPA28	1360	1	SE	30	35.9	16.5	11.5	142	2	QUEF.QUEI
SPA	SPA29	1354	2	SE	30	86.0	34.5	19.4	105	4	PINS.QUEF.QUEI.PINN
SPA	SPA30	1350	1	SW	20	18.9	8.8	13.8	53	2	QUEF.QUEI
SPA	SPA31	1342	1	SW	30	21.7	8.9	12.1	70	2	QUEF.QUEI
SPA	SPA32	1236	2	SW	30	20.3	9.5	13.2	63	1	QUEI
SPA	SPA33	1251	2	SW	20	20.7	10.8	13.8	65	1	QUEI
SPA	SPA34	1250	2	SW	20	22.2	10.8	11.1	101	2	QUEF.QUEI
SPA	SPA35	1267	2	N	30	27.0	12.8	16.0	57	2	QUEI.PINN
SPA	SPA36	1211	2	S	30	24.3	11.7	16.9	47	2	QUEI.PINN

Table S2- 2: List of target species for each study region, including their functional group and their phenophases. $_{obs}$EOS is the estimated EOS dates calculated from our image-derived method for each tree species in it's monospecific plots (species richness = 1) and for each region. For species that occur in monospecific stands in multiple plots within a given region, the EOS dates are averaged. Thus the SD of $_{theor}$EOS is the standard deviation for such cases. The units for the $_{obs}$EOS are julien day of year (DOY) and are number of days for SD of $_{obs}$EOS.

Study site	Species	Functional group	Phenophases*	
			$_{obs}$EOS	SD of $_{obs}$EOS
Finland	*Betula pendula*	Deciduous broadleaf	270	0
	Picea abies	Conifer	261.25	17.5
	Pinus sylvestris	Conifer	265.75	8.5
Germany	*Acer pseudoplatanus*	Deciduous broadleaf	NA	NA
	Fagus sylvatica	Deciduous broadleaf	295.75	4.92
	Fraxinus excelsior	Deciduous broadleaf	288.5	16.26
	Quercus petraea	Deciduous broadleaf	298	2.83
	Picea abies	Conifer	274.75	37.66
Italy	*Quercus ilex*	Evergreen broadleaf	217.50	70
	Castanea sativa	Deciduous broadleaf	254.5	62.93
	Ostrya carpinifolia	Deciduous broadleaf	307	0
	Quercus cerris	Deciduous broadleaf	303.5	3.54
	Quercus petraea	Deciduous broadleaf	312.5	0.71
Poland	*Betula pendula*	Deciduous broadleaf	NA	NA
	Carpinus betulus	Deciduous broadleaf	300	NA
	Quercus robur	Deciduous broadleaf	NA	NA
	Picea abies	Conifer	240.5	84.15
	Pinus sylvestris	Conifer	300	0
Spain	*Quercus ilex*	Evergreen broadleaf	259	72.12
	Quercus faginea	Deciduous broadleaf	281.33	49.65
	Pinus nigra	Conifer	282.5	27.58
	Pinus sylvestris	Conifer	207.33	8.14

Table S2- 3: Summary statistics of the observed image-based phenophase estimates for each study region.

REGION		Finland		Poland		Germany				Spain		Italy	
STRATA OR ROI		Understory	Overstory	Understory	Overstory	Understory	Overstory	Understory	Overstory	Understory	Overstory	Understory	Overstory
SAMPLING YEAR		2013		2012		2012		2013		2012		2012	
Onset (SOS)	Min (earliest)	125	125	101	101	96	97	110	110	102	102	96	96
	Max (latest)	128	129	113	105	124	129	115	115	132	150	289	123
	Range	3	4	12	4	28	32	5	5	30	48	193	27
	Mean	126.64	126.78	103.39	103.14	100.27	104.42	112.03	112.48	110.03	118.2	145.61	104.94
	SD	1.04	1.12	1.95	1.05	6.18	7.38	1.76	1.53	10.12	17.01	72.23	6.74
	outliers removed	1	1	0	0	1	0	0	1	2	2	*	1
	value of outlier	196	196	0	0	158	0	0	144	259, 294	179, 261	0	255
Offset (EOS)	Min (earliest)	210	196	159	181	141	179	158	177	126	188	183	168
	Max (latest)	300	270	314	300	315	300	297	310	353	310	355	355
	Range	90	74	155	119	174	121	139	133	227	122	172	187
	Mean	267.85	255.71	253.81	280.47	249.39	279.03	219.03	280.9	219.87	244.16	311.29	283.78
	SD	30.3	24.19	58.61	26.99	65.41	41.02	58.03	35.11	51.65	44.8	61.48	54.56
	outliers removed	0	0	0	0	0	0	0	0	0	0	0	0
	value of outlier	0	0	0	0	0	0	0	0	0	0	0	0
GSL	Min (shortest)	84	68	54	77	41	79	45	64	51	61	49	92
	Max (longest)	175	145	212	198	215	203	183	196	230	207	259	258
	Range	91	77	158	121	174	139	142	132	189	143	218	194
	Mean	135.67	126.46	149.26	187.06	147.26	174.61	107	167.37	108	125.43	165.68	187.42
	SD	30.91	26.3	59.27	27.41	65.56	42.64	57.67	36.61	48.65	48.4	82.02	50.83
	outliers removed	0	0	0	0	0	0	0	0	0	0	0	0
	value of outlier	0	0	0	0	0	0	0	0	0	0	0	0

* more than three values were "outliers" and so were not removed.

Table S2- 4: Summary of the random forests model outputs for each forest strata.

Strata	Evergreen Filter Size	Sample Size (raw data)	Predictor Variable	Variable Importance	Node Purity	Psuedo-Rsquare
Overstory	0.05	84	Tree species richness (e^H)	127.706	14473.051	-14.11
Overstory	0.05	84	Latitude	113.169	10132.464	
Overstory	0.05	84	Year	0	0	
Overstory	0.05	84	Exposition	11.462	11094.259	
Overstory	0.05	84	Canopy age	51.606	5034.61	
Overstory	0.05	84	Mean annual precipitation	77.924	8723.412	
Overstory	0.05	84	Mean diurnal temperature range	228.149	8661.879	
Overstory	0.05	84	Mean annual temperature	148.313	5652.745	
Overstory	0.05	84	Below-canopy light availability	165.799	13381.589	
Midstory	0.05	84	Tree species richness (e^H)	35.111	23606.363	-33.53
Midstory	0.05	84	Latitude	4.96	21421.684	
Midstory	0.05	84	Year	0	0	
Midstory	0.05	84	Exposition	-224.892	16521.898	
Midstory	0.05	84	Canopy age	23.22	12554.961	
Midstory	0.05	84	Mean annual precipitation	-67.681	14751.488	
Midstory	0.05	84	Mean diurnal temperature range	53.716	14653.359	
Midstory	0.05	84	Mean annual temperature	111.387	18107.05	
Midstory	0.05	84	Below-canopy light availability	91.075	22912.921	
Understory	0.05	84	Tree species richness (e^H)	594.213	29095.858	20.65
Understory	0.05	84	Latitude	470.611	24362.272	
Understory	0.05	84	Year	0	0	
Understory	0.05	84	Exposition	-33.783	15782.134	
Understory	0.05	84	Canopy age	78.057	9706.433	
Understory	0.05	84	Mean annual precipitation	189.29	12695.493	
Understory	0.05	84	Mean diurnal temperature range	108.951	7587.305	
Understory	0.05	84	Mean annual temperature	197.592	11171.531	
Understory	0.05	81	Below-canopy light availability	292.486	22023.328	
Overstory	0.33	143	Tree species richness (e^H)	110.947	14607.383	-13.30
Overstory	0.33	143	Latitude	184.349	10422.411	
Overstory	0.33	143	Year	0	78.419	
Overstory	0.33	143	Exposition	3.468	12181.444	
Overstory	0.33	143	Canopy age	91.475	5144.633	
Overstory	0.33	143	Mean annual precipitation	135.228	9522.843	
Overstory	0.33	143	Mean diurnal temperature range	269.516	9748.265	
Overstory	0.33	143	Mean annual temperature	149.696	5810.26	
Overstory	0.33	143	Below-canopy light availability	233.194	18197.951	
Midstory	0.33	143	Tree species richness (e^H)	51.216	25745.496	-26.67
Midstory	0.33	143	Latitude	50.429	22179.641	
Midstory	0.33	143	Year	0	83.209	
Midstory	0.33	143	Exposition	-20.092	17845.041	
Midstory	0.33	143	Canopy age	300.777	16296.202	
Midstory	0.33	143	Mean annual precipitation	52.262	17870.524	
Midstory	0.33	143	Mean diurnal temperature range	113.308	17471.493	
Midstory	0.33	143	Mean annual temperature	141.854	16367.635	
Midstory	0.33	143	Below-canopy light availability	166.511	26126.846	
Understory	0.33	143	Tree species richness (e^H)	396.674	32529.823	29.76
Understory	0.33	143	Latitude	459.677	32765.157	
Understory	0.33	143	Year	0	182.474	
Understory	0.33	143	Exposition	136.983	18818.797	
Understory	0.33	143	Canopy age	224.638	15731.436	
Understory	0.33	143	Mean annual precipitation	260.267	18665.289	
Understory	0.33	143	Mean diurnal temperature range	102.733	7910.891	
Understory	0.33	143	Mean annual temperature	305.541	15499.956	
Understory	0.33	143	Below-canopy light availability	628.822	39074.849	
Overstory	0.66	174	Tree species richness (e^H)	54.534	14535.737	-12.53
Overstory	0.66	174	Latitude	353.777	13606.545	
Overstory	0.66	174	Year	2.565	333.341	
Overstory	0.66	174	Exposition	14.344	11994.987	
Overstory	0.66	174	Canopy age	127.038	5500.57	
Overstory	0.66	174	Mean annual precipitation	158.828	16488.23	
Overstory	0.66	174	Mean diurnal temperature range	253.508	9406.99	
Overstory	0.66	174	Mean annual temperature	180.791	5875.432	
Overstory	0.66	174	Below-canopy light availability	208.817	15546.739	
Midstory	0.66	174	Tree species richness (e^H)	7.715	24503.625	-20.95
Midstory	0.66	174	Latitude	179.553	23740.688	
Midstory	0.66	174	Year	4.787	480.626	
Midstory	0.66	174	Exposition	28.102	18705.307	
Midstory	0.66	174	Canopy age	312.64	17924.427	
Midstory	0.66	174	Mean annual precipitation	163.807	20679.04	
Midstory	0.66	174	Mean diurnal temperature range	174.994	19898.735	
Midstory	0.66	174	Mean annual temperature	214.015	18334.87	
Midstory	0.66	174	Below-canopy light availability	119.673	28253.111	
Understory	0.66	174	Tree species richness (e^H)	242.044	33633.985	30.98
Understory	0.66	174	Latitude	540.508	37408.977	
Understory	0.66	174	Year	5.416	483.938	
Understory	0.66	174	Exposition	234.527	23713.905	
Understory	0.66	174	Canopy age	161.182	18163.113	
Understory	0.66	174	Mean annual precipitation	301.785	24281.936	
Understory	0.66	174	Mean diurnal temperature range	92.098	7412.842	
Understory	0.66	174	Mean annual temperature	398.677	22753.113	
Understory	0.66	174	Below-canopy light availability	842.874	60875.955	
Overstory	1	191	Tree species richness (e^H)	40.758	16346.522	-6.53

Table S2- 3: continued...

Overstory	1	191	Latitude	288.372	15979.626	
Overstory	1	191	Year	46.341	1762.541	
Overstory	1	191	Exposition	-9.911	19616.892	
Overstory	1	191	Canopy age	143.095	9669.121	
Overstory	1	191	Mean annual precipitation	130.953	9677.9	
Overstory	1	191	Mean diurnal temperature range	394.385	14200.327	
Overstory	1	191	Mean annual temperature	156.163	7860.625	
Overstory	1	191	Below-canopy light availability	202.827	15913.167	
Midstory	1	191	Tree species richness (e^H)	47.8	25347.998	-15.86
Midstory	1	191	Latitude	173.949	24365.389	
Midstory	1	191	Year	37.724	1823.527	
Midstory	1	191	Exposition	9.882	16112.543	
Midstory	1	191	Canopy age	298.725	18760.842	
Midstory	1	191	Mean annual precipitation	131.635	21875.395	
Midstory	1	191	Mean diurnal temperature range	276.13	22461.636	
Midstory	1	191	Mean annual temperature	211.034	20753.669	
Midstory	1	191	Below-canopy light availability	78.983	23715.586	
Understory	1	191	Tree species richness (e^H)	289.642	31395.287	29.39
Understory	1	191	Latitude	653.359	40927.058	
Understory	1	191	Year	20.159	975.235	
Understory	1	191	Exposition	233.086	23289.32	
Understory	1	191	Canopy age	100.824	13711.775	
Understory	1	191	Mean annual precipitation	390.189	28135.374	
Understory	1	191	Mean diurnal temperature range	89.218	9639.328	
Understory	1	191	Mean annual temperature	448.377	24914.127	
Understory	1	191	Below-canopy light availability	585.159	56690.266	

LIST OF APPENDIX CHAPTER 2 FIGURES

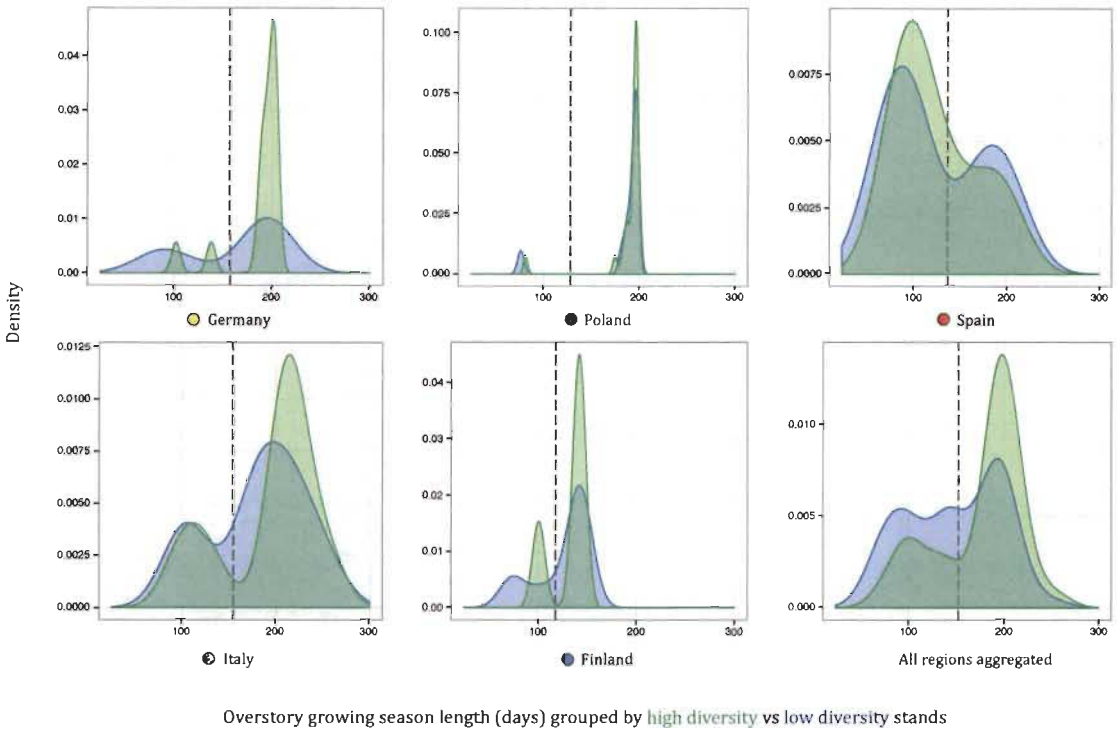

Figure S2 - 1: Kernel density estimates (y-axis) for the probability density function of stand-overstory growing season length grouped by low (blue) *vs.* high (green) stand tree species diversity for each region and for all plots aggregated together. For each region and again for all plots aggregated together, the vertical dashed line represents the split point between the bimodal distribution of GSLs which is separated at this point into stands with short growing seasons and stands with long growing seasons using k-means clustering.

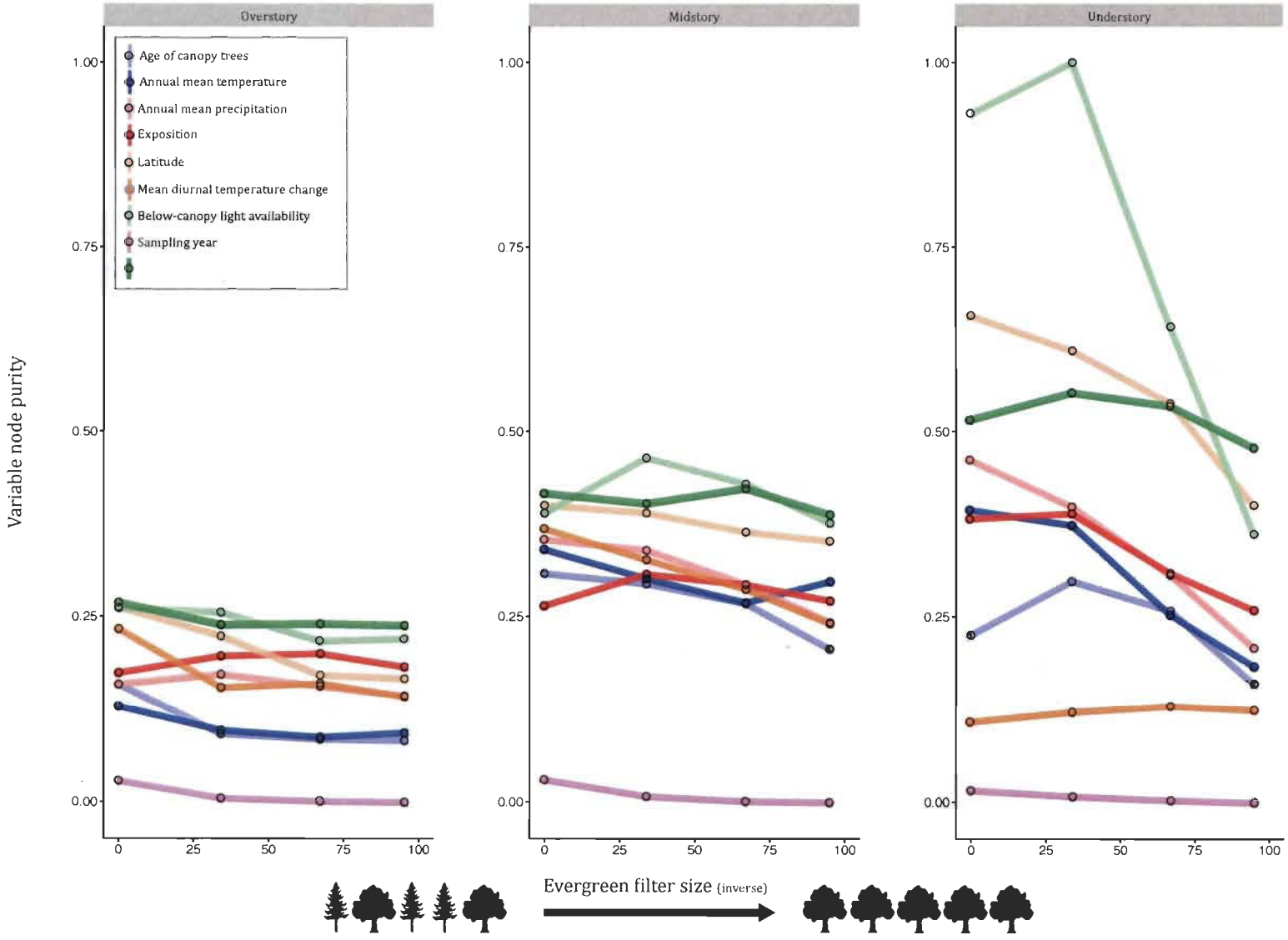
Overstory
Midstory
Understory
Age of canopy trees
Annual mean temperature
Annual mean precipitation
Exposition
Latitude
Mean diurnal temperature change
Below-canopy light availability
Sampling year
Variable node purity
1.00
0.75
0.50
0.25
0.00
0
25
50
75
100
Evergreen filter size (inverse)

Figure S2 - 2: Variable node purity scores for each predictor of the growing season length of each forest strata. For each panel, the x-axis indicates the evergreen filter level wherein the RF models were run at each level. The evergreen filter size is displayed as the inverse of values, such that with increasing values, the tolerance for evergreen presence decreases and, thus, more plots are removed. At 0 no plots are removed and at 100 plots containing any amount of evergreen trees are removed. The results of a random forests model show that the node purity of tree species diversity ($\mathbf{e}^{\mathrm{H}}$) in predicting growing season length increases from the overstory layer down to the understory layer.

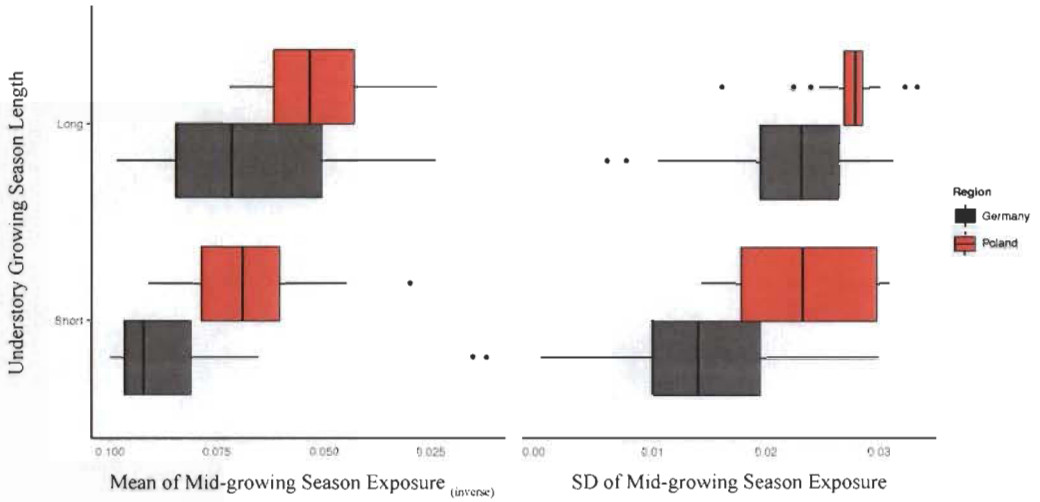

Figure S2 - 3: Box plots of the understory layer growing season length grouped as stands with short *versus* long growing seasons compared to the mid-growing season understory light availability for the German (black) and Polish (red) regions. Plot A is the inverse of the mean of mid-growing season (June — July) image exposure values and Plot B is the inverse of the standard deviation of mid-growing season exposure values. In both regions, stands with longer understory growing season lengths show higher mean understory light availability and more variation in light availability over time (SD of light availability values).

.3 Chapter 3 — Appendices

.3.1 Supplementary Methodology

Tree detection learning algorithm

We estimated the total area (percent of pixels in the image) covered by trees in each image by applying a multi-step image segmentation method developed by Hoiem *et al.* Hoiem *et al.* (2005). The goal of the method is to model geometric classes that depend on the orientation of a physical object with relation to the scene and with respect to the camera from a single image; that is to say, the underlying 3D geometric structure. Specifically, each image pixel is classified into one of a few geometric classes: *i)* the ground plane; *ii)* surfaces that stick up from the ground (vertical surfaces); *iii)* part of the sky plane. Further, vertical surfaces are subdivided into planar surfaces facing left, right or towards the camera and non-planar surfaces of either porous (e.g. trees and their leafy vegetation) or solid (e.g. a person or lamp post). Although this recognition approach differs from many approaches that instead model semantic classes (*e.g.,* car, house, person, vegetation), it has proven exceptionally powerful and efficient in cluttered outdoor scenes like urban streetscapes and, most relevant to our application here, in distinguishing human built structures from natural ones like trees.

First, for each image, pixels are grouped into what are termed *super-pixels* which are pixels assumed to correspond to a single label (*e.g.,* the ground or sky plane) and respect segment boundaries Felzenszwalb et Huttenlocher (2004) (*e.g.,* a boundary between a tree and a building). The super-pixel regions provide some spatial context and similarities to compute first order statistics (e.g. colour and texture) but are too scattered to build more complex geometric features on; those being features that can be used to estimate large-scale surfaces (*e.g.,* whole buildings or trees). As such, the system then applies a standard segmentation algorithm to group regions of the image into homogenous segments. However, it is unknown which segments would be correctly labelled, though some must be and,

as such, multiple hypotheses or numerous combinations of these rough segmentations are developed by varying the parameters of the algorithm.

Concretely, at both the level of the super-pixel and the larger region segments, a set of features are computed (*e.g.,* descriptors of colour and texture, location and shape and 3D geometry). Using training image data of urban scenes that have been ground-truthed with labels according to the geometric classes, learning the parameters to predict labels operates at two stages. First, the process of generating multiple segmentations of an image into geometrically homogeneous regions (*i.e.,* grouping super-pixels) is learned by estimating the likelihood that two super-pixels belong in the same region based on their features. Having done so, different hypotheses or combinations of segmentations are generated by varying the number of regions and the initialization of the algorithm. In the second stage, the final labelling of the geometric classes of image segments is learned by computing the features for each region and labelling them with a geometric class based on likelihood functions (*i.e.,* the likelihood that super-pixels have the same label and the confidence in each geometric label). Once labelled in this fashion, the optimal likelihood functions are then learned through training.

Finally, with our images segmented by this procedure and labelled with the geometric classes, we applied semantic labels to each pixel accordingly: ground (ground plane), sky (sky plane), building (vertical and oriented planar surfaces) and trees (vertical and non-planar meshes). The percent of tree cover in an image, as well as that of ground, sky and building, were calculated as the total number of pixels belong to that class divided by the total number of image pixels.

Modelling streetscape tree cover

We model the relationship between our streetscape tree cover metric and the dependent variable of true percent tree canopy using multiple linear regression and least squares. In doing so, we divided the the data into training and test

sets using a 70-30 % split and randomly sampling without replacement (Table S1). With the training sets, we build multiple polynomial regression models and cross-validate using 4-fold cross validation. After model validation we then test their performance on the unseen test datasets.

Considering our primary dependent variables of interest, for the true percent canopy cover we test the relationship with our streetscape metric and multiple spatial scales: at the city district levels of dynamic block, community district, school district and borough by computing the total percent tree canopy cover per block unit at each district level (*i.e.*, percent canopy cover in a given district polygon) and the associated mean of streetscape tree cover for all GSV sampling points inside each block unit (polygon). The mean unit (polygon) size at each district level, as well as their standard deviations, are provided in Table S2. Moreover, at each district level, some units had little or no GSV image sampling points in them due to missing or limited data at those locations. Therefore, we imposed a cutoff value for each district level representing the minimum number of GSV sampling points inside a unit in order to ensure the predicted mean streetscape values were representative of the area in question. Units not attaining the minimum number of GSV sampling points were removed from this portion of the analysis (Table S2)., wherein if the number of GSV sampling points associated with a given district unit was below the cutoff, they were removed (see the dynamic block level of Fig.5). We also note that these results were produced using only the E-W road-to-camera orientation which limited the number of GSV sampling points in some areas. In future applications we can acquire images only at the E-W orientation for the full extent of the city and thus have a more complete dataset to compute district-level means of streetscape tree cover.

Filtering the dataset

In order to minimize the multiple sources of systemic error when relating the streetscape tree cover metric from GSV images to the response variable derived from the existing representations of urban tree cover (*i.e.,* true percent canopy cover), we perform several filtering steps data. Specifically, we first remove all GSV sampling points that fall in a street intersection for two reasons. First, they are difficult to determine which of the crossing street segments they belong to and, hence their street orientation category. Second, since multiple streets converge at intersections, multiple GSV sampling points become stacked on or very near to each other. In this case they do not conform to our node and neighbouring point rules.

We also attempt to minimize, as much as possible, situations that could likely produce mismatches between our predictor of tree cover and the response variable. The fundamental issue in such cases is not whether our predictor is capturing trees present in the real-world scene, but whether those trees are represented in our response variables. There are several cases for which they are not. Thus, for the model training purposes that we focus on here, we wish to avoid areas that likely have high non-street tree cover in them or nearby. Accordingly, we remove any GSV sampling points located within 50 m of any city park. We do this also when considering the city district levels. We also remove sampling points who's FOV contained tree canopy cover derived from the land cover map, but which contained no street trees according to a recent NYC street tree survey data base. We also remove any rows of the final matrices for which any GSV sampling node neighbours are missing and, hence, only include sampling points that have two neighbouring points to either side. This filtering process was relatively greedy and reduced sample sizes substantially relative to the whole.

Finally, these filtering steps were of particular importance when learning the

weighting factors since their values or relative symmetry to each other are susceptible to such sources of noise in the data. As such, we manually selected the sampling point subsets used to learn the weighting factors by overlaying the sampling points on Google Earth imagery, as well as the landcover map, and manually selecting only street segments in which we thought the issues described above were minimized.

.3.2 A: Supplementary Results

LIST OF APPENDIX CHAPTER 3 TABLES

Figure Page

Table S3- 1: Summary of the sample sizes for all final regression models presented in Figures 3 and 5 of the main text. For the dependent variable of true percent canopy cover inside the 35 m FOV), each road-to-image orientation and after the data filtering steps, the sample sizes of each training and test set are provided. Moreover, for the data subsets used to learn the final neighbour-weighting factors are also provided.

[HTML]EFEFEF [HTML]EFEFEF**Road Orientation Category**	**Dataset associated with final regression model using true tree canopy cover as response**		
	Learning weighting factors	Training	Test
[HTML]EFEFEF1: N-S	702	3642	1561
[HTML]EFEFEF2: E-W	1643	3170	1358
[HTML]EFEFEF3: NE-SW	406	2240	960
[HTML]EFEFEF4: NW-SE	856	4902	2101

Table S3- 2: Summary statistics for the city district level analysis: we tested the relationship between our streetscape tree cover metric and the true percent canopy cover derived from a high resolution landcover map at four city district levels of increasing unit size (dynamic block, community district, school district and borough). The the total percent tree canopy cover per block unit was computed at each district level (*i.e.*, percent canopy cover in a given district polygon) and the associated mean of streetscape tree cover for all GSV sampling points inside each block unit (polygon) we computed and regression models were built to test the relationships.

District Level	Mean unit size (m2)	SD unit size (m2)	Cutoff value	Number of units	adjusted R-square	RMSE
|HTML|EFEFEF Dynamic Block	10720.81529	26424.99699	20	4129 (64)	0.76	0.122
Community District	8270427.327	7901235.102	800	51 (15)	0.56	3.73
|HTML|EFEFEF School District	17793949.67	19121444.96	1500	29 (9)	0.76	2.36
Borough	117440067.4	70329748.6	2000	4 (3)	0.96	0.47

.3.3 Methodology for an exploratory analysis on predicting street tree biomass

In an exploratory analysis using the New York City GSV dataset presented I explore the potential of computer vision models to estimate tree biomass in urban landscapes. I estimate the total aboveground biomass of all New York street trees within each GSV sampling point FOV using a preliminary subset of the 2015 NYC Parks Street Tree Census Data NYC Parks (2016). This dataset provided location, species and diameter at breast height measurements for all street trees within several contiguous regions of the city (n = 93,556 trees), however data for the full city extent was not released at this time. Following, we collected a set of diameter-based allometric regression equations for estimating total aboveground biomass and applied them to each tree in the dataset to obtain an estimate of individual tree aboveground biomass. To generalize a set of allometric equations that could be applied to each tree species (n = 132) we used a combination of sources. First, we applied the generalized allometric equations developed by Jenkins *et al.* Jenkins *et al.* (2003) to any species common to both datasets. For those remaining unmatched, we carried out an exhaustive literature search for published allometric equations for those species and applied the appropriate equations if found. For those still remaining, we matched trees species at the Genus level and applied the equations accordingly, or failing that, at the Family level. This framework resulted in 15 species groups and generalized allometric equations. For all trees falling inside a given GSV sampling point FOV, and at each FOV level (15, 25, 35 and 45 m), we summed the biomasses to obtain an aggregate measure of street tree biomass associated with every GSV sampling point (image).Though using allometric equations primarily developed for natural forest settings is not ideal for estimating urban tree biomass McHale *et al.* (2009), equations specific to urban trees are currently lacking. Our application of generalized equations grouped by functional types represents the best available option to estimate tree biomass from

field measurements. Moreover, volunteer-based field surveys may also be prone to measurement and identification errors. As such, we acknowledge that the biomass estimates we obtain for the street trees are relatively coarse and may be prone to error (we estimate 5-10% error margin).

The remaining methods and analysis to estimate the total street tree biomass present in a GSV FOV and relate these values to the sum of tree biomass as estimated by generalized allometric equations follows that of the main text's methods. In this case we substitute estimated sum of street tree biomass inside each GSV FOV with true percent tree cover inside each GSV FOV as the response variable.

.4 Conclusions — Appendices

LIST OF CONCLUSION FIGURES

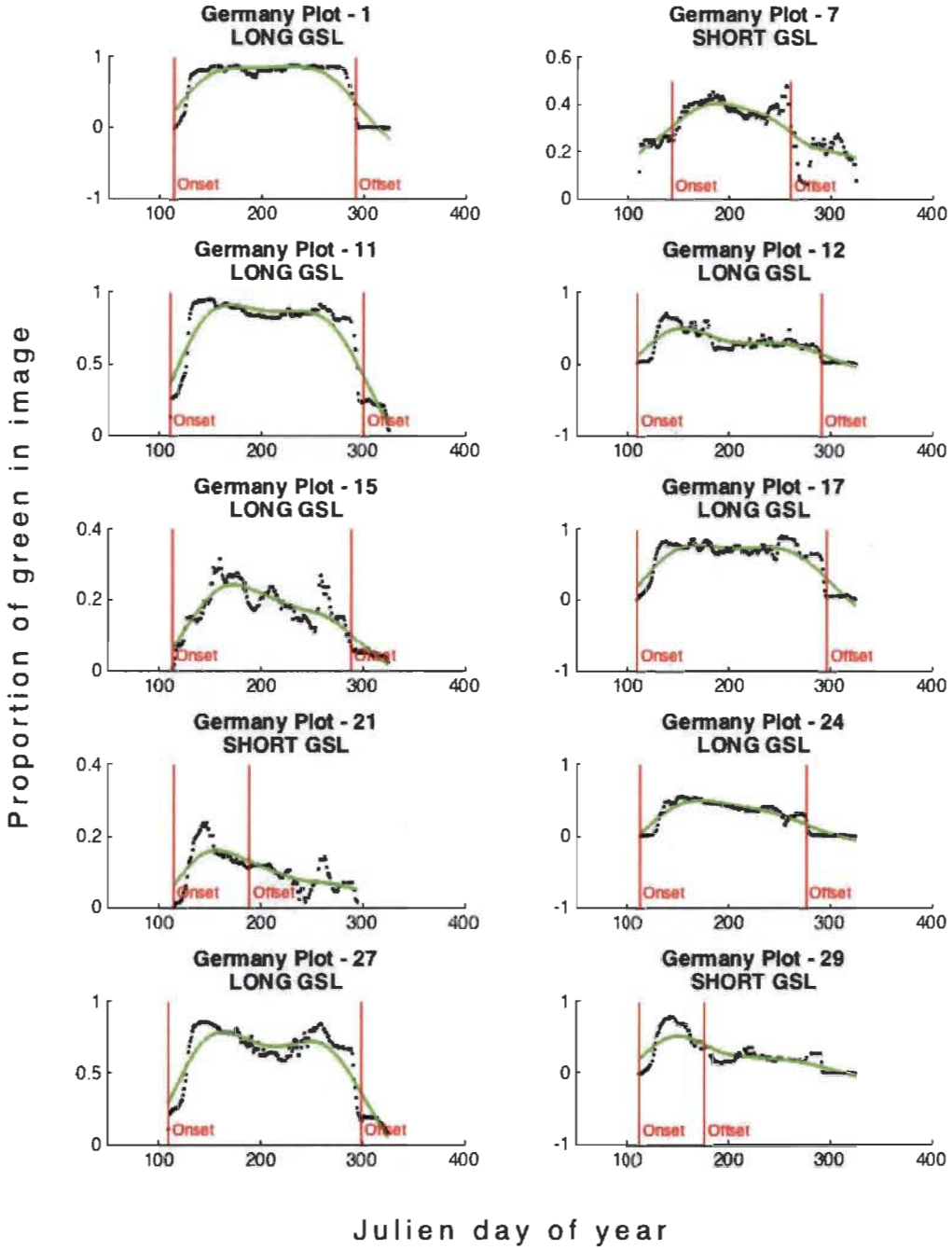

Figure C - 1: Subsample (n = 10) of plots and their estimated overstory seasonal patterns of leaf duration for the Chapter 2 study plots. Derived from time-series images of each plot, the x-axis denotes the day of year the image was taken and the y-axis represents the relative proportion of green pixels in the image which is used to estimate leaf duration. All plots are from the German study region.

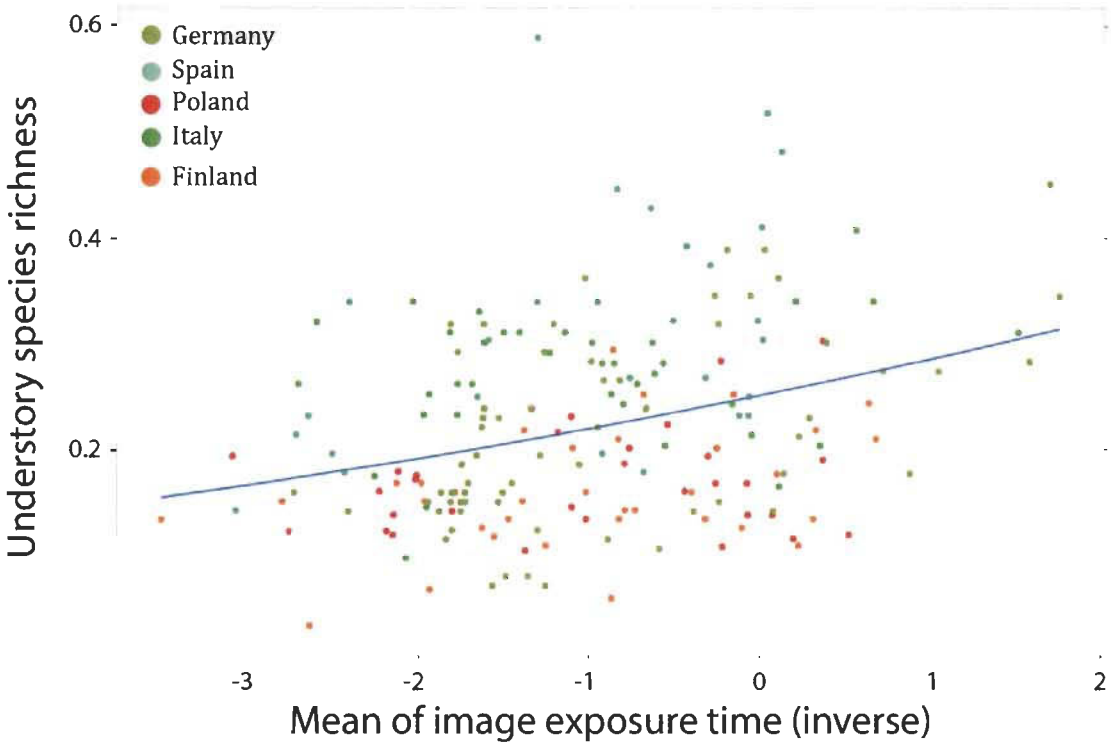

Figure C - 2: Plot understory species richness (y-axis) vs. the mean of the image inverse-exposure values from each plot image time-series (x-axis). The plot-level species richness is scaled by its associated regional species richness of understory species. The inverse of image exposure values can be used to estimate the amount of scene luminance and, hence a rough proxy for below-canopy light availability. The color of each point (plot) indicates the study region: Spain (red), Italy (orange), Germany (olive green) and Poland (turquoise)

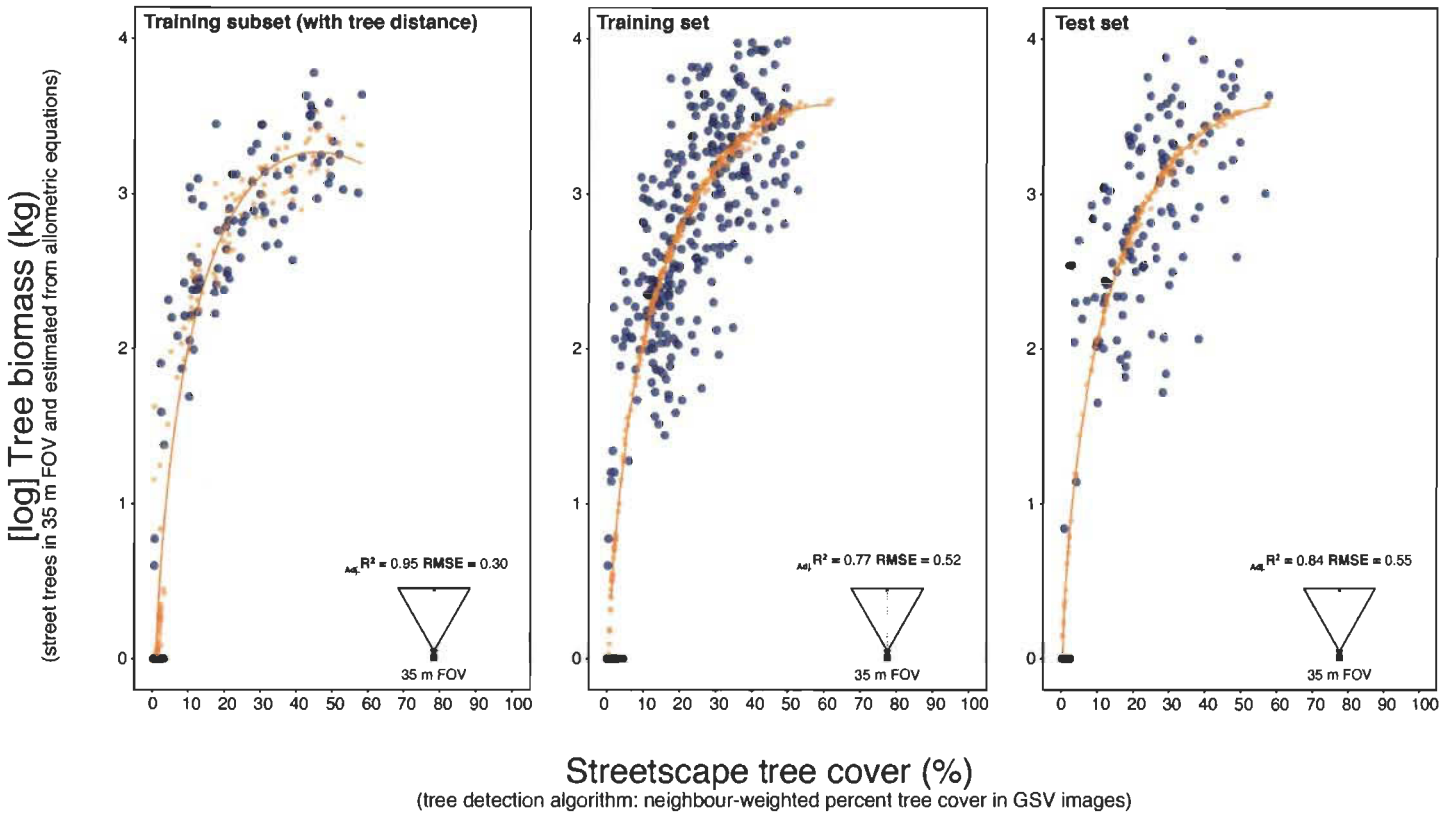

Figure C - 3: Final regression plots modelling the relationship between the streetscape tree cover (x-axis; neighbour-weighted percent) and the log of street tree biomass (kg) derived field surveys and allometric equations (y-axis) at the 35 m FOV level for each dataset: the data subset used to learn the weighting factors (left panel) which includes an additional predictor variable of the sum of tree distances to the GSV camera, the primary training set using all data all GSV sampling points (centre panel) and the unseen test data set (right panel). All data points correspond to GSV sampling points on east-west roads (road-to-camera orientation group 2). Small orange dots are the model's predicted values and the orange line is a smoothing line fit to the predicted values with a square-root polynomial. The adjusted r-square values and root mean squared-error values for the models are reported in the lower corner of each panel.